Dissertation zur Erlangung des Doktorgrades

der Fakultät für Chemie und Pharmazie

der Ludwig-Maximilians-Universität München

An endothelium-derived elastase as mediator of shear stress-induced outside-in signaling via integrin $\alpha_v\beta_3$

Theres Hennig

aus

Halle/Saale

2010

Erklärung:

Diese Dissertation wurde im Sinne von § 13 Abs. 3 bzw. 4 der Promotionsordnung vom 29. Januar 1998 von Herrn Professor Dr. Ulrich Pohl betreut und von Frau Professor Dr. Angelika Vollmar von der Fakultät für Chemie und Pharmazie vertreten.

Ehrenwörtliche Versicherung:

Diese Dissertation wurde selbstständig, ohne unerlaubte Hilfe erarbeitet.

München, am 11.02.2010

_____

Theres Hennig

Dissertation eingereicht am: 11.02.2010

1. Gutachter: Prof. Dr. Angelika Vollmar
2. Gutachter: Prof. Dr. Ulrich Pohl

Mündliche Prüfung am: 12.03.2010

Dedicated to my parents

CONTENTS

TABLE OF CONTENTS

INDEX OF FIGURES

INDEX OF TABLES

INTRODUCTION

I   INTRODUCTION

The vascular system continuously undergoes remodeling processes not only during the early development but also in the adult circulation, e.g. as consequence of exercise training or during the reproductive cycle. Vascular remodeling is as well a feature of vascular pathologies such as atherosclerosis, restenosis and collateral vessel growth [41].

Changes in blood flow conditions and especially alterations in shear stress are one principal stimulus for vessel remodeling and adaptation. Previously Gloe and colleagues were able to show that shear stress induces the release of fibroblast growth factor-2 (FGF-2) from endothelial cells [75]. This release process was not only dependent on the integrin $\alpha_v\beta_3$, but also on a serine protease with elastase activity [107].

1   THE VASCULATURE

The blood vessels as part of the entire cardiovascular system supply all organs with blood containing oxygen and nutrients essential for organ function and cellular integrity. The wall of a larger vessel is composed of three layers. The inner layer, the intima, is formed by a monolayer of endothelial cells and the basement membrane, whereas the media is composed of multiple layers containing variable amounts of elastic fibres and circular smooth muscle cells. The latter regulate the vessel width especially in small arteries and arterioles and are responsible for control of blood flow and flow resistance. The outer layer, the adventitia, mainly consists of connective tissue, containing a mixture of collagenous and elastic fibrils and fibroblasts (see Figure I.1) [155].

In the embryo, the first primitive vascular network is formed by bipotent precursor cells, the hemangioblasts. This de novo formation of a primary vessel plexus is termed vasculogenesis [101]. Hemodynamic forces and growth factors, especially vascular endothelial growth factor (VEGF), are critical in coordinating these processes and play a role in the ultimate shape of the vessel [185].
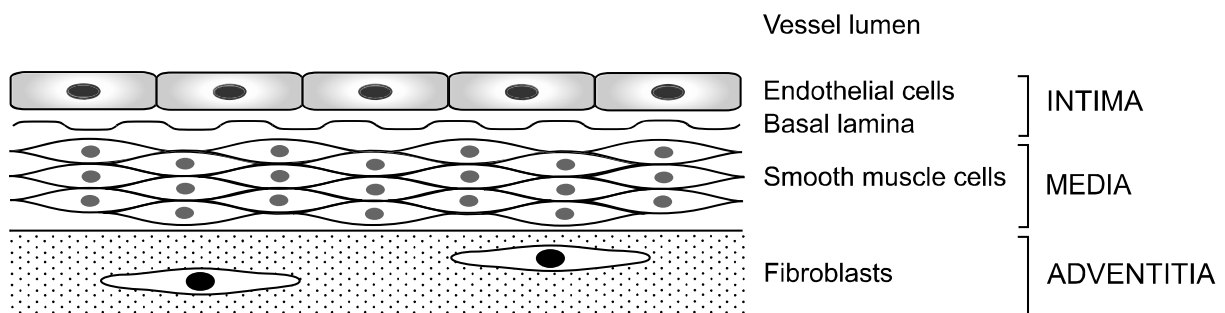
Figure I.1: The structure of the vessel wall

The division of the wall into three layers is the common structural pattern in all blood vessels with the exception of capillaries.

1.1   THE ENDOTHELIUM

The endothelium, a monolayer of cells, lines the inside of all blood vessels and therefore provides a barrier between the blood and the tissues. Endothelial cells can influence the underlying smooth muscle cells or circulating blood elements like platelets and white blood cells in a complex autocrine-paracrine set of interactions. Thereby they are involved in the regulation of vascular tone, permeability, angiogenesis, inflammation and coagulation. Endothelial cell injury, activation or dysfunction may lead to pathological states like atherosclerosis, thrombosis, hemostatic dysfunction or an altered inflammatory or immune response [185].

Due to their direct contact to the streaming blood, endothelial cells are constantly exposed to biochemical and biomechanical stimuli, especially to shear stress (see Figure I.2) [163].
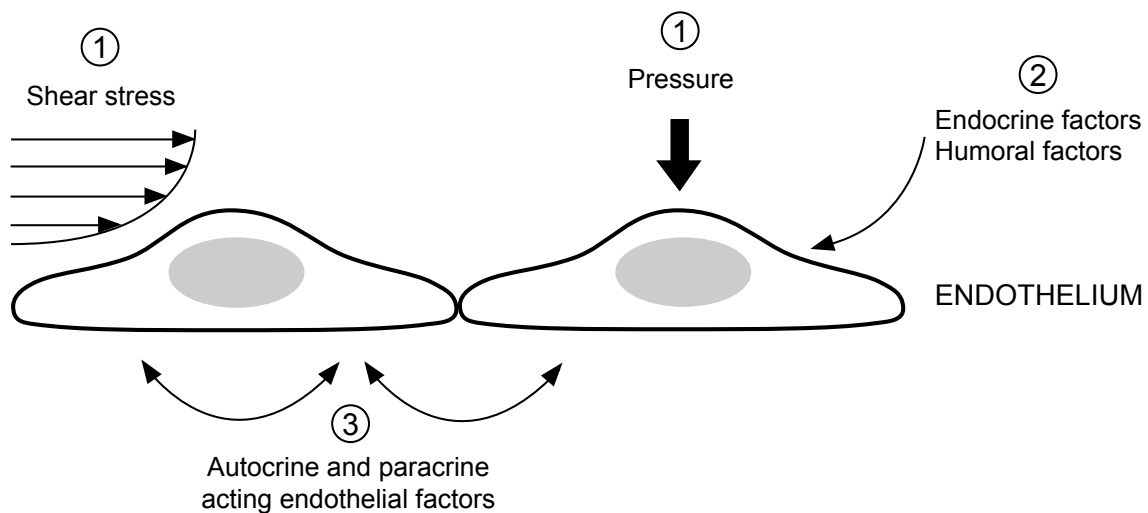
Figure I.2: Stimuli that affect the endothelium

Endothelial cells are influenced by (1) biomechanical stimuli like shear stress or hydrostatic pressure, (2) blood-borne humoral or endocrine stimuli or (3) endothelium and smooth muscle cell-derived stimuli acting in a paracrine or autocrine manner. Adapted from Paszkowiak and Dardik, 2003 [147].

The endothelium uniquely contains Weibel-Palade bodies, elongated storage organelles, that contain various substances, amongst others von Willebrand factor (vWF) and P-selectin [197]. Those proteins are targeted into the Weibel-Palade bodies for storage. In response to activating stimuli such as thrombin or shear stress, these vesicles are rapidly mobilized, fuse with the plasma membrane and thereby allow a prompt delivery of a number of bioactive substances [46,67].

2   HEMODYNAMIC FORCES

Arteries and veins are constantly exposed to distinct hemodynamic forces, which are generated by the blood flow. There are three principal types of hemodynamic forces acting on vascular cells: (1) the fluid shear stress, which acts in a longitudinal direction on the blood-endothelium interface and is directly related to the flow velocity profile, (2) the pulsatile cyclic stretch and (3) the compressive hydrostatic pressure [68]. Whereas cyclic stretch and pressure are transferred to the whole vessel wall due to their vertical orientation, the tangentially aligned shear stress is mainly sensed by the endothelium.

2.1   SHEAR STRESS

Shear stress is defined as the force per unit area applied to move parallel fluid layers or solid materials.

$$\tau = \frac{F}{A}$$

τ: shear stress $[N \cdot m^{-2}]$
F: the force applied $[N]$
A: the cross sectional area $[m^2]$
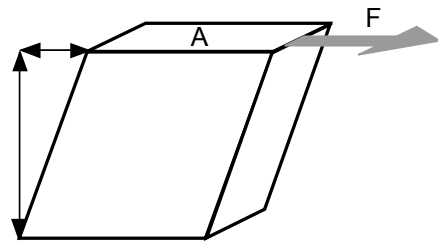
In vessels, the flowing blood exerts a force on the endothelial cell surface acting in flow direction. The occurring shear stress can be calculated using Hagen-Poiseuilles law, which is valid for ideal Newtonian fluids and laminar flows in stiff tubes [105]. Shear stress increases with elevated flow velocity, greater fluid viscosity and smaller vessel diameter.

Hagen-Poiseuille equation

$$\tau = \frac{4\mu Q}{\pi r^3}$$

τ: shear stress $[N \cdot m^{-2}]$ $[1\ N = 10^5\ dyn]$
μ: blood viscosity $[N \cdot s \cdot m^{-2}]$
Q: blood flow rate $[m^3 \cdot s^{-1}]$
r: vessel radius $[m]$

Blood is a non-Newtonian liquid, which means that its viscosity is not only dependent on the temperature but also on alterations in the strain [105]. Through the break-up of erythrocyte-aggregates and deformation of these cells, blood viscosity decreases with increasing flow velocities (shear thinning). In blood vessels the Poiseuille equation is only applicable with restrictions. The equation can be applied in vivo with the following assumptions: the blood is

considered as a Newtonian fluid, the vessel's cross-section is cylindrical, the vessel is straight with inelastic walls and the blood flow is steady and laminar [144].

Shear stress varies depending on heart minute volume, heart period and regional differences in vessel geometry and thereby varies in its magnitude, frequency and direction. Large arteries are defined by a high-pressure, pulsatile flow with shear stresses that cycle within systole and diastole, reaching relatively high levels of 10 to 70 dyn/cm². The highest values appear at bifurcations of large central arteries. Veins experience much lower shear stresses of 1-6 dyn/cm² with a lesser degree of force variation [144]. Flow disturbances occur in arterial segments with geometric irregularities, like curvatures, branches or bifurcations or upstream and downstream of stenoses [34].

Under normal physiological conditions, shear forces serve as an important signal to preserve the anti-thrombotic, anti-inflammatory, anti-oxidative stress and anti-apoptotic phenotype of the vascular endothelium. By contrast, lower flow velocities or disturbed, turbulent flows promote a proatherogenic and/or prothrombotic state and hence vascular pathologies like atherosclerosis and thrombosis. High shear levels are thought to play an important role during the formation of collateral arteries, termed arteriogenesis [26,162].

LAMINAR FLOW		DISTURBED FLOW
Chronic	Acute changes	Acute and chronic
1. Suppression of endothelial activation genes 2. Endothelial quiescence, anti-apoptotic, anti-inflammatory/atherogenic 3. Cytoskeleton/morphology adaption to flow	1. Induction of endothelial activation genes 2. Endothelial activation, release of vasoactive factors, survival, migration, ECM synthesis	1. Induction of inflammatory/atherogenic genes 2. Activation, migration, proliferation, apoptosis, leukocyte binding
Atheroprotection	Vascular remodeling Arteriogenesis	Atherosclerosis

Figure I.3: Effects of laminar and disturbed flow on endothelial cells

The image is adapted from Resnick et al., 2003 [163].

Short term changes in blood flow through arteries result in vasodilation via the release of vasoactive substances, like prostacyclin, nitric oxide (NO) and endothelium-derived hyperpolarizing factor (EDHF), and molecules reducing platelet aggregation [27,172,192]. Shear stress is the most potent physiological stimulus for NO production in endothelial cells [192].

A chronic high blood flow may induce vessel remodeling, that is the formation of new vessels [53,95] or a structural reorganization of blood vessels as observed in arteriogenesis. It has been shown that an elevated flow as a consequence of exercise causes the formation of new

capillaries (angiogenesis) and growth of arteries in the skeletal muscle. Furthermore, treatment with prazosin, an α1-antagonist that induces a threefold higher capillary flow, increased capillary growth in muscles [48,130,156]. By contrast, vessels that are not exposed to flow degenerate.

It has been shown that different growth factors, including FGF-2 and PDGF (platelet-derived growth factor), are released by cultured smooth muscle cells after shear stress exposure in vitro [164,182]. Furthermore, Gloe et al. demonstrated that in endothelial cells the release of FGF-2 strongly increases after shear stress exposure [75].

The endothelium, which is constantly exposed to shear stress, is able to sense this physical stimulus. This ability of the vascular endothelium to sense and respond to the blood flow was observed more than 150 years ago by Virchow [163]. Cells exposed to shear stress elongate and align in flow direction [163]. Shear stress signals are thought to be mediated by ion channels, mechanosensitive proteins like integrins, mechanosignaling via G-proteins, receptor tyrosine kinases (RTKs) or adhesion molecules like platelet endothelial cell adhesion molecule-1 (PECAM-1) (see Figure I.4). Intracellular components that have been linked to the mechanotransduction process are the mitogen-activated protein kinases (MAPK) [199]. The exact mechanisms of cell mechanotransduction, especially how cells sense hemodynamic forces, are not yet fully understood.
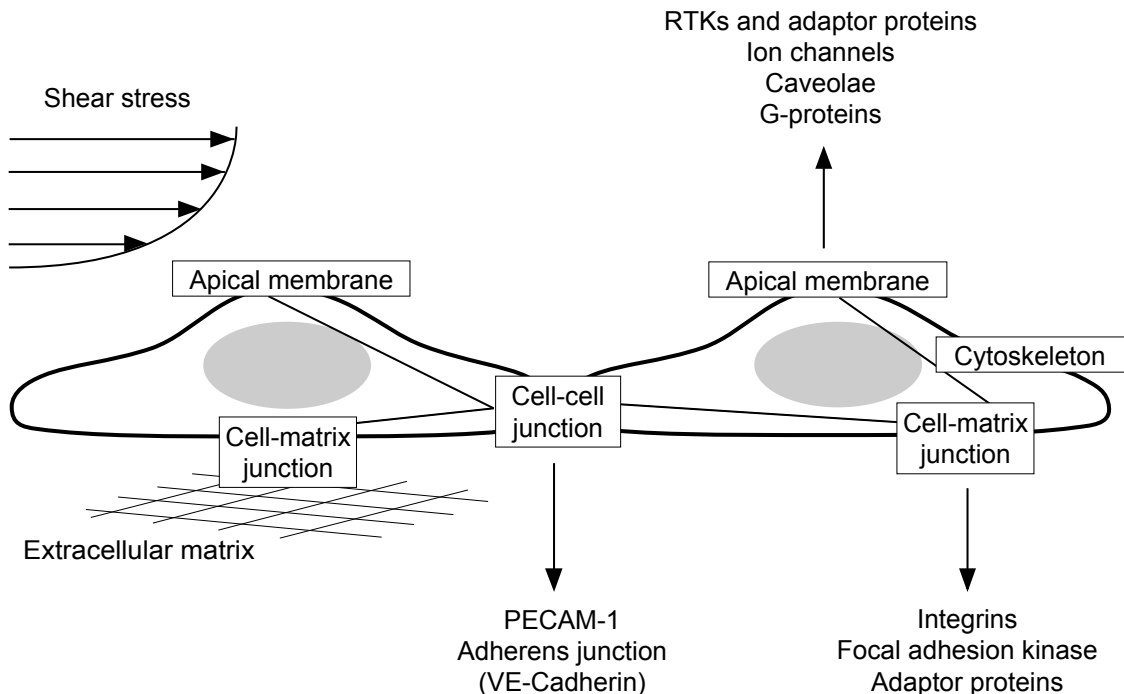
Figure I.4: Shear stress sensors on endothelial cells

Mechanosensors on the apical membrane, cell-cell junctions and cell-matrix junctions are connected by the cell cytoskeleton. All three types of mechanosensors can be activated via shear stress. Adapted from Resnick et al., 2003 [163].

3 ANGIOADAPTATION

Vessels dynamically adjust to changes in hemodynamic and metabolic conditions. Zakrzewicz et al. proposed the term angioadaptation to describe this set of processes [206]. It involves the reorganization of blood vessels via changes in vessel number or structural changes, which incorporate alterations in vessel diameter or wall mass. In detail, vessel sprouting or subdivision resulting in an increased vessel number is called angiogenesis. By contrast, the term pruning describes the loss of vascular segments. Structural changes in vessel diameter or mass are termed vascular remodeling (see Figure I.5). The lumen diameter can be regulated by the flow velocity: A higher blood flow leads to vasodilation whereas a decrease in flow velocity induces a constriction of the vessel. Since remodeling may result in an increase, decrease, or not change the amount of wall material, Mulvany subclassified these three settings as hypertrophic, hypotrophic and eutrophic remodeling [133]. Clinical conditions that involve vascular remodeling are summarized in Table I.1.

ANGIOADAPTATION

Angiogenesis			Remodeling			
Increased number (sprouting)	Increased number (intus-susception)	Decreased number (pruning)	Increased diameter	Increased wall mass	Decreased diameter	Decreased wall mass
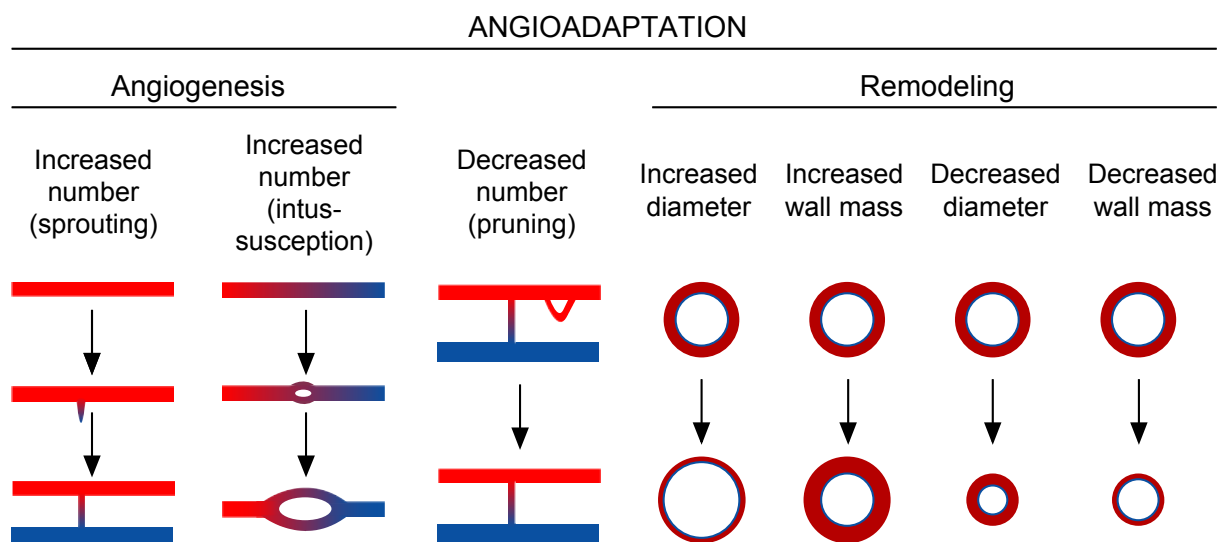
Figure I.5: Processes of angioadaptation

Image modified from Zakrzewicz et al., 2002 [206].

The remodeling procedure induced by chronic shear stress or other stimuli, can be divided into three steps: signal detection, release of substances and, finally, the remodeling process per se. At first, signals are detected by endothelial cells via mechanosensory molecules (see Figure I.4). As a response, these cells synthesize and release substances like matrix modulators (enzymes), growth regulators, cytokines or vasoactive substances. These molecules induce changes regarding cell growth, death, migration or the formation or degradation of extracellular matrix and thus influence the structural composition of the vessel. A description of the mechanisms of angioadaptation requires the identification of the processes by which shear stress or other stimuli are sensed and the characterization of

subsequent signaling pathways leading to structural changes, including angiogenesis and remodeling. The next two chapters will describe the two angioadaptive processes, angiogenesis and arteriogenesis, in detail.

Table I.1: Clinical conditions involving vascular remodeling [72]

Atherosclerosis
Plaque formation
Systemical arterial hypertension
Pulmonary hypertension
Stenosis of vein bypass graft
Restenosis after angioplasty
Collateral formation
Glomerular sclerosis
Arteriovenous fistula
Aneurysm
Patent ductus arteriosus
Venous hypertension
Neovascularization
Transplantation-induced arteriopathy
Neointimal hyperplasia

3.1   ANGIOGENESIS

Angiogenesis is the growth of new blood vessels by sprouting from preexisting ones or by intravascular subdivision (intussuception) in adult and embryonic tissue [59]. Physiological and pathophysiological conditions that involve angiogenesis are summarized in Table I.2.

Table I.2: Conditions involving physiological or pathophysiological angiogenesis [31,78]

Physiological angiogenesis	Pathophysiological angiogenesis
Embryonic development	Tumor growth and metastasis
Wound healing	Psoriasis
Menstrual cycle, ovulation, corpus luteum formation, embryo implantation	Chronic inflammation (rheumatoid arthritis, Crohns disease)
Exercise	Age-related macular degeneration
	Diabetic retinopathy
	Cardiovascular diseases (atherosclerosis)
	Endometriosis
	Adiposity

The angiogenic cascade of the sprouting mode is composed of a complex set of sequential steps (see Table I.3). In brief: Hypoxic, injured or diseased tissue synthesizes and releases angiogenic growth factors. Binding of these growth factors to their appropriate endothelial receptors leads to endothelial cell activation [58]. Removal of pericytes and vessel destabilization shifts the cells from a stable situation with less growth to a proliferating phenotype. Due to an increased cell permeability induced by VEGF, proteases and matrix components escape from the blood into the surrounding tissue. Proteases digest the basement membrane and the extracellular matrix and thereby release matrix-bound growth factors (VEGF, FGF-2). Endothelial cells migrate and proliferate through the reorganized matrix [16]. Adhesion molecules, namely the integrins $\alpha_v\beta_3$ and $\alpha_v\beta_5$, help to move the sprouting vessel. Matrix metalloproteinases are produced to rearrange the extracellular matrix. The interaction of angiopoetin-1 (Ang1) with its receptor Tie2 modulates the tube-like structure and decreases vascular permeability, thereby stabilizing the newly formed vessel. Pericytes, recruited by PDGF and TGF-β (transforming growth factor-β), are incorporated to further stabilize the new blood vessel [58,198].

Table I.3: Sequential process of normal sprouting angiogenesis [145]

Step	Process	Angiogenic factors
1	Vessel destabilization	Ang2/Tie2
2a	Vessel hyperpermeability	VEGF, VE-cadherin
2b	Matrix remodeling	TGF-β
3	Endothelial cell proliferation	VEGF, FGFs, EGF
4	Endothelial cell migration	Integrin $\alpha_v\beta_3$ and $\alpha_v\beta_5$, VEGF, FGFs
5	Cell-cell contact	VE-cadherin, ephrin-B2/Eph-B4
6	Tube formation	FGFs, PDGF, TNF-α, Eph-A2
7	Mesenchymal proliferation/migration	PDGF, Ang1/Tie2
8	Pericyte differentiation	TGF-β
9	Vessel stabilization	Ang1/Tie2, PDGF, VE-cadherin, TGF-β

3.2 REMODELING – ARTERIOGENESIS

The occlusion of a conduit vessel induces a rapid proliferation of preexisting collateral vessels involving an increase of their length and mass. The term arteriogenesis, which describes this phenomenon, was created more than 10 years ago by Schaper et al. [170]. Collateral artery growth after arterial occlusion is the most important tissue-saving, organ-saving and often life-saving vascular adaptive process [170].

The main elicitor for arteriogenesis is thought to be a rapidly increasing blood flow in these collaterals. This raised shear stress activates endothelial cells, leading to an upregulation of endothelial chemokines, mainly monocyte chemoattractant protein-1 (MCP-1), granulocyte-macrophage colony-stimulating factor (GM-CSF) and tumor necrosis factor-α (TNF-α),

adhesion molecules, like intercellular adhesion molecule-1 (ICAM-1) and endothelial nitric oxide synthase (eNOS) [198]. MCP-1 attracts circulating monocytes, which migrate into the vascular wall. After their transformation to macrophages, these cells produce proteases, fibronectin and proteoglycans, which remodel the extracellular matrix. The inflammatory cells release vascular growth factors, especially FGF-2, which induce an immense growth process with active proliferation of endothelial and smooth muscle cells [88]. Proteases alter the external elastic lamina and elastin, located in the adventitia and surrounding tissue, to give way to the growing vessel [198].
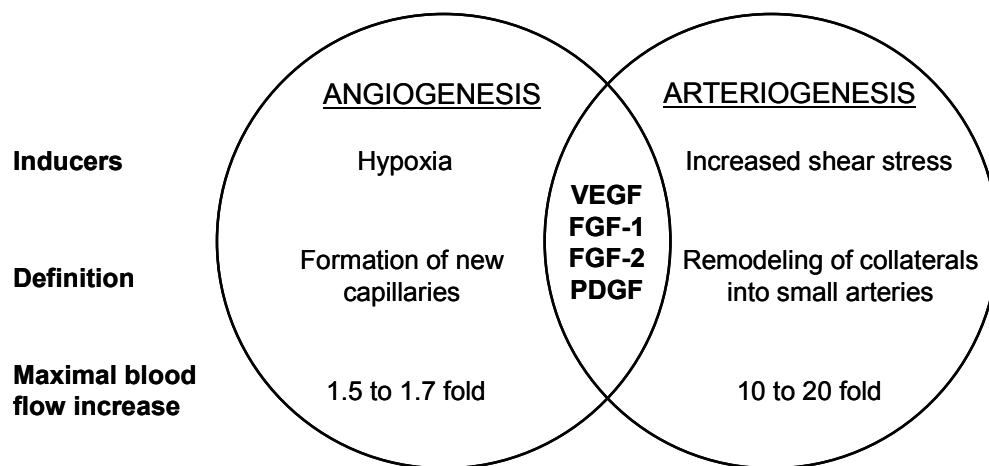
Figure I.6: Angiogenesis versus arteriogenesis

Image adapted from Buschmann and Schaper, 1999 and Schaper and Scholz, 2003 [25,170].

3.3 PROTEASES

Proteases are enzymes capable of hydrolyzing peptide bonds and thereby breaking down proteins. As mentioned above, extracellular proteolysis plays a crucial role in vascular remodeling processes and angiogenesis by degrading extracellular matrices [196]. Moreover, proteases are involved in the regulation of growth factor bioavailability, modulation of cytokine activity and receptor shedding [69]. Several pathological conditions including tumor growth, inflammatory diseases and cardiovascular conditions such as atherosclerosis and restenosis are linked to changes in protease activity [69]. By their mechanism of hydrolytic cleavage, proteases can be classified as serine proteases, cysteine proteases, metalloproteinases, threonine proteases and aspartate proteases. Furthermore, depending on their site of action they are classified as exo- or endopeptidases. Endopeptidases in contrast to exopeptidases cleave at the inner regions of peptide chains. Most proteases that act in the extracellular space are serine and metalloproteinase endopeptidases, acting at a neutral pH, and cysteine endopeptidases, which function optimally in acidic conditions. Protease action is regulated by specific activation mechanisms and specific inhibitors, including tissue inhibitors of metalloproteinases (TIMPs) or serine protease inhibitors [196].

3.3.1   Elastase

Our group was able to show that a serine protease with elastase activity is important for shear stress induced signaling processes [107]. Historically, the term elastase describes proteases having the ability to cleave elastin [17]. Different proteases from the metalloproteinase, cysteine and serine protease familiy have been shown to degrade elastin. However, the name elastase is now applied to neutrophil and pancreatic elastase, which are serine proteases belonging to the chymotrypsin family [87]. Both enzymes cleave elastin, but elastin is neither their only, nor necessarily their most important substrate [17].

Neutrophil elastase is primarily located in the azurophilic granules of polymorphonuclear leukocytes, but has also been detected in the nuclear membrane, the Golgi complex, the endoplasmic reticulum (ER) and the mitochondria of these cells. Furthermore, neutrophil elastase can be found in granules of monocytes [103]. The enzyme is essential for phagocytosis and defense against infection by invading microorganisms and participates in tissue remodeling and is thereby implicated in numerous diseases, including emphysema, chronic obstructive pulmonary disease, cystic fibrosis, acute respiratory distress syndrome, ischemia reperfusion injury and rheumatoid arthritis [193]. Pancreatic elastase is stored as an inactive zymogen in the pancreas. It is secreted into the intestines, where it is activated by trypsin and participates in digestion [17].

For humans, six genes have been described and are listed in NCBI [136]. These are one neutrophil (ELANE, synonym ELA2) and five pancreatic elastases (ELA1, 2A, 2B, 3A, 3B). The comparison of their coding sequences is shown in Figure I.7. Below, in Figure I.8, the six human genes are compared with the two porcine elastase genes that are listed in NCBI. The porcine ELS1 gene shows most homologies to the human ELA1 gene. Surprisingly, the porcine ELANE gene is not highly related to the human neutrophil elastase gene (ELANE), but to the human pancreatic elastase 2A and 2B. The sequence of human neutrophil elastase (human ELANE) parallels porcine pancreatic elastase (porcine ELS1) with 43% identical residues [179].
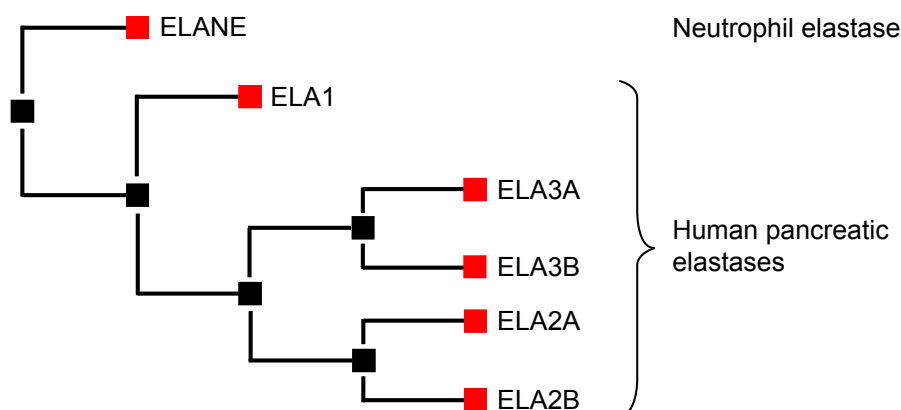
Figure I.7: Phylogenetic analysis of coding sequences of human elastases

The analysis was performed using the Phylogenetic web repeater [121].
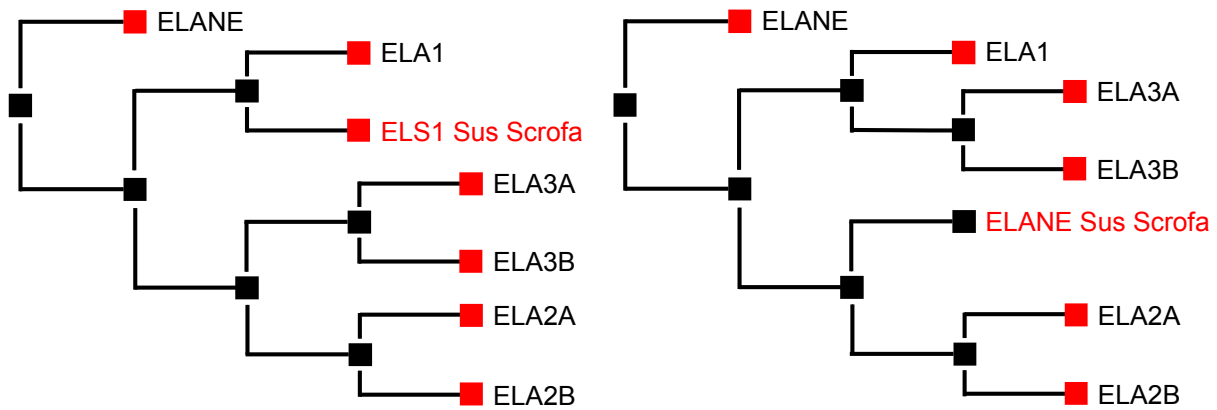
Figure I.8: Phylogenetic analysis comparing coding sequences of human and porcine elastases

The analysis was performed using the Phylogenetic web repeater [121].

3.4   FIBROBLAST GROWTH FACTOR-2

In 1974, the group around Gospodarowicz purified a protein from the bovine pituitary gland. Because of its ability to induce proliferation in 3T3 mouse fibroblasts and its basic isoelectric point of 9.6, the protein was called basic fibroblast growth factor (bFGF) [77]. Later, after more members of the FGF family had been found, the proteins were numbered serially and bFGF was renamed to FGF-2. To date, 22 members of the human fibroblast growth factor family and four major FGF receptor families called FGFR 1 to 4 have been identified [141].

FGF-2 is a heparin binding growth factor that affects the growth, differentiation, migration and survival of a wide variety of cell types. Its sequence is highly homologous across a wide range of species [139]. Especially the human and the bovine FGF-2 protein are extremely homologous; they show an amino acid sequence homology of 98.7% [1]. The human and the porcine FGF-2 protein are as well highly related.

FGF-2 has been found in all organs, solid tissues, tumors, and cultured cells examined [165]. Five different isoforms result from alternative initiations of translation: one AUG-initiated isoform of 18 kDa and four CUG-initiated forms of 22, 22.5, 24 and 34 kDa (see Figure I.9). Whereas the smaller 18 kDa form is primary localized in the cytosol, the others are predominantly found in the nucleus [140].
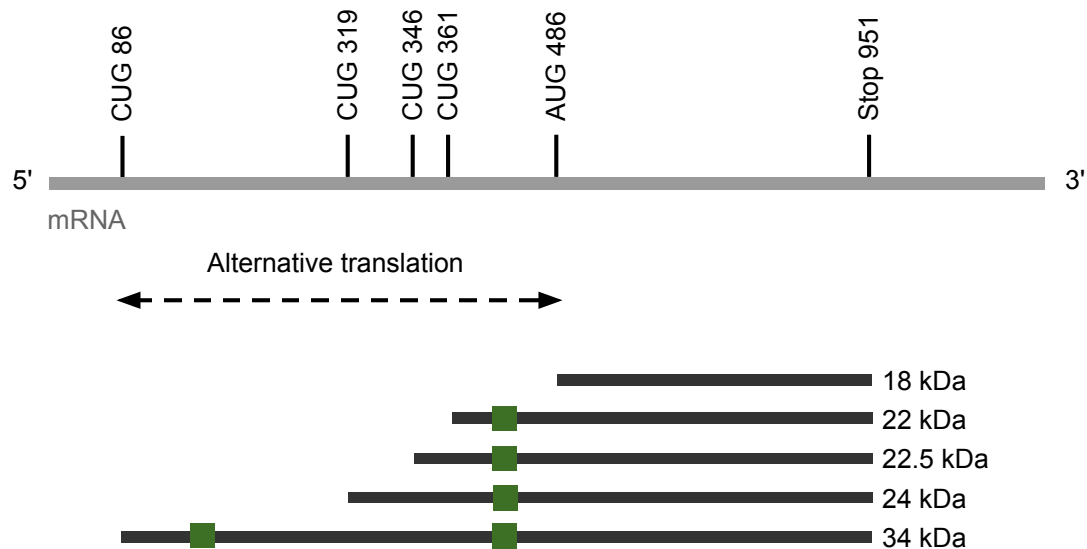
Figure I.9: The five different isoforms of FGF-2 as result of alternative translation
The green boxes represent the nuclear localization signal. Adapted from Okada-Ban et al., 2000 [140].

3.4.1   FGF-2 secretion

Known stimuli for the release of FGF-2 are estrogen [5], hypoxia [97], inflammatory cytokines [168], thrombin [43], nicotine [44] or elevated hydrostatic pressure [2]. Furthermore, it has been demonstrated that shear stress is a very potent stimulus for FGF-2 release from smooth muscle cells in vitro [182] and endothelial cells in vitro [75] and in vivo [115]. The knowledge of how cells, especially endothelial cells, sense this physical stimulus and transduce it to a biochemical signal represented by FGF-2 release is very limited. Gloe et al. showed that blocking the integrin $\alpha_v\beta_3$ inhibited the shear stress induced FGF-2 release, indicating that this integrin is involved in the mechanotransduction process [75].

FGF-2 lacks a consensus signal sequence for secretion, and is therefore not released via the classical protein secretion pathway that progresses through the ER and the Golgi apparatus. Initially, it was suggested that it was released as the result of cell damage, cell death and non-lethal membrane disruptions [45]. But as FGF-2 is also released from viable, undamaged cells, a secretion via a nonclassical ER/Golgi-independent pathway was suggested eventually [62]. Other proteins that are unconventionally secreted are fibroblast growth factor-1 (FGF-1), interleukin-1α (IL-1α), interleukin-1β (IL-1β) and the galectins [137,157]. Yet the molecular mechanisms of their secretion process stay elusive.

The group around Nickel was able to show that FGF-2 membrane translocation occurs in a folded conformation [10]. Furthermore they proposed that FGF-2 is initially recruited to the inner leaflet of plasma membranes followed by membrane translocation via heparan sulfate proteoglycans that form an extracellular trap facilitating the export of the growth factor [207]. In addition, a release via exosomes and vesicles was discussed [33,188].

3.4.2   FGF-2 signaling

Released FGF-2 signals via autocrine and paracrine mechanisms. It interacts with low-affinity heparin or heparan sulfate proteoglycans (HSPGs) on the cell surface. This interaction protects the growth factor against heat, acid denaturation and protease cleavage and increases its affinity to the receptor [40,205]. FGF-2 has two separate receptor binding sites which allow one FGF-2 molecule to bind two high affinity FGF receptors. Finally two receptors, two FGF-2 molecules and two heparan sulfate chains form a ternary FGF-FGFR-HSPG signaling complex [123]. FGF-2 activation of FGFR induces receptor dimerization and subsequently causes an autophosphorylation inside the cells and the initiation of signaling cascades.

3.4.3   Biological functions of FGF-2

FGF-2 exerts pleiotropic roles in many cell types and tissues. It stimulates cell migration, cell differentiation, cell proliferation and a variety of developmental processes and thereby regulates the growth and function of vascular cells. Furthermore, it is involved in angiogenesis, arteriogenesis (see chapter I.3.1 and I.3.2) and in the pathogenesis of vascular diseases such as atherosclerosis.

As FGF-2 knockout mice are viable, fertile and phenotypically indistinguishable from their wild-type littermates, the protein is not essential for embryonic development. These mice furthermore show no morphological defects in heart and vasculature, but exhibit reduced blood pressure [50,140], decreased vascular tone [209] and delayed wound healing [143]. These findings indicate that no vital function is absolutely dependent on FGF-2, which may be due to the redundant functions of several FGFs [140]. In contrast, FGFR1 and FGFR2 knockout are lethal in the embryonic stalk [208]. FGF receptor mutations are associated with birth defects involving craniosynostosis or skeletal abnormalities [24].

Clinical application of FGF-2 could be useful to stimulate wound healing and augment collateral artery development to relieve myocardial and peripheral ischemia. By contrast, FGF-2 inhibition may limit angiogenesis and thus tumor growth or blindness (diabetic retinopathy) or the restenosis that often follows vascular interventions such as balloon angioplasty [139].

4 MECHANOTRANSDUCTION

4.1 OUTSIDE-IN SIGNALING

The cellular plasma membrane creates a barrier between the inside and outside of the cell. In order to respond to its environment, bidirectional signaling across the plasma membrane is mediated by integrins. The transduction of chemical and mechanical signals from the extracellular space to the cytoplasm via integrins is called outside-in signaling (see Figure I.10) [159].
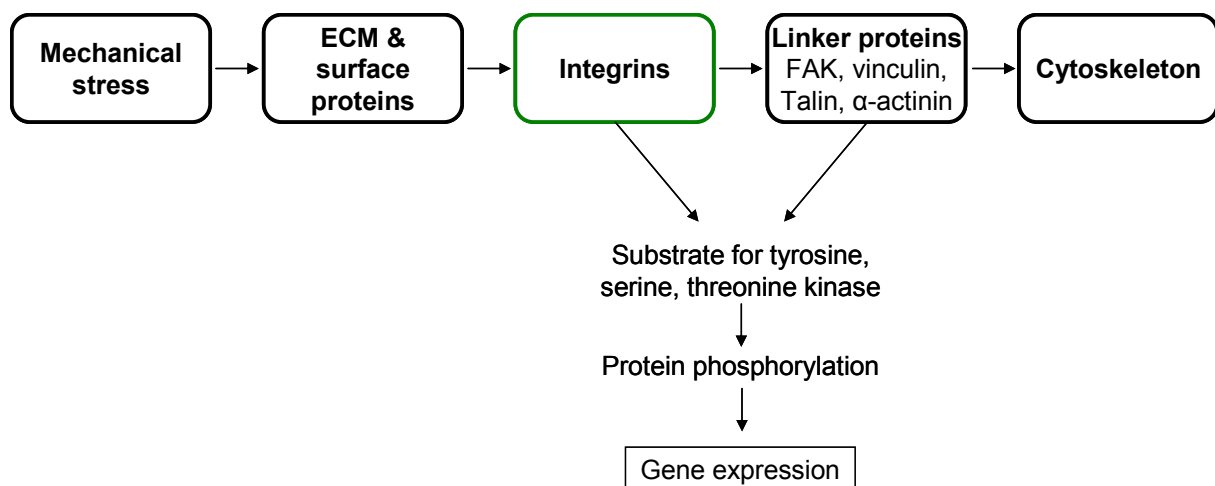
Figure I.10: Integrin outside-in signaling induced by mechanical stress

4.1.1 Extracellular matrix

The extracellular matrix (ECM) is important for the organization of a tissue and the connectivity of single cells. Beyond providing mechanical support, it has an active role in regulating cell shape, behavior and function [4]. The extracellular matrix is a complex molecular network of scaffolding elements, a mixture of adhesive glycoproteins, glycosaminoglycans and proteoglycans (see Table I.4). These molecules are produced intracellularly and continuously secreted into the matrix via exocytosis [123].

Table I.4: Components of the extracellular matrix [4,7]

Scaffolding elements	Glycoproteins	Proteoglycans
Collagen	Fibronectin	Perlecan
Elastin	Laminin	Syndecan
	Fibrinogen	Aggrecan
	Vitronectin	
	Tenascin	
	Thrombospondin	

Two biochemically and morphologically different structures of extracellular matrix can be separated in the vessel: the basement membrane and the interstitial matrix [81]. The basement membrane underlies the endothelium. It is composed of type IV collagen fibers, perlecan and laminin. The interstitial matrix located in between the cells mainly contains collagens of type I, III, V, VI, fibronectin and proteoglycans [112].

4.1.2   Integrins

The cells are linked to the extracellular matrix via integrins, a large family of homologous cell surface molecules that bind the ECM and therefore are responsible for cell adhesion [4]. They possess functions in hemostatis (platelet $\alpha_{IIb}\beta_3$) [175], leukocyte adhesion ($\alpha_L\beta_2$, $\alpha_M\beta_2$) [117], inflammation (leukocyte $\alpha_L\beta_2$ and α_4) [181], angiogenesis (endothelial $\alpha_v\beta_3$) [55], bone resorption (osteoclast $\alpha_v\beta_3$) [189] and cell migration (amongst others $\alpha_5\beta_1$ and $\alpha_v\beta_3$) [91].

Integrins are non-covalent bound heterodimers which are composed of an α- and β-subunit. In total 18 α- and 8 β-subunits form 24 heterodimers [186]. Each subunit contains an extracellular domain that interacts with molecular binding sites of the extracellular matrix, a transmembrane region, and a short cytoplasmic domain which associates with the actin cytoskeleton. Integrins bind extracellular matrix components like laminin, collagen, fibronectin, fibrinogen, vitronectin, thrombospondin or other cell adhesion molecules like VCAM or ICAM (vascular and intercellular adhesion molecule) [186]. These matrix molecules can mediate cellular effects via the integrin. Ligand binding induces integrin clustering, which results in the formation of highly organized intracellular complexes, known as focal adhesions that are connected to the cytoskeleton. This mode of signaling is called integrin outside-in signaling [159]. Adherent cells need the attachment to the extracellular matrix to proliferate and even to survive (anchorage dependence) [4]. By contrast, the ability of cells to control integrin activity from within is termed inside-out signaling.

Most integrin outside-in signals depend on the focal adhesion kinase (FAK) and thereby also src-family-kinases (SFKs). A subset, including the integrins $\alpha_1\beta_1$, $\alpha_5\beta_1$ and $\alpha_v\beta_3$, in addition, activates the adaptor protein Shc [81,177] (see Figure I.11).

Shear stress activates endothelial integrins [120,194]. Studies of Orr and colleagues showed that this integrin activation was specifically dependent on the underlying matrix component. Flow induced integrin $\alpha_2\beta_1$ activation in cells on collagen, but not on fibronectin or fibrinogen, conversely $\alpha_5\beta_1$ and $\alpha_v\beta_3$ were activated on fibronectin and fibrinogen, but not collagen [142]. Shear stress induced integrin activation starts within one minute and lasts for more than six hours [120]. Blocking integrins using anti-integrin antibodies or inhibitory RGD (arginine-glycine-aspartic acid) peptides attenuates the shear induced signaling [120].

The integrin $\alpha_v\beta_3$, known as vitronectin receptor, mediates the adhesion of cells to vitronectin but also to fibronectin and various other ligands [93]. Its key recognition motif is composed of three amino acids: arginine-glycine-aspartic acid (RGD). The integrin $\alpha_v\beta_3$ has been reported

to be present in focal contacts in endothelial cells [73]. This integrin is important for cell adhesion and migration, neointima formation, angiogenesis and bone resorption [108,109]. It was identified as a marker for angiogenic vascular tissues, and its inhibition using RGD peptides induced apoptosis [19,20]. Furthermore, in collateral vessels the integrin $\alpha_v\beta_3$ was upregulated in the vascular wall, indicating an increased outside-in signaling during arteriogenesis [28].

The Shc (Src homology 2 domain-containing transforming protein) adaptor protein family consists of three members. Whereas ShcA (here named Shc) is ubiquitously expressed, ShcB and C appear restricted to neuronal cells [161]. It has been shown that shear stress activation of the integrin $\alpha_v\beta_3$ is associated with an increased interaction of the integrin with Shc [36]. Jalali et al. were able to show that shear stress increased this association only in cells plated on fibronectin or vitronectin [98]. Furthermore, shear stress induced Shc tyrosine phosphorylation and the association of Shc with Grb2 (growth factor receptor-bound protein-2) [36]. Docking of Shc to integrins is linked to the activation of the MAP kinases ERK, JNK and p38 [114].
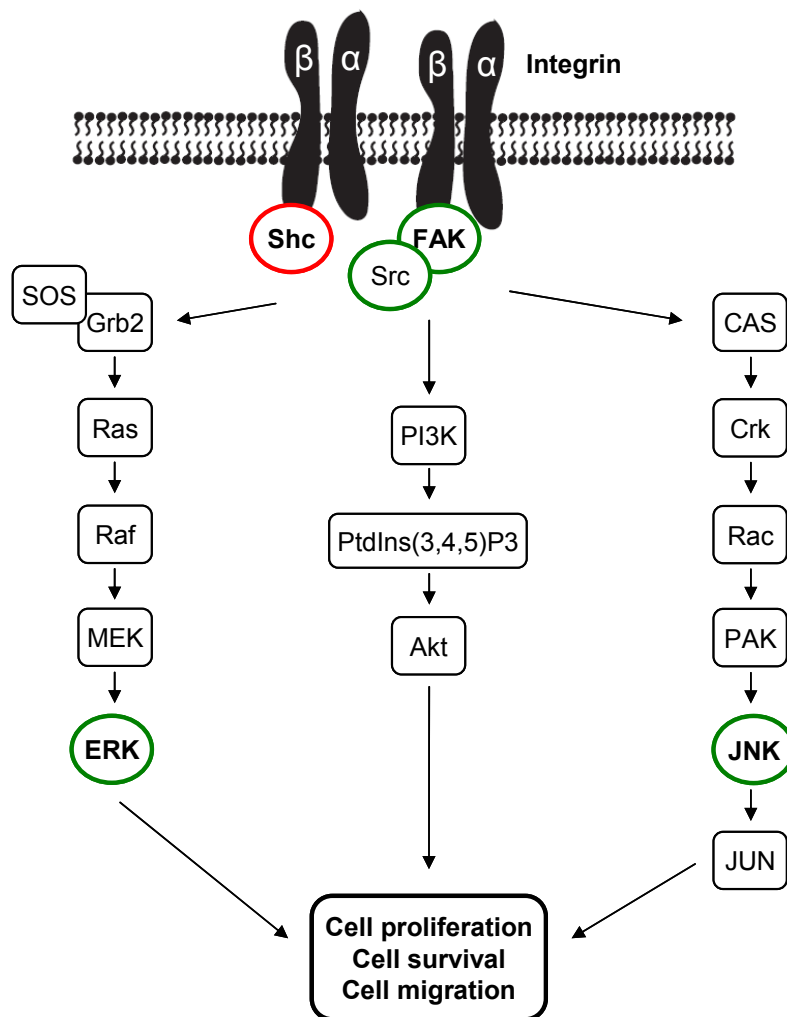
Figure I.11: Integrin signaling pathways

Integrin signaling affects cell proliferation, survival and migration via ERK, Akt and JNK. Furthermore, overexpression of FAK has been shown to activate p38 [3]. The binding of mechano-sensitive integrins to Shc is also linked to the activation of ERK, JNK and p38 [114]. Adapted from Guo and Giancotti, 2004 [81].

4.1.3   Focal adhesions

Inside the cells, the integrin cytoplasmic domains are clustered in dynamic structures called focal adhesions or focal contacts. A mass of proteins including α-actinin, talin, vinculin, paxillin, the focal adhesion kinase (FAK) and the integrin-linked kinase (ILK) are involved in these points and form discrete subcellular regions where the plasma membrane is in tight association with the underlying substrate [70,195]. Bundles of actin filaments, called stress fibers, terminate and are associated with the plasma membrane at focal adhesion sites. They are composed of filaments formed by the contractile interaction of actin, myosin, α-actinin and tropomyosin [104].

The focal adhesion kinase is a cytoplasmatic, non-receptor protein tyrosine kinase. Its N-terminal domain binds to sequences in the cytoplasmic domain of β-integrin subunits. The C-terminal region is rich in protein-protein interaction sites [146]. Cell adhesion or clustering of integrins results in a rapid autophosphorylation of FAK at Tyr397, creating a binding site for the SH2 domain-containing molecules, such as Src, to be recruited and activated. Interaction with Src accelerates FAK phosphorylation at Tyr407, Tyr576/577, Tyr861 and Tyr925. It has been suggested that Tyr576/577 phosphorylation elevates the kinase activity of FAK, while phosphorylation at Tyr925 confers the site for Grb2 binding which may lead to the activation of Ras and triggers the MAP kinase cascade [169]. FAK has been shown to be involved in arteriogenesis and cancer progression [28,128].

Shear stress causes a migration and orientation of endothelial cells in flow direction. In this process, focal adhesions are redistributed and FAK is recruited to focal adhesions, which is accompanied by changes in its phosphorylation [118,163]. The redistribution of integrins and focal contacts serves to strengthen EC adhesion at the points of greatest stress [12]. Thereby the cell cytoskeleton components are rearranged and stress fibers assemble [104].
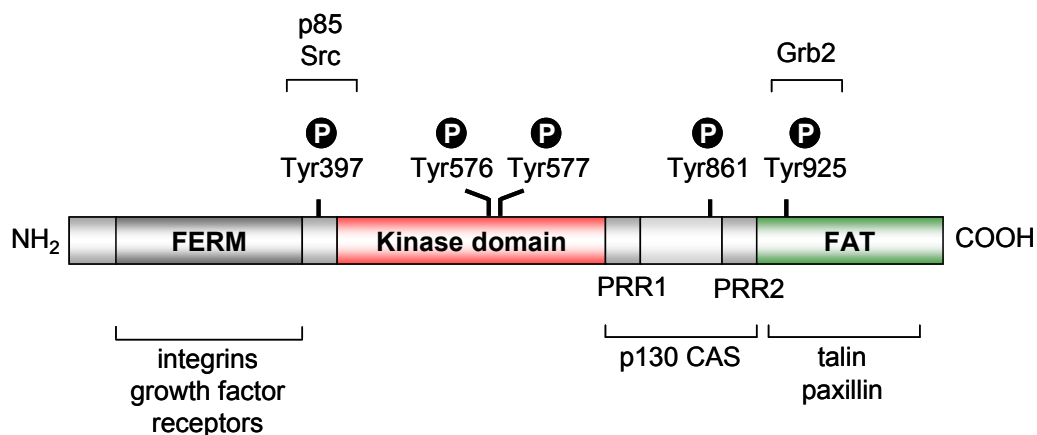
Figure I.12: Focal adhesion kinase domain structure and phosphorylation sites

FAK is composed of a FERM (protein 4.1, ezrin, radixin, moesin homology) homology that can bind integrins and growth factor receptors, a central catalytic domain and a FAT (focal adhesion targeting) domain, which not only directs FAK to adhesion complexes but also provides binding sites for other docking molecules [204]. PRR: Proline-rich region. Adapted from Mitra et al., 2005 [131].

4.2   THE MAP KINASE PATHWAYS

Mitogen-activated protein kinases (MAPK) are a group of serine/threonine kinases [148]. They are activated by an enormous array of distinct extracellular stimuli through dual phosphorylation at conserved threonine and tyrosine residues by upstream kinases (see Figure I.13) [203]. Mammals express five different families of MAPK: extracellular signal-regulated kinases (ERK1, ERK2), c-Jun N-terminal kinases (JNK1, JNK2, JNK3, also referred to as stress-activated protein kinases or SAPKs), p38 kinase isozymes (p38α, p38β, p38γ, p38δ), ERK3/4 and ERK5. The first three of the above are known to be implicated in human diseases [158].

Via phosphorylation of numerous proteins, including transcription factors, cytoskeletal proteins and kinases, the MAP kinases greatly influence gene expression, metabolism, cell division, cell morphology and cell survival [158].

Shear stress activates multiple signaling pathways that include the different members of the MAPK family. ERK, JNK and p38 are all activated but with different temporal patterns [9,99,120]. Azuma et al. furthermore demonstrated that the shear stress induced p38 activation leads to MAPK activated protein kinase 2 (MAPKAP kinase 2) activation followed by phosphorylation of heat shock protein 27 (Hsp27) [8,119].
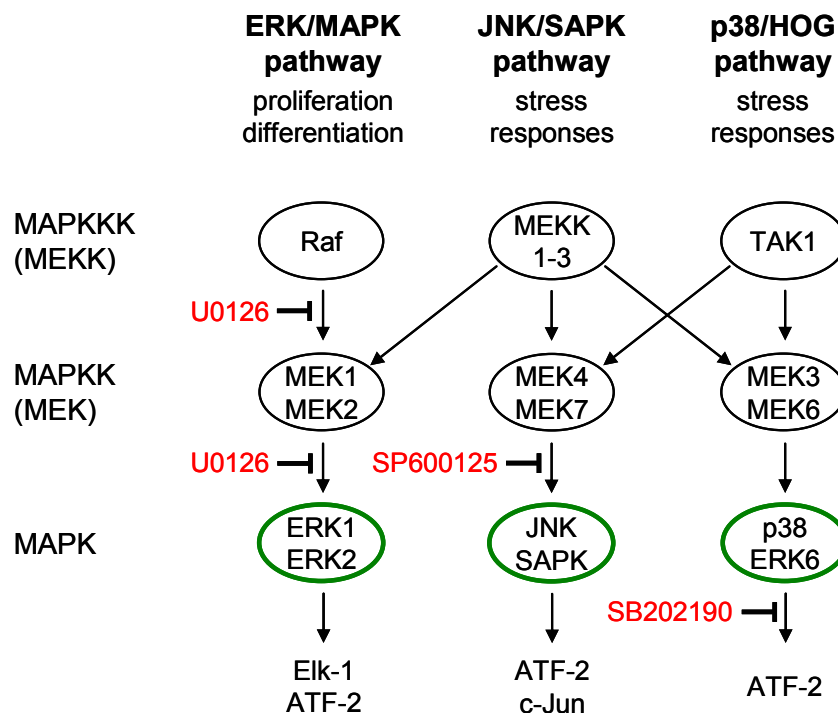
Figure I.13: MAPK pathways

Each MAPK pathway contains three steps comprising a MAP kinase kinase kinase (MAPKKK or MEKK), a MAP kinase kinase (MAPKK or MEK) and the MAPK [38]. MAPKKK phosphorylates and thereby activates MAPKK. Activated MAPKK in turn phosphorylates MAPK [203]. Common inhibitors of these three pathways are labeled in red. Image modified from Cobb, 1999 [38].

Heat shock proteins serve as molecular chaperones. They assist in the folding of proteins and are able to protect them from damage by environmental factors [60]. Furthermore, Hsp27 is known to inhibit apoptosis and modulate F-actin polymerization, preventing stress induced disruption of the cytoskeleton [39].

Hsp27 belongs to the family of small Hsps, which range in monomer size from 15 to 30 kDa, but form oligomeric complexes of 200 to 800 kDa. Phosphorylation occurs on three different serine residues: Ser16, Ser78 and Ser82 and is catalyzed by MAPKAP kinases 2 and 3, which are activated through phosphorylation by p38. An enhanced expression and phosphorylation of Hsp27 is seen as a response to estrogen [151], different forms of stress such as heat shock [111,166], oxidative stress [13] and shear stress [8,119,150], cytokines, thrombin and histamine [116]. As mentioned earlier, many of those stimuli also lead to a release of FGF-2.
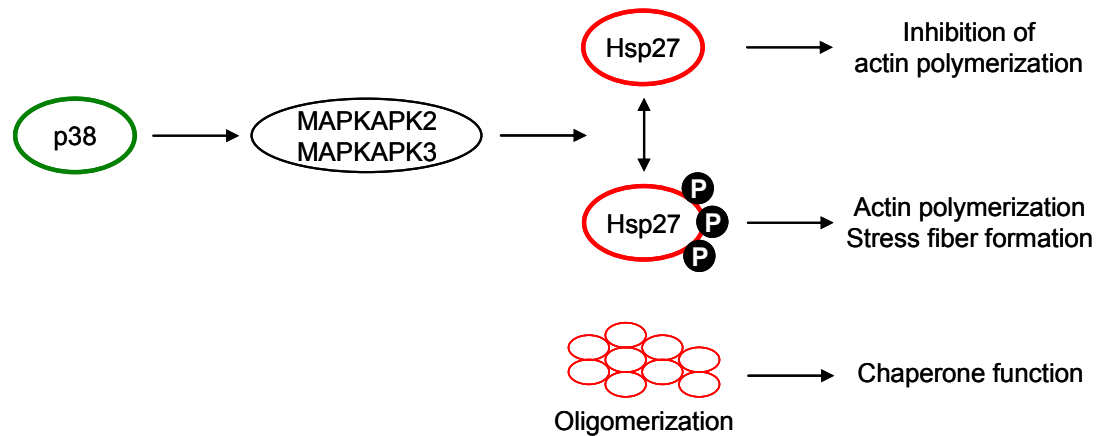
Figure I.14: Hsp27 phosphorylation is linked to its function

P38 phosphorylates MAPKAP kinase 2 and 3 (MAPKAPK 2 and 3), which phosphorylate Hsp27 on key serine residues [60]. In vitro, the non-phosphorylated form of Hsp27 inhibits actin polymerization, whereas the phosphorylated protein allows actin to polymerize [15,80].

5 AIM OF THIS STUDY

Chronic elevation of shear stress stimulates vessel remodeling and adaptation. These events require the control of cell proliferation, migration and differentiation, pivotal processes being mainly regulated by growth factors such as fibroblast growth factor-2 (FGF-2). Shear stress has already been shown to induce the release of FGF-2 from endothelial cells [75]. Thus, FGF-2 release may represent a necessary initial step in the adaptive remodeling process induced by shear stress. Our laboratory has demonstrated before that the shear stress-induced release of FGF-2 depends on the functional integrin $\alpha_v\beta_3$ [75], and also provided first evidence that a serine protease with elastase activity may play a pivotal role in the shear stress-induced signaling cascade leading to FGF-2 release [107]. Based on these findings, the aims of the present study were:

1. Functional characterization of the putative elastase mediating the shear stress-induced FGF-2 release

We wanted to clarify whether the endothelial enzyme shares substrate specificity with known elastases and whether endothelial cells express any of the two known elastases, pancreatic or neutrophil elastase. We further aimed to investigate whether this enzyme is stored in endothelial cells. Finally, we aimed to analyze the effect of this enzyme on the macrostructure and cleavage pattern of defined protein matrices.

2. Analysis of the shear stress-induced integrin $\alpha_v\beta_3$ activation and the role of elastase in this process

Since the integrin $\alpha_v\beta_3$ is involved in the shear stress-induced FGF-2 release, it was further aimed to analyze the impact of elastase on integrin $\alpha_v\beta_3$ outside-in signaling and parameters of integrin activation like focal adhesion assembly and reorganization of the cytoskeleton.

3. Intracellular signaling pathways and proteins involved in the FGF-2 release process

Based on the earlier demonstration of Christina Klarskov Mogensen of an elastase-mediated activation of p38 and Hsp27 [107], it was aimed to clarify whether this activation pathway plays a role in the shear stress-induced FGF-2 release and whether other MAP kinases are activated as well. We also wanted to analyze the role of Hsp27 in the release of FGF-2 by knockdown experiments.

MATERIALS AND METHODS

II   MATERIALS AND METHODS

1   MATERIALS

1.1   REAGENTS

Reagent	Company
2-Propanol	Merck KGaA
Acetic acid 100%	AppliChem GmbH
Acrylamide 30% (Mix 37.5:1)	Genaxxon Bioscience GmbH
Agarose	AppliChem GmbH
Ammonium hydroxide	Sigma-Aldrich Chemie GmbH
Ammonium persulfate	AppliChem GmbH
Aprotinin	AppliChem GmbH
Aqua ad iniectabilia	B. Braun Melsungen AG
Boric acid	AppliChem GmbH
Bromophenol blue	Sigma-Aldrich Inc.
Bovine serum albumin (albumin fraction V)	AppliChem GmbH
Bovine serum albumin (acetylated)	Aurion
Calcium chloride	Sigma-Aldrich Chemie GmbH
Coomassie brilliant blue G-250	AppliChem GmbH
Dimethyl sulfoxide	AppliChem GmbH
Disodium ethylenediaminetetraacetic acid	AppliChem GmbH
Disodium hydrogen phosphate dihydrate	AppliChem GmbH
Ethanol	Merck KGaA
Ethidium bromide	Sigma-Aldrich Inc.
Ficoll-Paque Plus	GE Healthcare
Formaldehyde 37%	AppliChem GmbH
Glutaraldehyde	Calbiochem
Glycerol	AppliChem GmbH
Glycine	AppliChem GmbH
Heparinase I (from Flavobacterium heparinum)	Sigma-Aldrich Inc.
Hydrochloric acid	Merck KGaA
Leupeptin	AppliChem GmbH
Magnesium chloride	Fluka Chemie AG
Methanol	AppliChem GmbH
Nonfat dried milk powder	AppliChem GmbH
Paraformaldehyde	Merck KGaA
Phenylmethylsulfonyl fluoride	Sigma Aldrich Chemie GmbH

Potassium chloride	Merck KGaA
Potassium dihydrogene orthophosphate	Merck KGaA
Saponin	Sigma-Aldrich Inc.
Sodium azide	Sigma-Aldrich Chemie GmbH
Sodium chloride	AppliChem GmbH
Sodium deoxylcholate	AppliChem GmbH
Sodium dodecylsulfate	AppliChem GmbH
Sodium fluoride	Merck KGaA
Sodium hydroxide	AppliChem GmbH
Sodium orthovanadate	Alexis Corporation
Tetramethylethylenediamine	AppliChem GmbH
Tris	AppliChem GmbH
Triton X-100	AppliChem GmbH
Tween 20	AppliChem GmbH
Uranly acetate	Merck KGaA
Xylene cyanol	Sigma-Aldrich Inc.
β-Mercaptoethanol	AppliChem GmbH

Unless stated otherwise, all buffers were prepared using deionized water. If necessary, pH was adjusted by addition of hydrochloric acid or sodium hydroxide solutions, respectively.

1.2   TECHNICAL EQUIPMENT

Flow cytometer	FACSort (Becton Dickinson)
Confocal laser scanning microscope	Leica TCS SP5 (Leica Microsystems)
Fluorescence microscope	Axiovert 200M (Carl Zeiss) Axiophot (Carl Zeiss) equipped with a AxioCam MRm (Carl Zeiss)
Imaging system for western blot analysis (CCD camera)	Digital CCD Camera (ORCA-ER) (Hamamatsu Photonics)
Thermocycler for real time PCR	Light Cycler 1.5 (Roche)
Thermocycler for PCR	Mastercycler ep gradient S (Eppendorf AG)
Table centrifuge for microcentrifuge tubes	EBA 12 (Hettich Zentrifugen)
Cooling centrifuge for microcentrifuge tubes	Biofuge Primo R (Heraeus Instruments)
Cooling centrifuge for falcon tubes	Megafuge 1.0R (Heraeus Instruments)
ELISA plate reader	Infinite F200 (Tecan)
Cell counter	Coulter AcT 8 (Beckman Coulter)
PH measurement	PHM 82 Standard pH Meter (Radiometer Copenhagen)

1.3   CELL CULTURE

All sterile work was performed using an air flow work bench (LaminAir HB2448, Heraeus Instruments). Before usage, all instruments were autoclaved by means of a steam sterilizer (H&P Labortechnik AG). The cells were cultivated in a humidified incubator (Sanyo CO_2 Incubator Model MCO-17AI, Sanyo Electric Co. Ltd.) at 37°C and aerated with 5% of carbon dioxide. To control cell appearance and behavior, a light microscope (Fluovert FU, Leitz) was used.

Cell culture reagents and tools	Company
Accutase	PAA Laboratories GmbH
Antibiotic antimycotic solution (Amphotericin B, Penicillin, Streptomycin)	Sigma-Aldrich Chemie GmbH
Cell culture dishes, 6 and 24 well plates	BD Biosciences (BD Falcon)
Collagen G	Biochrom AG
Collagenase A	Roche
Cryovials	Biozym Scientific GmbH
Dulbecco's Modified Eagle Medium	Gibco Invitrogen
Dulbecco's Modified Eagle Medium without phenol red	Sigma-Aldrich Chemie GmbH
Endothelial Cell Growth Medium	Promocell
Fetal calf serum	Biochrom AG
Fibronectin	Harbor Bio-Products
Hank's balanced salt solution	Apotheke Innenstadt, University-Clinic of Munich
L15 Medium (Leibovitz)	Sigma-Aldrich Inc.
Supplement Mix	Promocell
Trypsin-EDTA solution	Sigma-Aldrich Chemie GmbH

Fetal calf serum (FCS) was heat inactivated at 56°C for 30 minutes and stored at 20°C. In cell culture, two sterile phosphate buffers were used, one without calcium and magnesium ions (PBS-), the other one containing these ions (PBS+) (see composition below). These buffers were either prepared in the laboratory or obtained from the local dispensary (Apotheke Innenstadt, University-Clinic of Munich).

PBS (pH 7.4)		
NaCl	137	mM
KCl	2.68	mM
Na_2HPO_4	8.1	mM
KH_2PO_4	1.47	mM
in Aqua ad iniectabilia		

PBS Ca^{2+}/Mg^{2+} (pH 7.4)		
NaCl	137	mM
KCl	2.68	mM
Na_2HPO_4	8.1	mM
KH_2PO_4	1.47	mM
$MgCl_2$	0.42	mM
$CaCl_2$	0.90	mM
in Aqua ad iniectabilia		

1.3.1 Isolation of primary endothelial cells

1.3.1.1 PAEC – Porcine aortic endothelial cells

All experiments were performed using endothelial cells from pig aortas (PAEC – porcine aortic endothelial cells). The isolation of these cells has been described previously by Gloe et al. [74].

The aortas were obtained directly from the local slaughterhouse. After washing them several times with sterile PBS+, surplus fat and connective tissue were removed. Subsequently, the aortas were sliced lengthwise and clamped in specially-designed metallic frames. The inner surface of the vessel was covered with 2 ml of a collagenase A solution (1 mg/ml, activity > 0.15 U/mg) at 37°C for 1 hour, leading to the dissolution of the endothelial cells. They were scraped off and cultivated in PAEC growing medium in the incubator at 37°C in standard plastic culture dishes. After reaching confluence, cells were frozen and thawed when needed (see chapter II.1.3.3).

PAEC growing medium	
FCS	10 %
Antibiotic antimycotic solution	1 %
in DMEM	

PAEC starving medium	
FCS	1 %
Antibiotic antimycotic solution	1 %
in DMEM	

1.3.1.2 HUVEC – Human umbilical vein endothelial cells

Human umbilical cords were kindly provided by the gynecological hospital of the Ludwig-Maximilians-Universität Munich (Campus Innenstadt and Großhadern).

The central vein in the umbilical cords was rinsed with PBS+ and incubated with a collagenase A solution (1 mg/ml, activity > 0.15 U/mg) for 10 minutes at 37°C. Then the dissolved primary endothelial cells were washed out with warm HUVEC growing medium (a 1:1 mixture of HUVEC growing medium I and II), centrifuged at 1,200 x G for 5 minutes and cultivated in standard plastic culture dishes in the incubator at 37°C.

HUVEC growing medium I			HUVEC growing medium II	
FCS	20 %		Supplement Mix	2.5 %
Antibiotic antimycotic solution	1 %		in Endothelial Cell Growth Medium	
in DMEM				

1.3.2   Cell passaging

Cells were subcultured at 90 to 100% confluence. After washing the cells with PBS-, a solution containing 0.5% trypsin and 0.2% EDTA was added (1 ml per 78.2 cm² flask). Due to the proteolytic activity of trypsin and the ability of EDTA to catch bivalent cations as a chelating agent, adherent cells detach from the culture dish. This process, which was observed using the light microscope, takes 5 to 10 minutes at 37°C. Detached cells are characterized by a rounded cell shape. To inactivate trypsin, 5 ml of PAEC or HUVEC growing medium, which both contain at least 10% of serum, were added. This cell solution was then diluted by adding the required volume of growing medium. Depending on the planned experiment and the required cell confluency dilutions in a ratio of 1:2 to 1:4 were used. Subsequently, the cells were cultivated in growing medium. For all experiments PAEC of passage 2 to 5 and HUVEC of passage 1 to 2 were used.

1.3.3   Freezing and thawing

For long-time cell storage, cells were frozen. For this purpose, endothelial cells were incubated with trypsin for approximately 2 to 5 minutes, centrifuged and resupended in a respective amount of freezing medium. Afterwards, cell solutions were added to cryovials, frozen for 24 hours at -80°C and thereafter stored for preservation in liquid nitrogen (-196°C).

Freezing medium	
DMSO	10 %
in FCS	

Cells were quickly defrosted in a water bath. Subsequently, they were added to plastic culture dishes containing growing medium of 37°C and placed in the incubator. After 24 hours, cells were subcultured.

1.4   ISOLATION OF LEUKOCYTES FROM HUMAN AND PORCINE BLOOD

As a positive control for neutrophil elastase, mononuclear cells were isolated from human and porcine blood. For this purpose, 4 ml Ficoll-Paque were carefully covered with 5 ml of the blood sample containing the anticoagulant heparin (Heparin-Natrium-25000-ratiopharm, Ratiopharm). The falcon tube containing these two layers was centrifugated for 12 minutes at 1,400 x G and 8°C without using the centrifuge brake. The emerging layer between plasma and Ficoll-Paque (see Figure II.1), called buffy coat, was removed with a pasteur pipette and collected in another tube. This cell solution was centrifuged for 10 minutes at 1,000 x G. Afterwards, the cell pellet was lysed and used for protein or RNA analysis.
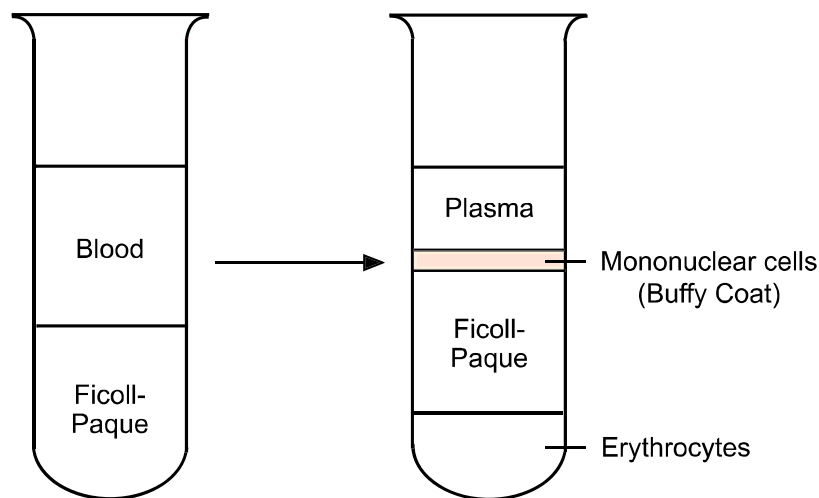
Figure II.1: Ficoll gradient centrifugation for white blood cell isolation
The buffy coat containing the mononuclear cells (here in light red) was isolated via Ficoll centrifugation.

1.5   PREPARATION OF HUMAN AND PORCINE PANCREATIC TISSUE

Human pancreas was provided by the University-Clinic of Munich (Foundation HTCR – Human tissue and cell research). Porcine pancreas was obtained directly from the Walter-Brendel-Centre of Experimental Medicine (Munich).
The frozen pancreatic tissue was added to a mortar in a box filled with dry ice. Liquid nitrogen was poured rapidly into the mortar and the pancreas was mechanically grinded with a pestle until pulverized. Subsequently, the powder was lysed for protein or RNA analysis.

2   METHODS

2.1   CELL STIMULATION AND INHIBITION

2.1.1   Shear stress

2.1.1.1   Cone and plate apparatus

For shear stress application, a self-made cone and plate apparatus was used (see scheme and photograph in Figure II.2).
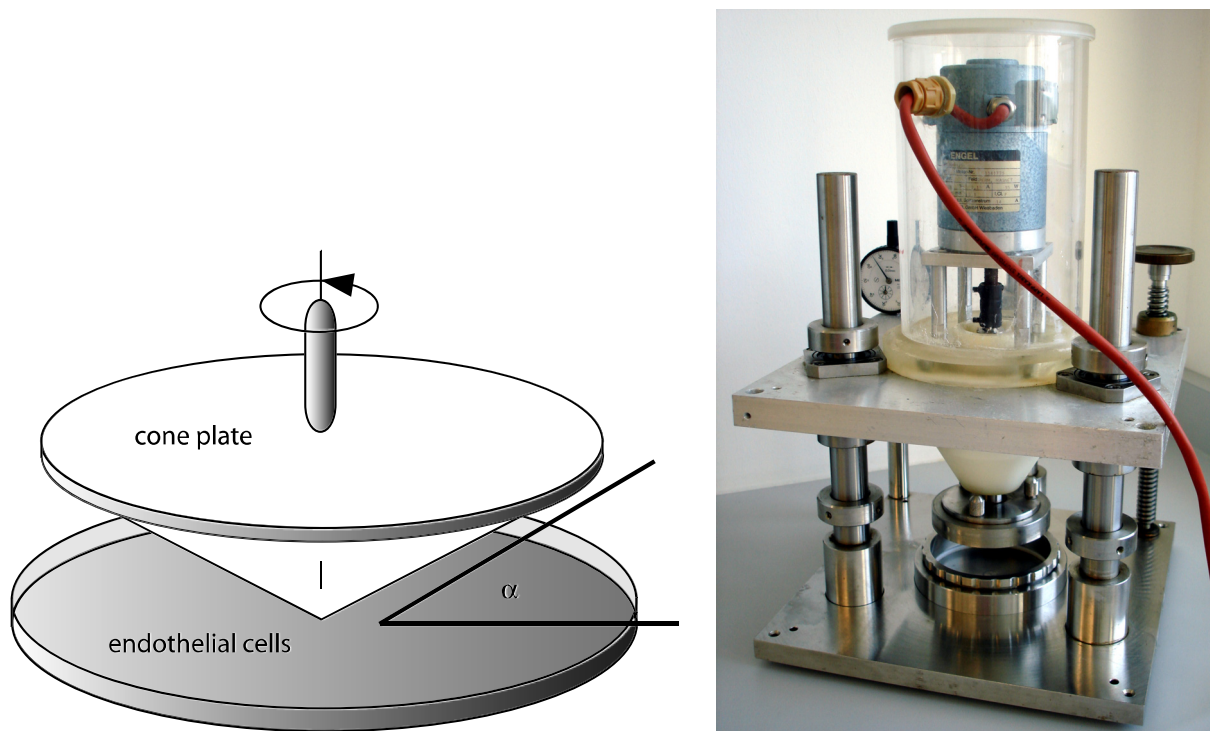
Figure II.2: Cone and plate apparatus

Shear stress was adjusted using the following equation:

$$\tau = \frac{\mu\omega}{\alpha}$$

τ: shear stress [N $\cdot$ m^{-2}] [1 N = 10^5 dyn]
μ: viscosity of the medium [N $\cdot$ s $\cdot$ m^{-2}]
ω: angular velocity [s^{-1}]
α: angle of the cone

Unless stated otherwise, glass plates, measuring 10 cm in diameter, were coated with collagen G (10 µg/ml), which mainly consists of collagen type I. Some additional experiments were performed using fibronectin (10 µg/ml) as coating agent. Confluent cells were transferred in a 1:1 ratio from 10 cm plastic culture dishes onto these glass plates, which were

placed in plastic petri dishes (Greiner Bio-One). The cells were left in PAEC growing medium overnight (24 h) until they reached confluency. 30 minutes prior to the planned experiments, the medium was changed to 7 ml of PAEC starving medium (without phenol red). After this time, one of the glass plates was put in the metal cylinder of the shear stress apparatus and covered with the pre-used 7 ml of starving medium. Now the metal cylinder was inserted into the apparatus, the cone was lowered and a shear stress of 16 dyn per cm² was applied. By modification of the angular velocity of the cone, a particular shear stress was applied. Another glass plate, which was left in the petri dish as a control, was put in the same incubator. After 2 hours of stimulation with shear stress, cell supernatants were collected, centrifuged for 5 minutes at 1,200 x G and frozen for storage. The cells were rinsed with PBS- and 1 ml of lysis buffer was added. These samples were frozen as well. For western blot analysis of elastase and von Willebrand factor in cell supernatants, they were concentrated in a 1:10 ratio using centrifugal columns (Vivaspin 4, 10,000 MWCO, Sartorius Stedim Biotech).

2.1.1.2   Parallel plate apparatus

For immunofluorescence experiments a parallel plate apparatus (see Figure II.3) was used for shear stress experiments. This system consists of a pump (Ismatec IPS-12, Ismatec SA) connected to tubes and a μ-slide from Ibidi. The pump presses the medium through the tubes and the slide. During the experiment the slides were placed onto a 37°C heating plate.

Prior to the planned experiment, the uncoated slide was incubated for 30 minutes with collagen G (10 μg/ml). Afterwards it was rinsed with 1 ml of Aqua ad iniectabilia and left under the bench until completely dry. Next, 100 μl cell suspension containing approximately 30,000 cells was filled into the slide. Subsequently, the slide was incubated at 37°C. After cell attachment, the two reservoirs of the slide were each filled with 500 μl PAEC growing medium. When the cells were confluent, L15 medium was used, since these shear stress experiments were performed outside a CO_2 incubator. This medium is buffered by salts, free amino acids and galactose, preserving a physiological pH. The slide was connected to the tubes of the flow apparatus and a shear stress of 16 dyn per cm² was applied, corresponding to a flow of 12.8 ml per minute. The calculation was performed using the equation below [64]. After applying shear stress, the cells were prepared for fluorescence microscopy as described in chapter II.2.7.3. Finally, cells were mounted using the Vectashield mounting medium (Vector Laboratories) and analyzed by confocal laser scanning microscopy.

$$\tau = \frac{6\mu Q}{bh^2}$$

τ: shear stress $[dyn \cdot cm^{-2}]$
μ: viscosity $[0.01\ dyn \cdot s \cdot cm^{-2}]$
Q: flow rate $[0.213\ cm^3 \cdot s^{-1}]$
b: channel with [0.5 cm]
h: channel height [0.04 cm]
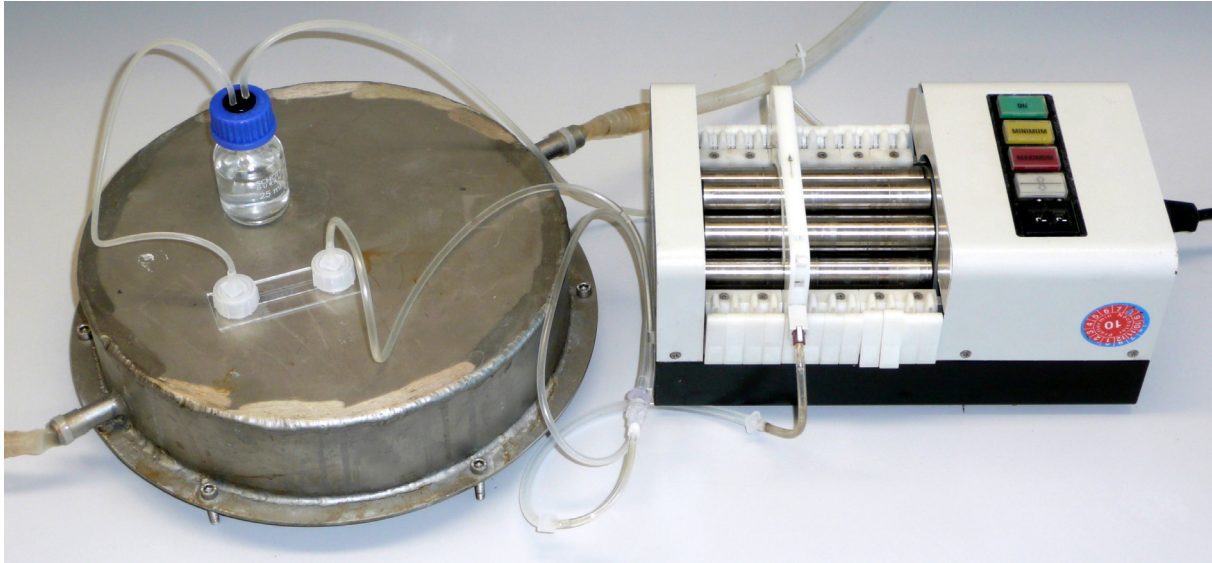
Figure II.3: Parallel plate apparatus

2.1.2   Stimulation with porcine pancreatic elastase

Porcine pancreatic elastase (Serva Electrophoresis GmbH) was diluted in a concentration of 1 mg/ml in Tris buffer (10 mM, pH 8.5). According to the manufacturer's information, 1 mg enzyme had an activity of 232 units. 1 unit is defined as the amount of enzyme that catalyzes the hydrolysis of 1 µmol N-acetyl-L-alanyl-L-alanyl-L-alanine methyl ester per minute at 25°C and pH 8.5. Confluent cells were rinsed twice with PBS+. Then Hank's balanced salt solution was added for 2 hours at 37°C (drying cabinet). Since Hank's solution does not contain FCS, and thus no growth factors, cells should synchronize their cell cycle during this time. Cells were stimulated with 0.5 U/ml of elastase, according to findings of Klarskov Mogensen [107]. Incubation time depended on the type of experiment (5, 10, 30 or 60 minutes). In cases where the cell supernatants were needed for further experiments, they were collected. Afterwards the cells were washed with PBS- and ice-cold lysis buffer was added (1 ml per 10 cm dish, 200 µl per 6 well).

Hank's balanced salt solution (pH 7.4)	
NaCl	8 g
KCl	0.4 g
$MgSO_4$ x 7 H_2O	0.13 g
$MgCl_2$ x 6 H_2O	0.07 g
$CaCl_2$ x 2 H_2O	0.13 g
Na_2HPO_4 x 2 H_2O	0.15 g
KH_2PO_4	0.06 g
Glucose x H_2O	0.06 g
$NaHCO_3$	0.3 g
in Aqua ad iniectabilia	ad 1,000 ml

2.1.3   Inhibition

Inhibition of elastase, integrin or MAPK activity was performed by applying the particular inhibitor (see Table II.1). In shear stress as well elastase treatment experiments, inhibitors were added to the culture dish 30 minutes prior to beginning the stimulation. The concentrations mentioned in Table II.1 were used.

Table II.1: Inhibitors

Inhibitor	Concentration	Target	Company
MeOSuc-Ala-Ala-Pro-Val-chloromethylketone	50 µM	Neutrophil elastase [180]	Bachem AG
Chymostatin	10 µg/ml	Serine and cysteine proteases chymotrypsin, chymase, cathepsin A, B, C, G, H, L, neutrophil and pancreatic elastase [171]	Sigma-Aldrich Inc.
Abciximab	1 µg/ml	Integrin $\alpha_v\beta_3$, platelet integrin $\alpha_{IIb}\beta_3$ (GpIIb/IIIA) [187]	Lilly
SB202190	10 µM	P38 MAPK	Upstate
U0126	10 µM	MEK1, MEK2	Calbiochem
SP600125	10 µM	JNK1, JNK2, JNK3	Calbiochem
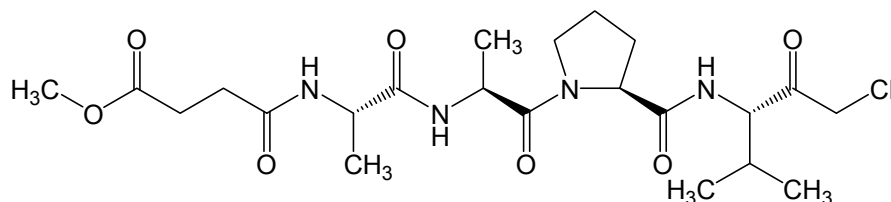
Figure II.4: MeOSuc-Ala-Ala-Pro-Val-chloromethylketone

2.2   CELL TRANSFECTION

2.2.1   Gene silencing by RNA interference

RNA interference (RNAi, RNA silencing), a natural process in eukaryotes, is a phenomenon that leads to post-transcriptional gene silencing. It is based on the fact that double-stranded RNA induces the suppression of specific genes that contain a complementary sequence. The mechanism of RNAi was discovered by Andrew Z. Fire and Craig F. Mello in Caenorhabditis elegans [61]. For this finding they received the Nobel Prize in Physiology or Medicine in 2006. Double-stranded RNA (dsRNA) is recognized and cleaved by the enzyme Dicer. The resulting small double-stranded RNAs, called small interfering RNAs (siRNA), are 21 to 23 base pairs in length and have a single stranded 3' overhang of 2 nucleotides on either end. The siRNA is integrated in the RNA-induced silencing complex (RISC), a riboprotein complex.

After that, the sense strand of the siRNA is eliminated and the now activated RISC is able to bind and cleave mRNA containing a complementary sequence.
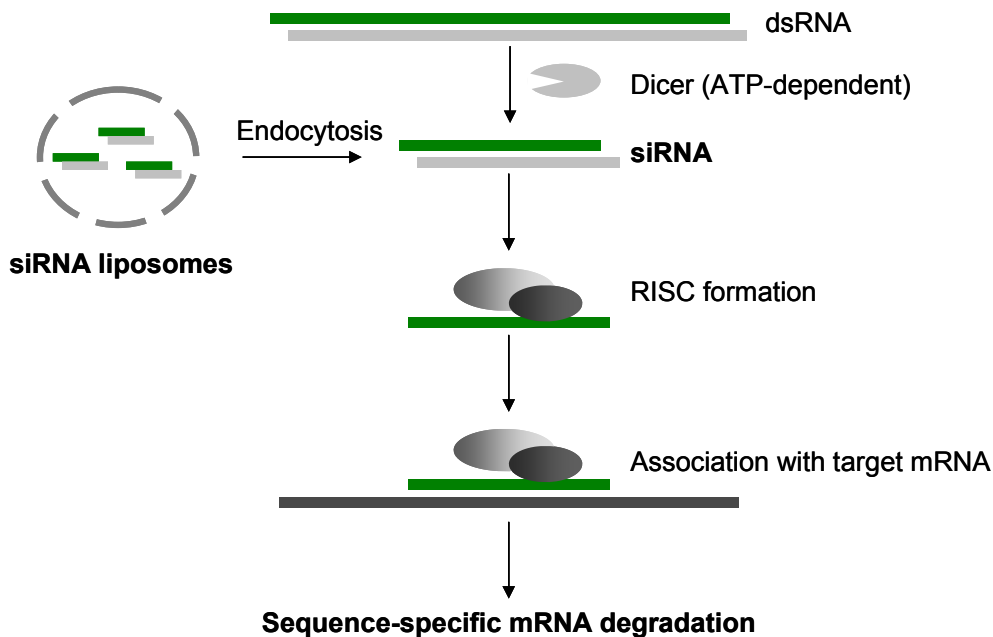
Figure II.5: RNA interference

SiRNA containing liposomes are able to cross the cell membrane. After incorporation into the RISC complex, the siRNA mediates target sequence specificity for subsequent mRNA cleavage.

2.2.1.1   Cell transfection with synthetic siRNA

To induce Hsp27 gene silencing, synthetic siRNA against porcine Hsp27 (Eurofins MWG GmbH) was transferred into PAEC using the HiPerFect Transfection Reagent from Qiagen. For this purpose, PAEC were seeded onto 6 well plates. After 8 hours and 50 to 80% cell confluency, siRNA at concentrations of 5, 20 or 50 nM plus the required amount of HiPerFect reagent were added. The reagent contains a lipid that enables an effective siRNA uptake. After 24 or 48 hours cells were lysed. Knockdown efficiency was controlled by analyzing the samples with western blot (see chapter II.2.6.3). Best Hsp27 downregulation was observed at siRNA concentrations of 20 nM and incubation times of 48 h. Therefore silencing experiments were always performed for 48 hours using 20 nM of Hsp27 and control siRNA.
To measure the changes in FGF-2 release induced by Hsp27 knockdown, cells were transfected and stimulated with elastase (see chapter II.2.1.2). Cell supernatants were collected for FGF-2 determination (see chapter II.2.3). To ensure Hsp27 protein downregulation cells were always lysed and analyzed via western blotting.

Table II.2: Sequences of Hsp27 and control siRNA

siRNA	Sequence	
Hsp27 siRNA	Sense	GGAUGAGCACGGCUUCAUU
	Antisense	AAUGAAGCCGUGCUCAUCC
Control siRNA	Sense	UUCUCCGAACGUGUCACGU
	Antisense	ACGUGACACGUUCGGAGAA

2.3   QUANTITATIVE FGF-2 DETERMINATION

The concentration of FGF-2 in the supernatant was measured using a sandwich ELISA kit for quantitative FGF-2 determination (Quantikine bFGF ELISA, provided by R&D Systems) according to the manufacturer's instructions. The absorbance was measured at 450 nm (reference wavelength 550 nm).

2.4   QUANTITATIVE ELASTASE DETERMINATION

Quantitative measurement of elastase activity in cell supernatants was performed using methoxysuccinyl-Ala-Ala-Pro-Val-p-nitroaniline (MeOSuc-Ala-Ala-Pro-Val-pNA, Bachem AG), a specific substrate for neutrophil and porcine pancreatic elastase [32,134]. The rate of enzymatic hydrolysis was monitored by the increase in absorbance due to the release of the yellow reaction product p-nitroaniline.

The substrate peptide was dissolved in 50% ethanol (20 µg/µl). A calibration curve was generated using porcine pancreatic elastase in 8 different concentrations (0, 0.072, 0.145, 0.290, 0.580, 1.160, 2.320, 4.640 U/ml). 50 µl of each sample and standard solution were pipetted into a 96 well plate. To each well 1 µl of the substrate solution was added. The plate was then incubated for 30 minutes at 37°C. The absorbance was measured at 405 nm (reference wavelength 620 nm) using an ELISA plate reader system (Infinite F200, Tecan).
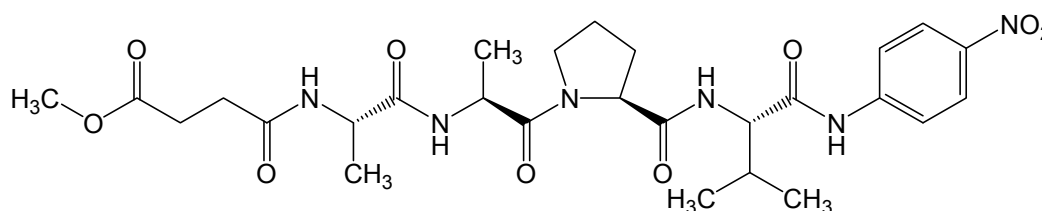
Figure II.6: MeOSuc-Ala-Ala-Pro-Val-pNA

2.5   QUANTITATIVE DETERMINATION OF VWF

The Imubind vWF ELISA kit (American Diagnostica Inc.) was used for quantification of vWF in cell supernatants. Since this assay did not recognize porcine vWF, it was performed

with supernatants from HUVEC according to the manufacturer's instructions. The absorbance was measured at 450 nm.

2.6   PROTEIN BIOCHEMISTRY

2.6.1   Sample preparation

Cells were rinsed with PBS+ and lysis buffer was added (1 ml per 10 cm dish, 200 µl per 6 well). After an incubation period of 10 minutes at 4°C, the lysed cells were scraped off the culture dish with a rubber policeman and transferred into a microcentrifuge tube. Soluble cell fragments were chopped and dissolved using an insulin syringe (BD MicroFine 0.30 x 8 mm 1 ml U-40, Becton Dickinson). Non-soluble fragments were removed by centrifugation at 15,000 x G at 4°C for 10 minutes. The supernatant was collected and, if not used right away, was stored at -20°C.

Lysis buffer (pH 7.4)		
Tris	20	mM
NaCl	137	mM
EDTA pH 8.0	2	mM
Glycerol	10	%
Sodium deoxylcholate	0.1	%
Aprotinin	10	µg/ml
Leupeptin	10	µg/ml
PMSF	1	mM
NaF	0.5	mM
Na_3VO_4	0.5	mM

Prior to each experiment, a stock solution of the lysis buffer was prepared. Sodium deoxylcholate was used as detergent. The inhibitors, namely aprotinin, leupeptin, phenylmethylsulfonyl fluoride (PMSF), sodium fluoride and sodium orthovanadate, were always freshly added to this buffer. Aprotinin acts as inhibitor of serine proteases, while leupeptin and PMSF additionally block cysteine proteases. Sodium fluoride inhibits phosphatases, while orthovanadate specifically inhibits tyrosine phosphatases.

Sodium orthovanadate needs to be activated before its usage. Therefore a 200 mM solution of Na_3VO_4 was adjusted to a pH of 10.0. The resulting yellow solution was boiled until colorless. After cooling the solution to room temperature, the pH was readjusted. Subsequently, the solution was boiled again. This procedure was repeated until the solution stayed uncolored at room temperature. Aliquots were stored at -20°C.

2.6.1.1   Isolation of the extracellular matrix

For ECM isolation cells were treated and stimulated as described above and lysed with a solution containing 0.1% Triton X-100, 0.1 M NH₄OH and 1 mM PMSF [18]. After 3 minutes of incubation, the lysed cell solution was collected. The ECM which was left on the culture dish was washed 4 times with PBS- and sample buffer (4x) was added. Subsequently, the ECM was scraped off the culture dish using a rubber policeman.

Cell dissolving buffer	
Triton X-100	0.1 %
NH₄OH	0.1 M
PMSF	1 mM

2.6.2   Protein quantification

To determine the quantitative amount of protein in the samples, the bicinchoninic acid assay (BCA™ Protein Assay Reagent A/B, Perbio) was performed. This method is based on the fact that under alkaline conditions bivalent cuprous ions react with proteins resulting in monovalent copper (biuret reaction). These reduced cuprous cations are able to react with two molecules of bicinchoninic acid producing a purple-colored end product. The amount of the resulting complex is proportional to the protein present.
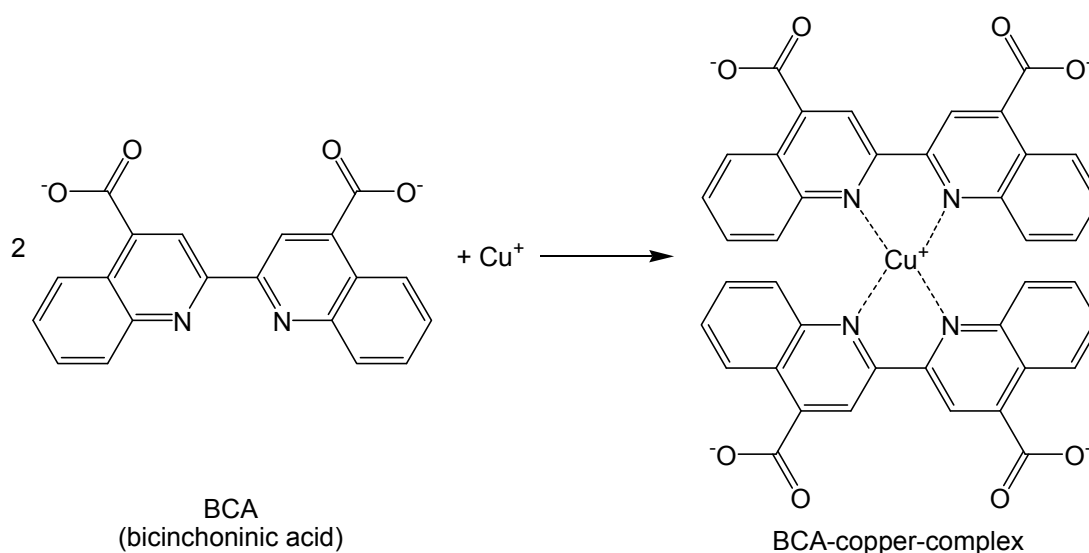
Figure II.7: The reaction of BCA with cupric ion

Reaction of two molecules BCA and one Cu⁺-ion forming a purple colored complex

To establish the calibration curve, a 0.2% solution of bovine serum albumin (BSA, 2 mg/ml) was used. According to the manufacturer's instructions, the protein standards as well as the samples were incubated for 30 minutes at 37°C with the BCA reagent in 96 well plates (Corning Incorporated). The calibration curve was measured in duplicate, every sample in triplicate. The absorbance of the emerging BCA-complex was determined at 550 nm.

2.6.3   Western blotting

2.6.3.1   One dimensional gel electrophoresis

The sodium dodecylsulfate-polyacrylamide gel electrophoresis (SDS-Page) is a method to separate proteins depending on their molecular mass in an electric field. For small gels the Mighty Small II SE 250/SE 260 mini vertical unit from Amersham Biosciences was used. Large gels were prepared with the SE 600 Series Electrophoresis Unit from Hoefer.

Depending on the size of the gel, 10 µg or 40 µg of protein were mixed in a 4:1 ratio with sample buffer (4x) and heated to a temperature of 95°C for 5 minutes. The sample buffer contains the anionic tenside sodium dodecylsulfate which destroys the secondary and tertiary protein structure and inhibits protein-protein interactions, causing the formation of negatively charged SDS-protein complexes with constant charge to mass ratios. This means that a negative charge is applied to each protein in proportion to its mass. Additionally, β-mercaptoethanol disrupts disulfide bonds. The denatured protein samples were applied onto a polyacrylamide gel containing a separating and a stacking gel part. This gel electrophoresis method refers to the discontinuous system of Laemmli [110].

Proteins move slower in gels with high percentages of acrylamide. Therefore the concentration of acrylamide in the separation gel was chosen depending on the molecular weight of the respective protein (see Table II.3). The stacking gel always contained 4% of acrylamide.

For gel polymerization, ammonium persulfate (APS) was needed as initiator for gel formation and N,N,N',N'-tetramethylethylenediamine (TEMED) was used as catalyst. After adding the electrophoresis buffer to the separation unit, voltage was applied (Power Pack P25, Biometra, voltage maximum capacity, current: 20–35 mA). Thus the negatively charged SDS-protein complexes migrate to the anode. Smaller proteins migrate faster than larger ones. To determine molecular masses, a molecular weight marker (PageRuler[TM] Prestained Protein Ladder, Fermentas) with colored proteins of a certain molecular mass was also added to the gel.

Sample buffer 4x

Tris (pH 6.8)	250	mM
SDS	8	%
Glycerin	40	%
Bromophenol blue	0.02	%
β-Mercaptoethanol	400	mM

Table II.3: Acrylamide concentrations in the separating gel

Protein	Separating gel concentration
FAK, fibronectin, laminin, vWF	7 %
ERK, ILK, JNK, p38, Shc, vitronectin	10 %
Elastase, Hsp27	12 %

Separating gel 12%

Acrylamide/Bis-Acrylamide 30%/0.8% (w/v)	40	%
Tris (pH 8.8)	375	mM
SDS	0.1	%
APS	0.05	%
TEMED	0.05	%

Stacking gel 4%

Acrylamide/Bis-Acrylamide 30%/0.8% (w/v)	13	%
Tris (pH 6.8)	125	mM
SDS	0.1	%
APS	0.05	%
TEMED	0.1	%

Electrophoresis buffer

Tris	124	mM
Glycin	960	mM
SDS	0.5	%

2.6.3.2   Semi-dry blotting

To transfer proteins from polyacrylamide gels to a nitrocellulose membrane, the semi-dry blotting method was performed. Therefore a self-made blotting unit was used. The membrane (Nitrocellulose Blotting Membran, Peqlab Biotechnologie GmbH) and two sheets of blotting paper (Gel Blotting Papier, Schleicher & Schuell BioScience GmbH) were trimmed to the size of the gel. The blotting unit as well as the membrane and the filter paper were moisturized with transfer buffer. Then the following setup was used:

Cathode

Soaked blotting paper
Gel
Membrane
Soaked blotting paper

Anode

A current was applied (voltage maximum capacity, current [mA]: area [cm²] x 0.8). Again, the negatively charged SDS-protein complexes move towards the positive pole. Thereby they migrate out of the gel into the membrane. Blotting time depended on the molecular weight of the protein and therefore varied from 1 to 3 hours. Next, the membrane was blocked for 1 hour under gentle agitation using 5% skimmed milk powder in TBS-Tween (TBS-T).

Transfer buffer		
Glycin	39	mM
Tris	48	mM
SDS	0.037	%
Methanol	10	%

TBS-T (pH 7.5)		
Tris	50	mM
NaCl	150	mM
Tween 20	0.1	%

2.6.3.3   Detection

The membrane was incubated with the respective antibody solution overnight at 4°C under gentle agitation. The antibody was either dissolved in TBS-T buffer with skimmed milk or albumin (BSA) using the dilution mentioned in Table II.4.

After removal of the first antibody, the membrane was washed 3 times for 5 minutes with TBS-T buffer. Then the horseradish peroxidase-labeled secondary antibody was added. The membrane was incubated for 1.5 hours at room temperature under gentle agitation.

After again washing 3 times for 5 minutes, the protein was detected using a Chemiluminescence Detection Kit for Horseradish Peroxidase (AppliChem GmbH), which is a luminol-based substrate. This kit includes two solutions, one containing luminol the other stable peroxide. These two were mixed in a 1:1 ratio. When incubating the blot with the mixture, the enzyme horseradish peroxidase catalyzes the decomposition of hydrogen peroxide. Luminol oxidation creates an exitated state, releasing photons of light when decaying to ground state. The appearing luminescence was visualized with the Digital CCD Camera from Hamamatsu Photonics, connected to a computer equipped with the Wasabi imaging software (Hamamatsu Photonics).

Table II.4: Primary antibodies for western blotting

Antigen	MW [kDa]	Isotype	Dilution	Provider and product number
FAK	125	Mouse monoclonal IgG$_1$	1:200 3% milk powder	Santa Cruz sc-1688
Fibronectin	220	Rabbit polyclonal Ig fraction of antiserum	1:200 5% BSA	Dako A0245
GAPDH	36	Mouse monoclonal IgG$_1$	1:1,000 5% BSA	Chemicon MAB374
Hsp27	27	Rabbit polyclonal IgG	1 :1,000 3% milk powder	Upstate 06-478
Laminin	~ 200/400	Rabbit polyclonal	1:1,000 5% BSA	Sigma-Aldrich Inc. L9393
Neutrophil elastase (antibody No.1)	29	Mouse monoclonal IgG$_1$	1:200 3% milk powder	Santa Cruz sc-53388
Neutrophil elastase (antibody No. 2)	29	Mouse monoclonal IgM	1:200 3% milk powder	Santa Cruz sc-59335
P38 MAPK	38	Rabbit monoclonal IgG	1:1,000 5% BSA	Cell Signaling 9212
Pancreatic elastase	28	Rabbit IgG	1:1,000 3% milk powder	Rockland 200-4168
Phospho-FAK (Tyr397)	125	Rabbit polyclonal IgG	1:1,000 5% BSA	Calbiochem 341292
Phospho-FAK (Tyr576/577)	125	Rabbit polyclonal	1:1,000 5% BSA	Cell Signaling 3281
Phospho-FAK (Tyr925)	125	Rabbit polyclonal	1:1,000 5% BSA	Cell Signaling 3284
Phospho-Hsp27 (Ser82)	27	Rabbit polyclonal	1 :1,000 5% BSA	Cell Signaling 2401
Phospho-p38 MAPK (Thr180/Tyr182)	38	Rabbit monoclonal IgG	1:1,000 5% BSA	Cell Signaling 9215
Phospho-p44/42 MAPK (Thr202/Tyr204)	42/44	Mouse monoclonal IgG$_1$	1:2,000 5% BSA	Cell Signaling 9106
Phospho-SAPK/JNK (Thr183/Tyr185)	46/54	Rabbit monoclonal IgG	1 :1,000 5% BSA	Cell Signaling 4671
Shc	46/52/66	Rabbit polyclonal IgG	1:1,000 3% milk powder	Upstate 06-203
β-tubulin	55	Mouse monoclonal IgG$_1$	1:10,000 5% BSA	Sigma-Aldrich Inc. T4026
Vitronectin	65/75	Rabbit polyclonal IgG	1:200 5% BSA	Santa Cruz sc-15332
vWF	270	Rabbit, IgG fraction of antiserum	1:100 5% BSA	Sigma-Aldrich Inc. F3520

Table II.5: Secondary antibodies for western blotting

Antibody	Dilution	Provider
Goat anti-rabbit IgG, HRP conjugate	1:5,000 in 5% milk powder	Calbiochem
Goat anti-mouse IgG, HRP conjugate	1:5,000 in 5% milk powder	Calbiochem
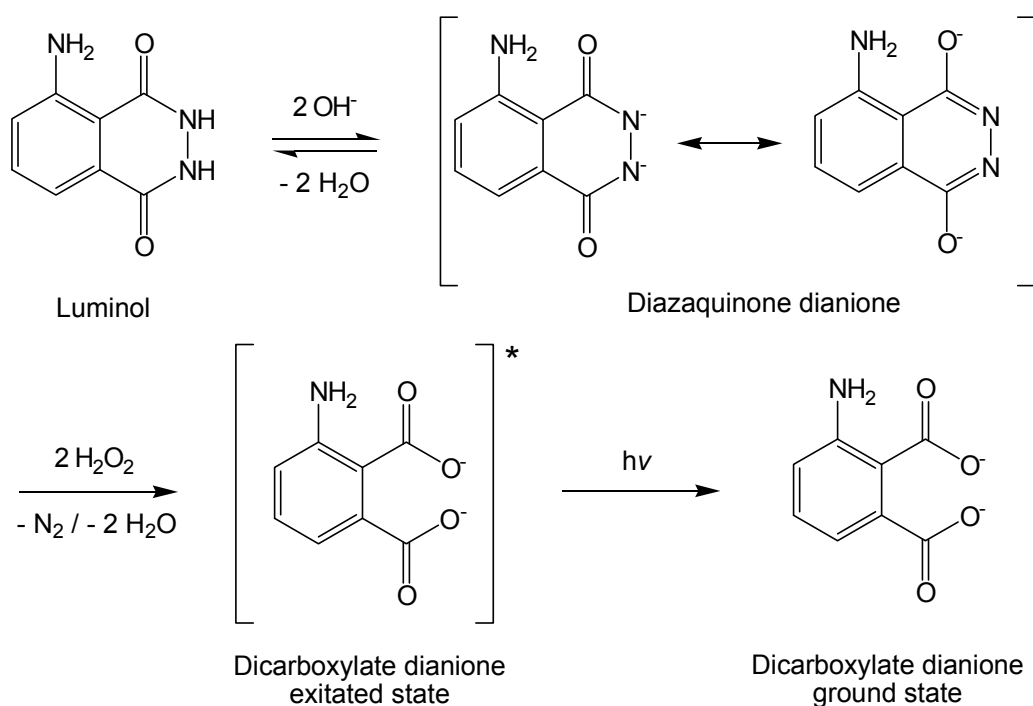
Figure II.8: Luminol chemiluminescence reaction

2.6.3.4   Membrane stripping

The removal of primary and secondary antibodies from a western blot membrane is called stripping. When using one membrane for more than one antigen detection, it is useful to remove the already bound interfering antibodies. For this purpose, the membrane was incubated for 1 hour at room temperature with the stripping solution mentioned below.

Stripping buffer (pH 2.8)	
Glycine	0.2 M
NaCl	0.5 M

2.6.4   Unspecific protein detection

Coomassie brilliant blue stains proteins because it accumulates at their basic side chains. This method was used to investigate the degradation properties of elastase on different extracellular matrix proteins (see Table II.6).

The extracellular matrix proteins mentioned in the table below were incubated for 1 hour at 37°C with 0.5 or 2.5 U/ml of porcine pancreatic elastase. Next, a SDS-Page as described in chapter II.2.6.3.1 was performed. Therefore 90 µl of each solution were mixed with 30 µl of the sample buffer. The polyacrylamide gel was incubated with the Coomassie staining

solution under agitation overnight. The following day, the gel was destained with a solution of 10% acetic acid. After around 4 hours blue protein bands were observed.

Coomassie staining solution	
Coomassie brilliant blue	0.7 mM
Acetic acid	10 %
2-Propanol	25 %

Table II.6: Extracellular matrix proteins

ECM protein	Source	Concentration used	Provider
Bovine collagen G (consists mainly of collagen I)	Bovine calf skin	300 µg/ml	Biochrom AG
Human collagen, type IV	Human placenta	300 µg/ml	BD Biosciences
Human fibronectin	Human plasma	1 mg/ml	Harbor Bio-Products
Mouse laminin (laminin-1)	Engelbreth-Holm-Swarm tumors	300 µg/ml	Harbor Bio-Products
Human vitronectin	Human plasma	100 µg/ml	R&D Systems

Table II.7: Expected size of uncleaved extracellular matrix proteins

ECM protein	Composition/Expected bands in SDS-Page
Collagen type I	α1 chain ~ 139 kDa, α2 chain ~ 129 kDa dimer ~ 290 kDa, trimer ~ 400 kDa
Collagen type IV	α1 chain ~ 185 kDa, α2 chain ~ 170 kDa additional band at 160 kDa
Fibronectin	220 kDa monomer
Laminin	α chain ~ 400 kDa β chain ~ 230 kDa, γ chain ~ 220 kDa
Vitronectin	Monomeric glycoprotein detected as a mixture of 65 kDa and 75 kDa polypeptides

2.6.5   Immunoprecipitation

Immunoprecipitation is a technique to isolate a particular protein out of a solution by using a specific antibody. The sample volume equivalent to 150 µg of protein was incubated for 2 hours at 4°C with 5 µg antibody and 100 µl Protein G Beads (µMACS^{TM} Protein G MicroBeads, Miltenyi Biotec). The tubes were gently agitated. Thereby a protein-antibody-beads-complex is formed.

Immunoprecipitation was performed using a magnetic separation unit (µMACS Separator) and the corresponding columns (µ Columns) from Miltenyi Biotec. The samples were added to the columns. The magnetic beads and all bound molecules stick to the column, whereas the residual sample flows through. Subsequently, the columns were rinsed 4 times with 200 µl of lysis buffer. To detach the precipitates from the microbeads, 20 µl of sample buffer, which

was heated to 95°C, was added and collected after passing the column. Then a SDS-Page and a western blot were performed corresponding to chapter II.2.6.3.

To ensure equal protein loading, a part of each cell lysate used for immunoprecipitation experiments was separately analyzed in western blots using the particular detection antibody.

Table II.8: Precipitation antibodies for immunoprecipitation

Antigen	Isotype	Provider and product number
FGF-2	Mouse monoclonal IgG$_{1\kappa}$	Upstate, 05-118
Integrin $\alpha_v\beta_3$	Mouse monoclonal IgG$_1$	Chemicon, MAB1976

2.6.6   Enzyme-linked immunosorbent assay

Similar to a western blot, an enzyme-linked immunosorbent assay (ELISA) is an immunological technique to specifically detect antigens. It is performed in 96 well plates using specific antibodies and an enzymatic reaction for detection.

To determine the protein-protein interaction of Hsp27 and FGF-2, a double sandwich ELISA mixing two commercially available ELISA kits one for Hsp27 (PathScan phospho-Hsp27 (Ser78) Sandwich ELISA Kit, Cell Signaling), the other for the detection of FGF-2 (Quantikine bFGF ELISA, R&D Systems), was developed. Firstly, 100 µl of each cell lysate and 100 µl of the sample diluent (PathScan) were mixed and vortexed. Then 100 µl of this solution were added to a multiwell plate (PathScan), which was pre-coated with a Hsp27 antibody by the manufacturer, and incubated for 2 hours at 37°C. The fluid in the plate was then discarded and the wells were washed 4 times with 200 µl of wash buffer (PathScan). Subsequently, 200 µl of a FGF-2 antibody conjugated with horse radish peroxidase (Quantikine) were added and incubated for 2 hours at room temperature. The washing procedure was then repeated using the Quantikine wash buffer. Next, 200 µl of the substrate solution, an equal mixture of solution A (hydrogen peroxide) and B (3,3',5,5'-tetramethylbenzidine), were added and the plate was incubated for 30 minutes in the dark. At last 50 µl of the stop solution (1 M sulfuric acid) were added. The absorbance was measured at 450 nm (reference wavelength 550 nm).
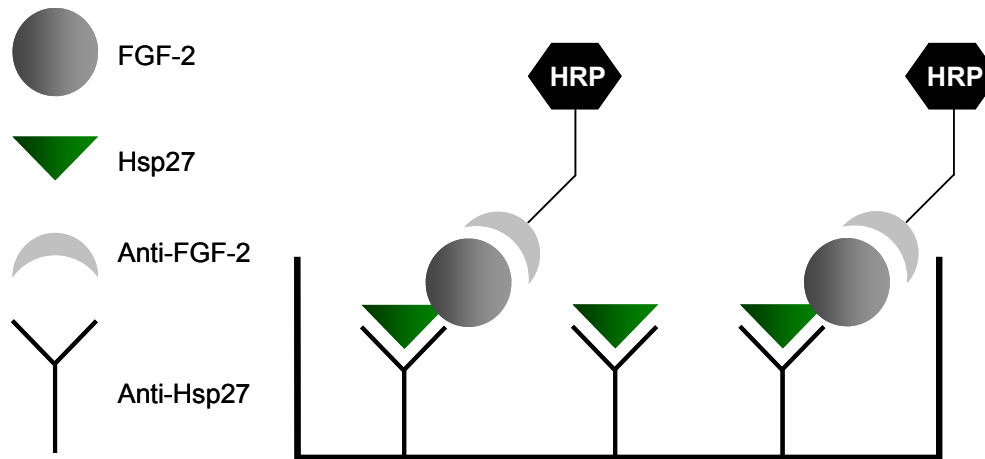
Figure II.9: Illustration of the self-made Hsp27-FGF-2 ELISA

Self-made Hsp27-FGF-2 ELISA: Firstly, Hsp27 was bound to the microwell plate coated with an Hsp27 antibody. Secondly, FGF-2 was detected by using an FGF-2 antibody conjugated with horse radish peroxidase (HRP).

2.7   MICROSCOPY

2.7.1   Fluorescence microscopy

Fluorescence microscopy is an effective method for the subcellular localization of fluorescently labeled proteins. Fluorescence is the property of molecules or chemical groups, called fluorophores, to absorb high-energy short-wavelength light and emit low-energy long-wavelength light. Antibodies labeled with fluorescent dyes, e.g. from the Alexa Fluor family, are used in fluorescence microscopy. These molecules differ in their excitation and emission wavelength and therefore allow multicolor detection. A fluorescence microscope usually consists of a light source, in most cases a high pressure mercury lamp, an excitation filter, a dichroic beam-splitter, an emission filter, a detector and a camera. An optimal separation of the excitation light and the fluorescence emission emanating from the sample is a basic requirement of the microscopes optical system. The inverted microscope Axiovert 200M or the upright microscope Axiophot (Carl Zeiss) was used to perform fluorescence microscopy.

2.7.2   Confocal laser scanning microscopy

A confocal laser scanning microscope is equipped with a confocal pinhole that eliminates out-of-focus light. Thus a much higher resolution can be obtained. The laser beam is focused to a point and scanned across the sample. A photomultiplier tube (PMT) detects the emitted fluorescence. In this study a Leica TCS SP5 (Leica Microsystems) microscope equipped with an argon (488 nm) and two helium-neon lasers (543 nm, 633 nm) was used.
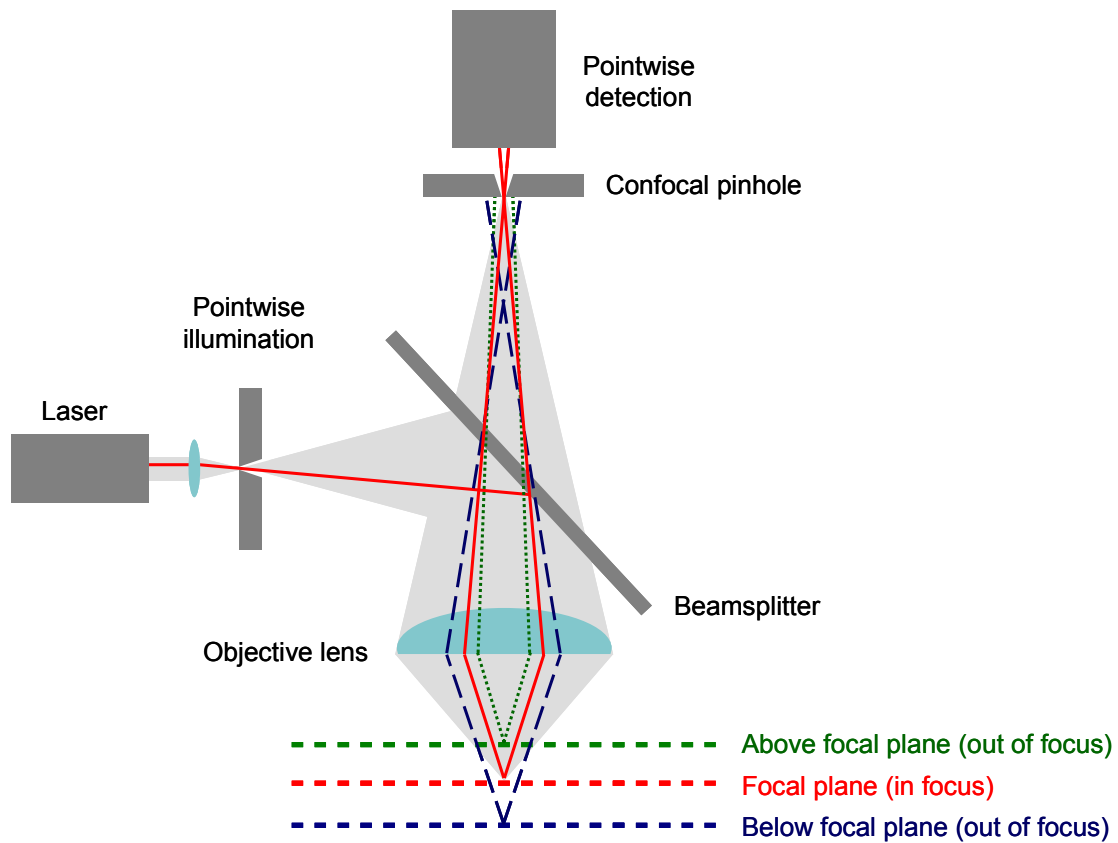
Figure II.10: Confocal scanning laser microscope

The light pathway of a confocal scanning laser microscope: Line-by-line scanning by a focused laser beam and pixel-by-pixel detection using a photomultiplier tube (PMT).

2.7.3   Fluorescence staining

Unless stated otherwise, glass coverslips (Ø 13 mm) were coated with collagen G (10 µg/ml), while incubating them for 30 minutes at 4°C followed by 30 minutes at 37°C. Some additional experiments were performed using fibronectin coating (10 µg/ml). PAEC were seeded onto these coverslips that were placed in 24 well plates. After 24 hours and at 100% confluency, cells were stimulated with shear stress or porcine pancreatic elastase as described in chapter II.2.1.1.2 and II.2.1.2. Subsequently, cells were washed with PBS+ and fixed with 3.7% formaldehyde in PBS+ for 10 minutes followed by another wash step. Cell permeabilization with 0.3% Triton X-100 in PBS+ was performed for 3 minutes. Then cells were washed 3 times and 1% BSA in PBS+ was added to block unspecific protein binding sites. After an incubation period of 30 minutes, the primary antibody solution was added and left there overnight at 4°C. The next day, the fixed cells were washed at least 3 times. Following, the secondary antibody was added and incubated for 30 minutes in the dark. Finally, the coverslips were removed with tweezers and were transferred upside-down on a drop of Mounting Medium (Shandon Immu-Mount, Thermo Scientific) onto an object holder. Coverslips were sealed with transparent nail polish. Microscopy was performed by using either the confocal laser scanning microscope Leica TCS SP5 (Leica Microsystems,

objectives: 40x NA 1.25; 63er NA 1.4 oil) or one of two fluorescence microscopes (Axiovert 200M (Carl Zeiss), objective: 63x NA 1.2 oil or Axiophot (Carl Zeiss), objective: 100x NA 1.3 oil). The appropriate objective, resolution and distance between two optical slices (z-step size) are indicated in the figure legend.

Table II.9: Primary antibodies for immunofluorescence

Antigen	Isotype	Dilution	Provider and product number
Collagen type IV	Rabbit polyclonal IgG	1:400 in 1% BSA	Abcam ab19808
FAK	Rabbit polyclonal IgG	1:100 in 1% BSA	Santa Cruz sc-558
Fibronectin	Rabbit polyclonal Ig fraction of antiserum	1:200 in 1% BSA	Dako A0245
ILK	Mouse monoclonal IgG$_{2b}$	1:100 in 1% BSA	Santa Cruz sc-20019
Laminin	Rabbit polyclonal	1:50 in 1% BSA	Sigma-Aldrich Inc. L9393
LAMP1	Rabbit polyclonal	1:100 in 1% BSA	Sigma-Aldrich Inc. L1418
Neutrophil elastase	Mouse monoclonal IgM	1:50 in 1% BSA	Santa Cruz sc-59335
Vitronectin	Rabbit polyclonal IgG	1:50 in 1% BSA	Santa Cruz sc-15332
vWF	Rabbit, IgG fraction of antiserum	1:100 in 1% BSA	Sigma-Aldrich Inc. F3520

Table II.10: Other fluorescent molecules

Fluorescent dye	Dilution	Provider
Alexa Fluor 488 phalloidin	1:40 in PBS+, 1% BSA	Molecular Probes Inc.
DAPI	1:2,000 in PBS+, 1% BSA	Invitrogen

Table II.11: Secondary antibodies for immunofluorescence

Antibody	Dilution	Provider
Alexa Fluor 488 chicken-anti-mouse IgG	1:200 in PBS+, 1% BSA	Invitrogen
Alexa Fluor 546 goat-anti-rabbit IgG	1:200 in PBS+, 1% BSA	Invitrogen

2.7.4   Electron microscopy

PAEC were dissolved using accutase and fixed in a mixture of 0.1% glutaraldehyde and 4% formaldehyde, which was freshly prepared from paraformaldehyde (in Sorensen's buffer). All further steps were performed by our collaboration partners at the Institute of Anatomy (Ludwig-Maximilians-Universität, Munich). Cells were embedded in Lowicryl (Polysciences

Inc.). Using an ultramicrotome (Ultracut E Microtome, Reichert-Jung), ultrathin sections of 90 nm were cut and collected in nickel grids. The grids were left to dry overnight. The next day, sections were washed with water, rinsed with PBS- and incubated with glycine (50 mM) for 20 minutes. The grids were then washed 3 times for 5 minutes each with PBS- and incubated in blocking solution for 30 minutes at room temperature (Blocking solution for goat-gold conjugates, Aurion). After shortly rinsing the section with PBS- containing 1% BSA-c (acetylated bovine serum albumin from Aurion), they were either incubated with a mixture of the anti-elastase and anti-vWF antibody or with buffer at room temperature overnight. Then, the grids were washed with PBS- BSA-c, incubated with secondary antibodies and washed again with PBS-. 2% glutaraldehyde was added for 10 minutes. After rinsing the grids in a drop PBS- and subsequently washing them 3 times with water, they were stained with uranyl acetate for 20 minutes and rinsed with water. The grids were examined in a Philips CM-10 Transmission Electron Microscope (Philips).

Sorensen's buffer (ph 7.4)	
KH_2PO_4 (15 M/l)	18.2 ml
Na_2HPO_4 (30 M/l)	81.8 ml

Table II.12: Primary antibodies for electron microscopy

Antigen	Isotype	Dilution	Provider and product number
Neutrophil elastase	Mouse monoclonal IgM	1:100	Santa Cruz sc-59335
vWF	Rabbit, IgG fraction of antiserum	1:200	Sigma-Aldrich Inc. F3520

Table II.13: Seconary antibodies for electron microscopy

Antibody	Dilution	Provider
Gold-labeled (6 nm)-goat-anti-mouse	1:40	Aurion
Gold-labeled (10 nm)-goat-anti-rabbit	1:40	Aurion

2.8 FLOW CYTOMETRY

Flow cytometry is a widely used method for the quantitative analysis of cell properties, which are relative cell size, granularity and fluorescence intensity. This technology can be used for a range of applications such as cell counting, cell cycle analysis, determination of cell viability and apoptosis or analysis of protein expression and localization. A flow cytometer consists of the following components: a fluidics system, an optical system, an electronic system and a computer. A cell sorter (FACS – fluorescence activated cell sorting) additionally separates the cells, based on their specific scattering and fluorescent characteristics.

In flow cytometry, the cells are injected into the center of a sheath flow, hydrodynamically focused and single cells are delivered to the laser beam. Forward and side scatter as well as fluorescence intensities at several wavelengths of each cell can be rapidly, simultaneously measured. The low angle forward scatter intensity is approximately proportional to the cell diameter while the orthogonal (90°) scatter intensity is roughly proportional to the degree of complexity and the amount of granular structures within the cell.
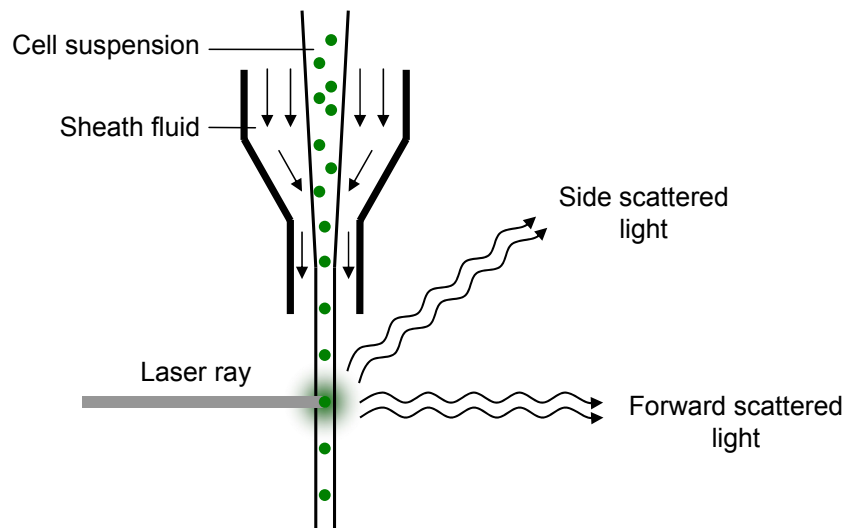
Figure II.11: Flow cytometry – hydrodynamic focusing and light scatter

Different cell types vary in their surface molecules, which are classified in the clusters of differentiation (CD) nomenclature. The analysis of expression patterns of CD molecules is the basis of cell immunophenotyping by flow cytometry. For this, fluorochrome-labeled antibodies are used. Common fluorescent dyes include fluorescein isothiocyanate (FITC), AlexaFluor 488, green fluorescent protein (GFP) or phycoerythrin (PE).

The phenotyping of PAEC and HUVEC was performed using the BD FACSort from Becton Dickinson equipped with one 488 nm laser which is able to measure three colors simultaneously. The cytometer was connected to a computer, where data was analyzed with the CellQuest software (Becton Dickinson). Sheath fluid (BD FACSFlow^TM), cleaning (BD FACSClean Solution) and rinsing solution (BD FACSRinse Solution) were also provided by Becton Dickinson.

2.8.1 CD31 expression

Platelet endothelial cell adhesion molecule (PECAM-1/CD31), an endothelial cell surface marker protein, was used to determine the purity of the primary endothelial cell cultures. For this purpose, confluent cells were rinsed with PBS- and 1 ml of accutase was added per 10 cm

dish to induce cell detachment and separation in single cells. The enzymatic reaction was stopped by adding 3 ml of FCS-containing medium. The cell solution was centrifuged and the supernatant discarded. Afterwards, the cell pellet was dissolved in 1 ml PBS+ containing 10% FCS and 1% sodium azide. Cells were counted and each tube was filled with 1 million cells. The samples were centrifuged and the supernatants were discarded. One tube was incubated with the CD31-PE-labeled antibody, another with the isotype control antibody (mouse IgG_1 PE, Becton Dickinson). After an incubation period of 1 hour at 4°C, cells were centrifuged and washed 3 times with PBS+, 10% FCS, 1% NaN_3. Subsequently, the cells were analyzed by flow cytometry.

Table II.14: CD31 antibodies for flow cytometry

Antigen	Isotype	Dilution	Provider and product number
Porcine CD31 PE	Mouse monoclonal IgG_1	1:200 PBS+, 3% BSA	AbD Serotec MCA1746PE
Human CD31 PE	Mouse $IgG_{1κ}$	1:33 PBS+, 3% BSA	BD Pharmingen 555446

2.8.2   Release of vWF

To examine whether shear stress induces the release of vWF indicating the exocytosis of Weibel-Palade bodies, the amount of vWF inside the cells was analyzed by flow cytometry. Less intracellular vWF staining would be an indication for the release of this protein. After shear stress treatment (see chapter II.2.1.1), cells were detached as described in chapter II.2.8.1. They were fixed with 0.5% formaldehyde for 15 minutes, permeabilized with 0.5% saponin for 20 minutes and washed with PBS containing 10% FCS and 1% sodium azide. Then the vWF antibody or the isotype control (mouse IgG_1, BD Pharmingen) was added and incubated at 4°C for 60 minutes. Again, the cells were washed and incubated with the secondary antibody (anti-mouse PE, BD Pharmingen) for 30 minutes. After repeating the washing procedure for 3 times, the samples were measured. Saponin was constantly present during antibody incubations and washes, with exception to the last wash step.

Table II.15: vWF antibody for flow cytometry

Antigen	Isotype	Dilution	Provider and product number
Human vWF	Mouse monoclonal $IgG_{1κ}$	1:20 in PBS+, 3% BSA	Dako M0616

2.9   POLYMERASE CHAIN REACTION

The invention of the polymerase chain reaction (PCR) was a revolution in molecular biology. PCR is a technique that allows the amplification of specific regions of a DNA strand. In 1993, Kary B. Mullis received the Nobel Prize in Chemistry for investigating the PCR [132].

Every PCR involves three major steps. The sequence of these steps is called cycle and is repeated around 20 to 40 times. Every cycle consists of the DNA denaturation, the primer hybridization and the synthesis of new double-strands by a DNA polymerase. Denaturation of DNA at temperatures of 94°C melts the DNA to single strands. Afterwards a temperature of around 50 to 65°C is used to allow primers to bind at their complementary sequence, the so called annealing. Primers are short oligonucleotides that serve as starting point for DNA replication. In the final elongation step the polymerase synthesizes the complementary strand by adding dNTPs (deoxynucleoside triphosphates), using the existing single strand as template.
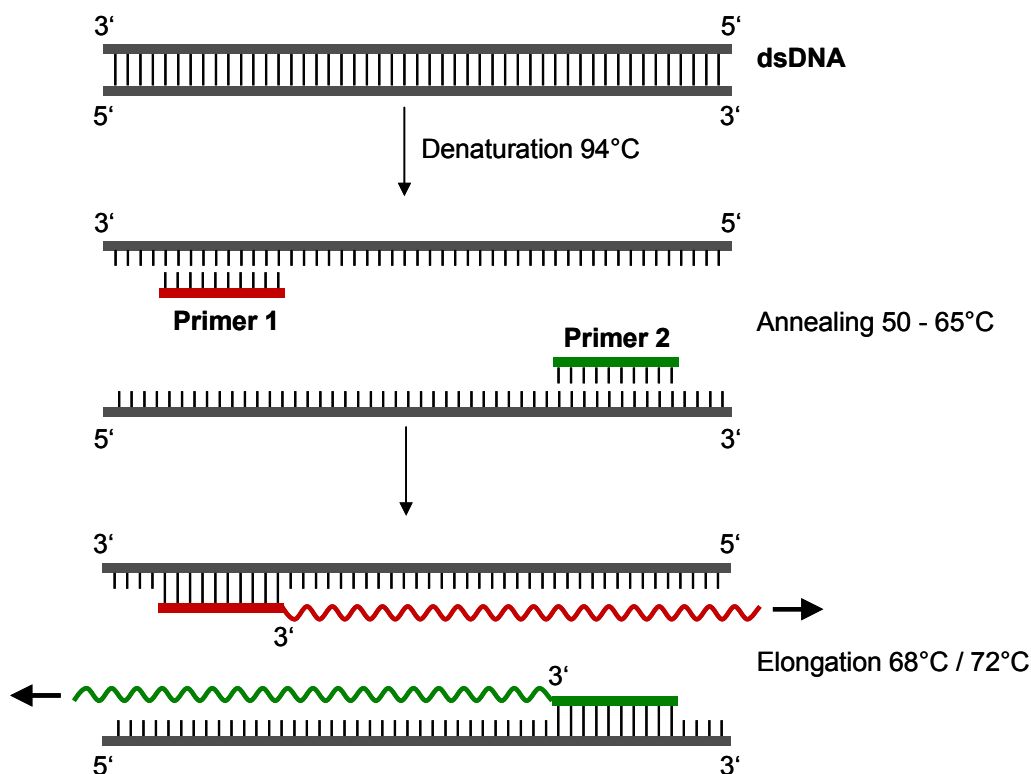
Figure II.12: Polymerase chain reaction

DNA-dependent DNA polymerases can only act on DNA templates. To investigate gene transcription, this means RNA analysis, the enzyme reverse transcriptase, which transcribes single-stranded RNA into complementary DNA (cDNA), is used. This reverse transcription followed by a PCR is called reverse transcription-PCR (RT-PCR).

2.9.1   Isolation of mRNA

RNA isolation is the first step when performing RT-PCR. For this, the RNeasy Mini Kit from Qiagen was used. For cell lysis, a denaturing guanidine thiocyanate buffer containing ß-Mercaptoethanol, which additionally inactivates RNases, was used. Afterwards, the cell lysate was chopped using QIAShredder columns, which were provided by Qiagen as well. By adding ethanol, the RNA was precipitated and bound onto silica-based membrane columns. After several different washing steps, the RNA was eluted using RNase free water.

2.9.2   RT-PCR

For RT-PCR the Titan One Tube RT-PCR Kit from Roche was used. Primers were designed with the Primer 3 software [167] and obtained from Eurofins MWG GmbH with the exception of the primers for ELANE Homo sapiens, which were obtained from Biomers.net. The manufacturer's instructions were followed. The respective protocol including the single steps and the temperature profile is listed in Table II.17. Thermocycling was performed using a Mastercycler ep gradient S from Eppendorf. Additionally, all samples were analyzed for β-actin as internal control. RT-PCR products were separated and detected via agarose gel electrophoresis.

Table II.16: Primers used for RT-PCR (HSA: Homo sapiens, SSC: Sus scrofa, AT: Annealing temp.)

Primer	Sequence		AT [°C]	Product length [bp]
ELANE [HSA]	Forward Reverse	CGTAAACTTGCTCAAACGACATC CCCTCACGAGAGTGCAGACGTT	56	241
ELA1 [HSA]	Forward Reverse	GCTATGTCCAGCTGGGTGTT AGCAGAGACCTGGGTGAAGA	55	364
ELA2A/B [HSA]	Forward Reverse	CCCTGCAGTACAGCTCCAAT CTGGAGCAGGTGGCATAGTC	56	429
ELA3A/B [HSA]	Forward Reverse	GACCTACCAGGTGGTGTTGG GGCTTGCTATGGTCTCCTCA	56	571
ELANE [SSC]	Forward Reverse	CAGCCTCTCCACCAATGAAC CATTGCAGCTGGAAATGATG	53	376
ELS1 [SSC]	Forward Reverse	AACCTGAACCAGAACGATGG ATCACCCTGACATCCAGAGC	53	380
β-actin	Forward Reverse	CCAAGGCCAACCGCGAGAAGATGAC AGGGTACATGGTGGTGCCGCCAGAC	53-56	586

Table II.17: RT-PCR protocol

Step	Time	Temperature	Cycles
Reverse transcription	30 min	50°C	
Denature template	2 min	94°C	
Denaturation Annealing Elongation	30 s 30 s 45 s	94°C see Table II.16 68°C	10 x
Denaturation Annealing Elongation	30 s 30 s 45 s (+ 5 s per cycle)	94°C see Table II.16 68°C	25 x
Prolonged elongation	7 min	68°C	

2.9.3   Real time RT-PCR

Real time RT-PCR allows the quantitative determination of RNA expression. It was performed using a Light Cycler 1.5 (Roche) and the QuantiTect SYBR Green RT-PCR Kit (Qiagen) according to the manufacturer's instructions. SYBR Green I binds double-stranded DNA molecules. The fluorescence of the emerging complex was quantified at the end of elongation time. Cycling conditions as mentioned in Table II.19 were used. The results were normalized to 18S rRNA as endogenous reference gene.

Table II.18: Primers used for real time RT-PCR (SSC: Sus scrofa)

Primer	Sequence		Product length [bp]
FGF-2 [SSC]	Forward Reverse	TCAAAGGAGTGTGTGCGAAC CAGGGCCACATACCAACTG	161
18S rRNA	Forward Reverse	TCAAGAACGAAAGTCGGAGG GGACATCTAAGGGCATCACA	488

Table II.19: Real time RT-PCR protocol

Step	Time	Temperature
Reverse transcription	20 min	50°C
PCR initial activation step	15 min	95°C
Cycling Denaturation Annealing Elongation Data acquisition	 15 s 30 or 50 s 30 s 5 s	 94°C 60°C 72°C 77°C (FGF-2), 81°C (18S rRNA)

2.9.4   Agarose gel electrophoresis

A mixture of 1% agarose in TBE buffer was boiled in a microwave oven until the agarose was dissolved. The solution was left to cool down to approximately 40 to 50°C. After the addition of ethidium bromide (0.05 μg/ml), the solution was transferred to the electrophoresis unit (Peqlab Biotechnologie GmbH). After gel polymerization, TBE electrophoresis buffer containing additional ethidium bromide was added. The DNA marker (2Log DNA Ladder, New England Biolabs) and the samples containing sample buffer in a 1:6 ratio were loaded onto the gel. Electrophoresis was performed at 100 mA using a Phero-Stab 0310 power supply from Biotec-Fischer. The fluorescence of the PCR products intercalated with ethidium bromide was documented with a Gel Doc 1000 station from Bio-Rad.

TBE buffer (pH 8.3)		
Tris	89	mM
Boric acid	89	mM
EDTA	2.5	mM

Sample buffer 6x		
Tris (pH 7.6)	10	mM
Bromophenol blue	0.03	%
Xylene cyanol	0.03	%
Glycerol	60	%
EDTA	60	mM

3   STATISTICS

Every experiment was performed at least three times. Data are expressed as mean values ± SEM. Statistical tests were performed using SigmaStat version 2.03 statistic software (SPSS Inc.). To compare two samples, the paired t-test was used. For the comparison of more than two samples, one-way analysis of variance for repeated measures (ANOVA RM) followed by the Student-Newman-Keuls test was applied. In cases where data were not normally distributed the ANOVA on ranks was used for statistical testing. The test that was used is indicated in the respective figure legend. P-values less than 0.05 were considered significant.

RESULTS

III RESULTS

1   CELL CHARACTERIZATION

1.1   CD31 STAINING OF PAEC AND HUVEC

CD31 (PECAM-1) cell surface staining of PAEC and HUVEC was performed to monitor the purity of the endothelial cell populations. For this purpose, cells of passage II were analyzed by flow cytometry. In PAEC cultures 96% of the cells were positive for CD31 (mean fluorescence intensity: isotype 25.6 vs. CD31 229.3), indicating that less than 4% of these cells were negative for CD31, as smooth muscle cells are. In HUVEC cultures 97% of the cells were CD31-positive (mean fluorescence intensity: isotype: 14.9 vs. CD31 280.2) (Figure III.1).
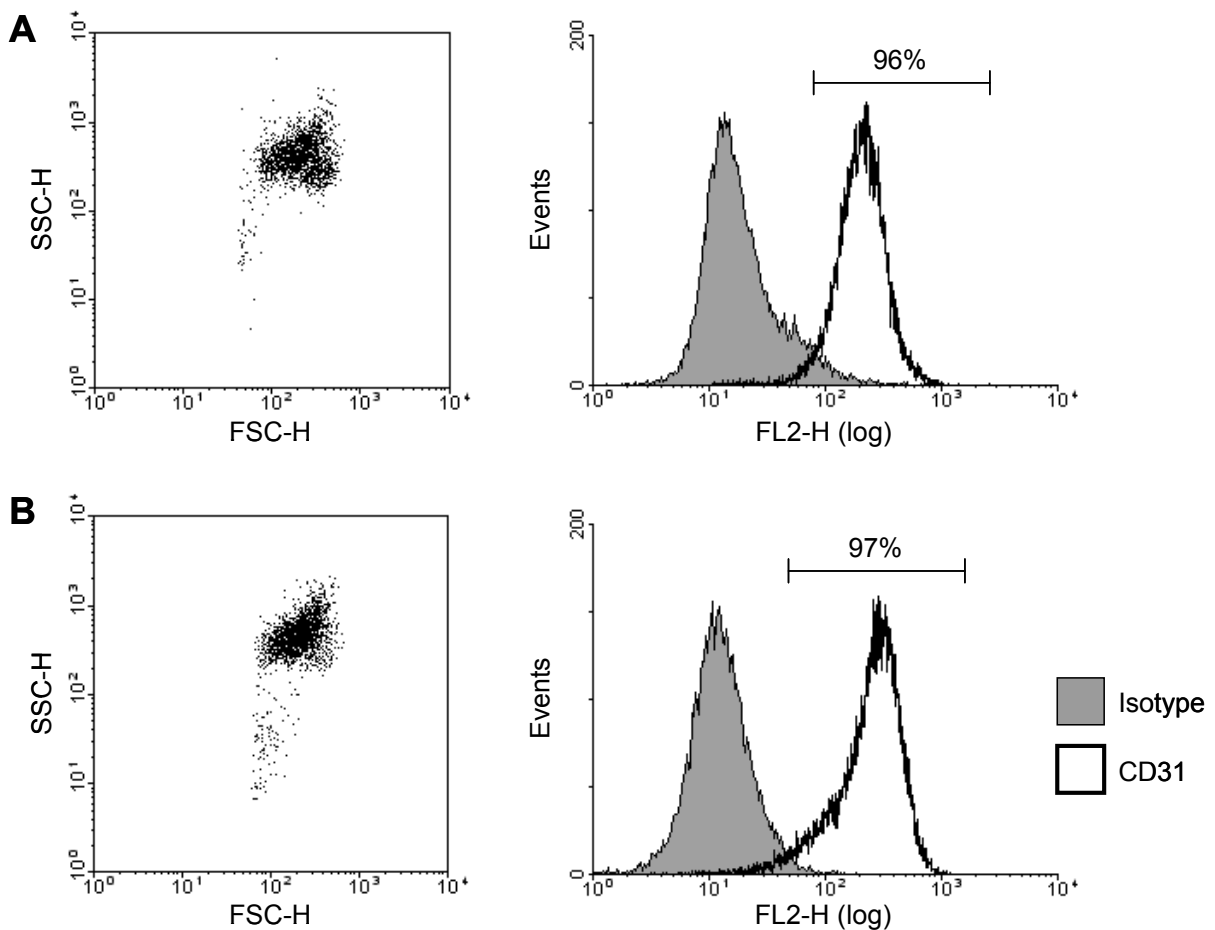
Figure III.1: Endothelial cell culture purity tested via flow cytometry

PAEC (A) and HUVEC (B) were stained for CD31 and analyzed in a flow cytometer. The *left panel* shows a representative dot plot (FCS-H vs. SSC-H) of the cell populations (10,000 cells). The *right panel* displays the fluorescence histogram of 50,000 cells. The filled grey curves represent the isotype control whereas the empty curves are the CD31 stained cell population. For PAEC two and for HUVEC three independent cell populations were analyzed. One representative histogram is shown.

2   ELASTASE AS PART OF THE MECHANOTRANSDUCTION CASCADE

2.1   SHEAR STRESS-INDUCED FGF-2 RELEASE IS ELASTASE DEPENDENT

Porcine aortic endothelial cells were kept under static conditions or exposed to a shear stress of 16 dyn per cm^2 for about 120 minutes using the cone and plate apparatus. Supernatants were collected and the concentration of FGF-2 in these samples was measured. While the FGF-2 concentration in supernatants of static control cells amounted to 106.5 ± 23.7 pg/ml, its concentration in supernatants of sheared cells was more than 3 times higher (344.2 ± 65.1 pg/ml, $p < 0.001$). To check whether elastase influences this shear stress-induced FGF-2 release, elastase activity was blocked using an unspecific and a specific inhibitor for elastase. Inhibition of elastase with the non-specific serine protease inhibitor chymostatin as well as with the specific inhibitor MeOSuc-Ala-Ala-Pro-Val-chloromethylketone significantly reduced the shear stress-induced increase in FGF-2 (167.6 ± 73.3 pg/ml and 153.0 ± 73.4 pg/ml respectively). Abciximab, an integrin $\alpha_v\beta_3$ blocker, abolished FGF-2 secretion into the supernatant (124.9 ± 18.7 pg/ml) (Figure III.2), which was already demonstrated by Gloe et al. [75].
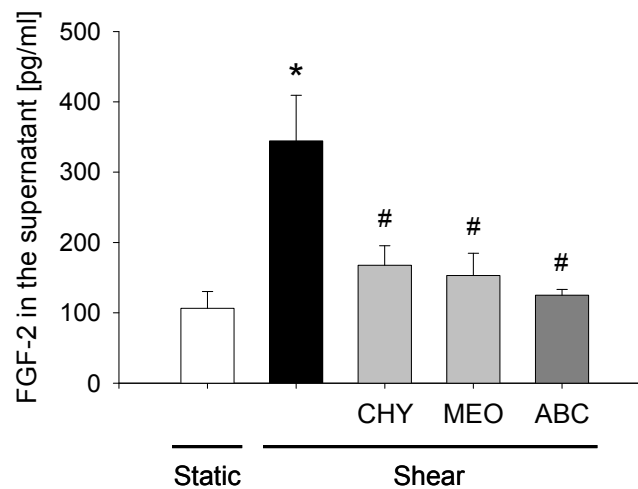
Figure III.2: Shear stress-induced FGF-2 release depends on elastase and integrin $\alpha_v\beta_3$

Quantification of FGF-2 in cell supernatants after the application of shear stress (16 dyn/cm^2, 120 minutes) is shown in comparison to static controls. Elastase inhibition was performed using chymostatin (CHY, 10 µg/ml) or MeOSuc-Ala-Ala-Pro-Val-chloromethylketone (MEO, 50 µM). The integrin $\alpha_v\beta_3$ was blocked with abciximab (ABC, 1 µg/ml) (n = 7, mean + SEM; * $p < 0.001$ vs. static, # $p < 0.001$ vs. shear, ANOVA RM, Student-Newman-Keuls).

2.2   ELASTASE IS RELEASED UPON SHEAR STRESS STIMULATION

To check whether elastase is released by shear stress exposure, the supernatants were analyzed. After 120 minutes of shear stress exposure, a significantly higher elastase activity was detected in the extracellular compartment compared to static control cells (static 0.0619 ± 0.0103 U/ml, shear 0.2036 ± 0.0288 U/ml). The activity was measured using the specific substrate MeOSuc-Ala-Ala-Pro-Val-p-nitroaniline. In order to investigate whether integrin $\alpha_v\beta_3$ activation was needed for elastase release, the integrin was blocked using abciximab. Integrin $\alpha_v\beta_3$ inhibition did not affect the shear stress-induced release of elastase (shear + ABC 0.1454 ± 0.0120 U/ml) (Figure III.3A).

In order to confirm elastase release upon shear stress, western blot analysis was performed using an antibody that detects human neutrophil elastase. In supernatants of PAEC and HUVEC exposed to shear stress the enzyme was detected whereas control supernatants showed no band in western blot (Figure III.3B).
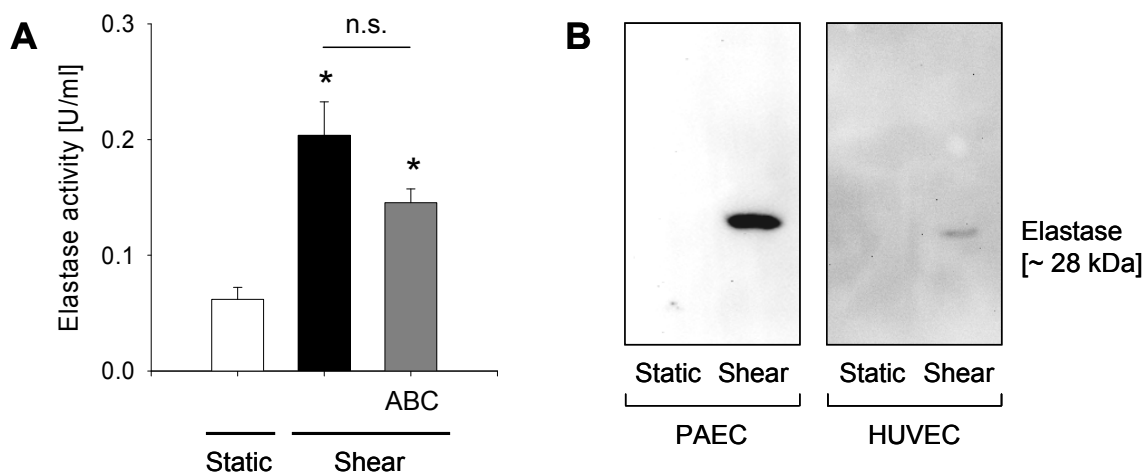
Figure III.3: Shear stress induces the release of an enzyme with elastase activity

(A) Elastase activity in supernatants of cells under static conditions and cells exposed to shear stress for 120 minutes was measured using the specific substrate MeOSuc-Ala-Ala-Pro-Val-p-nitroaniline (MeOSuc-Ala-Ala-Pro-Val-pNA) (1 µg/ml). Integrin $\alpha_v\beta_3$ was inhibited with abciximab (ABC, 1 µg/ml) (n = 20, mean + SEM, * p < 0.05 vs. static, n.s. = not significant, ANOVA RM on Ranks, Student-Newman-Keuls). (B) The concentrated supernatants of untreated cells and cells exposed to 120 minutes of shear stress were analyzed by western blot using an anti-neutrophil elastase antibody (antibody No. 2).

3   CHARACTERIZATION OF ENDOTHELIAL ELASTASE

3.1   ENDOTHELIAL ELASTASE DIFFERS FROM PANCREATIC AND NEUTROPHIL ELASTASE

In order to figure out whether the released elastase was indeed neutrophil or pancreatic elastase, RT-PCR experiments of cell lysates of PAEC and HUVEC were performed. As leukocytes are known to contain neutrophil elastase, human and porcine mononuclear cells were isolated with Ficoll gradient centrifugation and used as positive control for this elastase. Extracts from human and porcine pancreas were used as positive control for the pancreatic elastases. RT-PCR experiments revealed that neither neutrophil nor pancreatic elastase are expressed in PAEC as well as in HUVEC on mRNA level (Figure III.4).
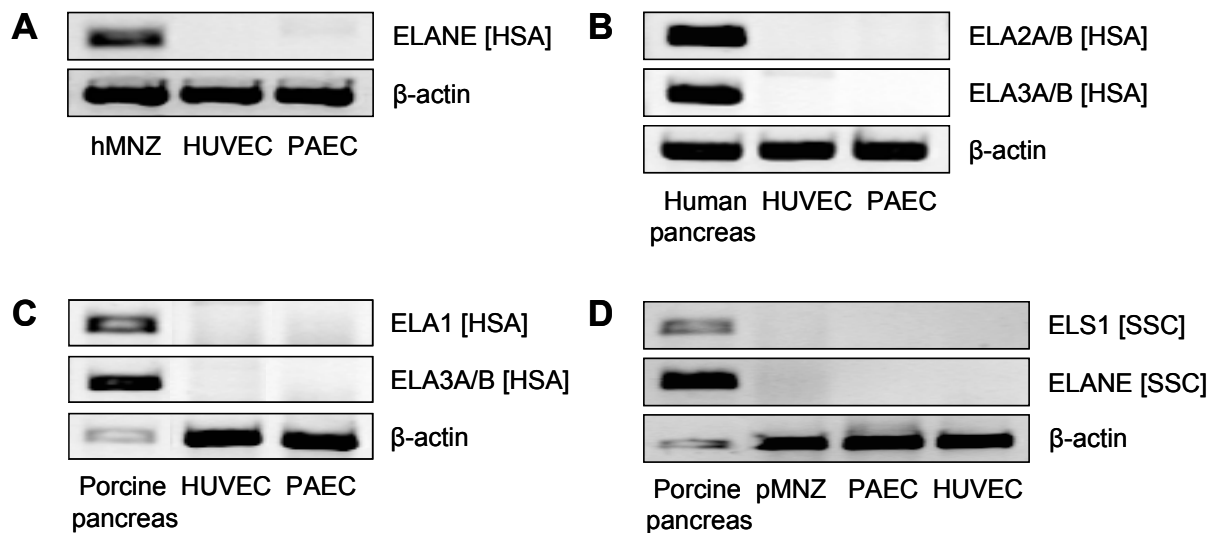
Figure III.4: No endothelial mRNA expression of neutrophil and pancreatic elastase

RT-PCR of PAEC and HUVEC was performed to detect mRNA expression of (A) human neutrophil elastase [ELANE], (B)/(C) human pancreatic elastases (ELA1, ELA2, ELA3) and (D) porcine elastases (ELS1, ELANE (the porcine ELANE mRNA was not detectable in porcine mononuclear cells but in porcine pancreas)). As controls human and porcine mononuclear cells (hMNZ, pMNZ) and pancreatic extracts from human and pig were used. β-actin served as internal control for each sample. HSA = Homo sapiens, SSC = Sus scrofa.

To investigate elastase expression on protein level, western blot analysis using antibodies against human neutrophil elastase (antibody No. 1) and pancreatic elastase was performed. As expected, and in correlation with RT-PCR data, neither neutrophil nor pancreatic elastase was detected in western blots of PAEC and HUVEC. Surprisingly, another antibody against neutrophil elastase (antibody No. 2) that was used for the detection of elastase in cell supernatants (see Figure III.3) was effective in detecting the enzyme in both endothelial cell types, maybe due to cross-reactions.

These results suggest that neither neutrophil nor pancreatic elastase are expressed in endothelial cells, but that another not yet described elastolytic enzyme, showing homology to neutrophil elastase, is present in endothelial cells and released upon shear stress exposure (Figure III.3). For the rest of this manuscript this enzyme will be termed endothelial elastase.
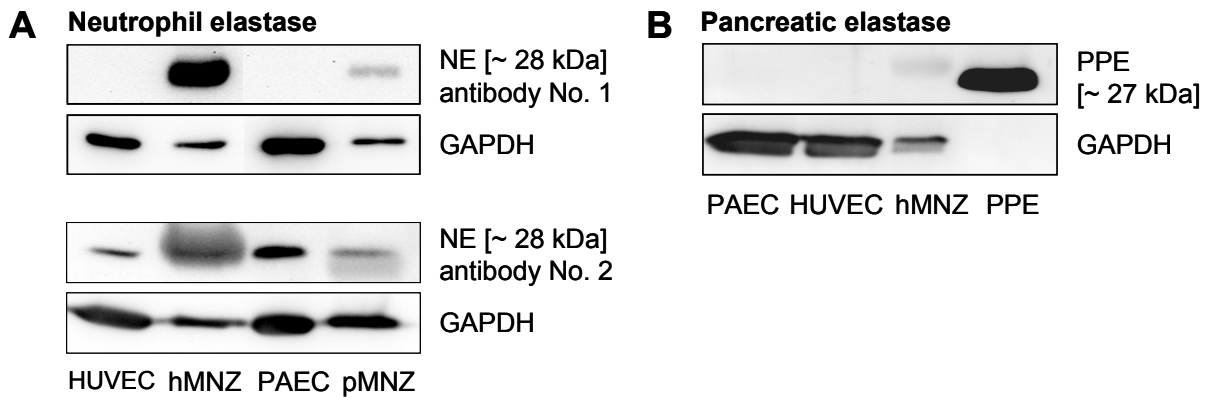
Figure III.5: Endothelial elastase detectable with an antibody against neutrophil elastase

(A) Endothelial elastase was analyzed by using two neutrophil elastase (NE) antibodies, probably raised against different epitopes of the enzyme. The *upper panel* shows a western blot with antibody No. 1, which does not recognize endothelial elastase, which antibody No. 2 does (*lower panel*). (B) An antibody against porcine pancreatic elastase (PPE) failed to detect endothelial elastase. GAPDH was used to control protein loading. HMNZ, pMNZ = Human and porcine mononuclear cells.

4   INTRACELLULAR STORAGE OF ENDOTHELIAL ELASTASE

4.1   ENDOTHELIAL ELASTASE COLOCALIZES WITH VWF

Since it was shown that an elastase mediates the shear stress-induced FGF-2 release, the release and intracellular storage of this enzyme was further examined using the neutrophil elastase antibody mentioned in chapter III.3.1.

Weibel-Palade bodies are prominent secretory vesicles in endothelial cells. These bodies contain among other substances von Willebrand Factor (vWF), a protein involved in platelet adhesion and coagulation. Since Galbusera et al. demonstrated that vWF is released from Weibel-Palade bodies upon shear stress, these endothelial vesicles were investigated here [67].

In immunofluorescence experiments (Figure III.6), endothelial elastase was found to colocalize with vWF in the cytosol, indicating endothelial elastase to be also stored in Weibel-Palade bodies. In contrast, cytosolic colocalization with LAMP1 (lysosomal-associated membrane protein-1), a lysosomal protein, was not detected.

To confirm the finding that elastase and vWF colocalize in Weibel-Palade bodies, electron microscopy using double immunogold labeling was performed. The negative control did not show any unspecific binding of immunogold particles. In positive samples a colocalization of elastase and vWF at cell border areas and inside the cytoplasm was detected (Figure III.7).
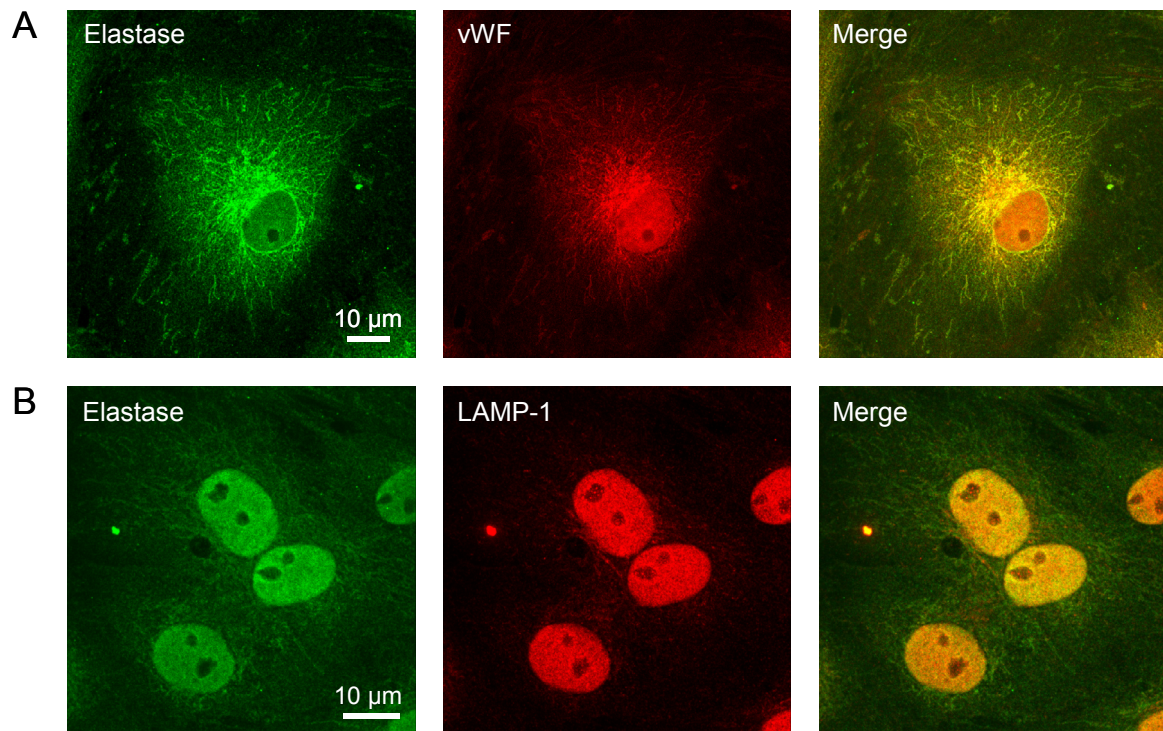
Figure III.6: Colocalization of endothelial elastase and vWF

The intracellular distribution of (A) elastase (anti-NE, antibody No. 2) and vWF (63x objective, pixel size: 0.08 x 0.08 µm, z-step size: 0.25 µm, projection) or (B) elastase (anti-NE, antibody No. 2) and LAMP-1 (40x objective, pixel size: 0.06 x 0.06 µm, z-step size: 0.5 µm, projection) was analyzed with confocal laser scanning microscopy.
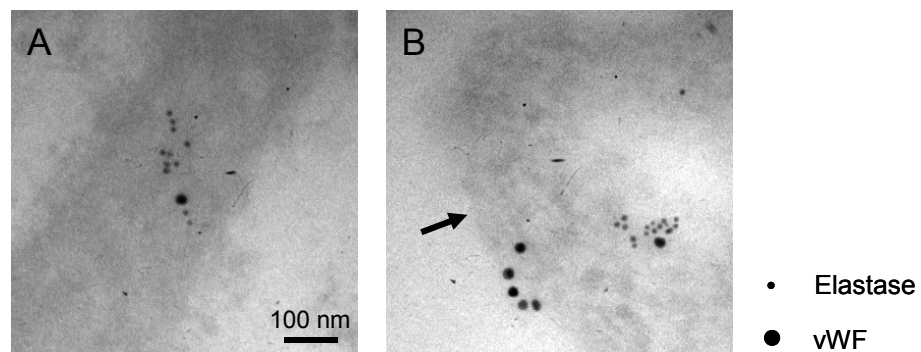
Figure III.7: Electron microscopy of endothelial elastase and vWF

Double-labeling immunogold electron microscopy of elastase (small 6-nm immunogold particles) (anti-NE, antibody No. 2) and vWF (large 10-nm immunogold particles) was performed in untreated PAEC: (A) image of the cytosolic region, (B) image of the cell border area (the arrow indicates the cell border).

4.2   ENDOTHELIAL ELASTASE AND VWF ARE RELEASED UPON SHEAR STRESS STIMULATION

To investigate whether both proteins – vWF and endothelial elastase – are released upon shear stress stimulation, flow cytometry and western blot analysis was performed. Flow cytometry experiments revealed that after 240 minutes of shear stress 30% less vWF was detectable inside the cells (mean cell fluorescence: static 37.0 ± 1.6 vs. shear 27.1 ± 2.4) indicating release of vWF upon shear stress. This finding was confirmed using western blot analysis. Whereas after 120 minutes of shear stress no change in the amount of intracellular stored vWF was noticed, after 240 minutes less vWF was detected in cell lysates of sheared cells compared to static cells. The same was true for endothelial elastase (Figure III.8).
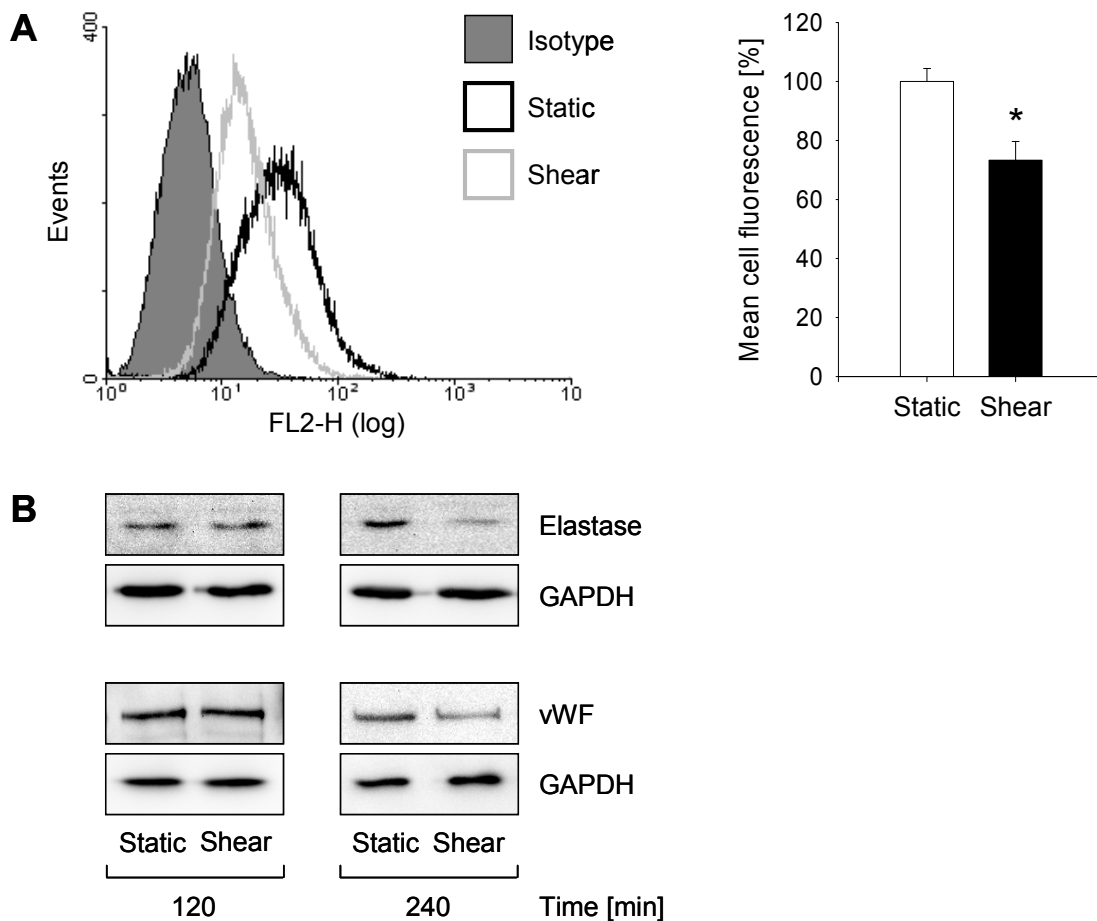
Figure III.8: Shear stress induces the release of vWF – intracellular analysis

(A) Flow cytometry of static PAEC and cells exposed to shear stress (16 dyn/cm², 240 minutes) (n = 5, mean + SEM, * p < 0.05 vs. static, paired t-test) showing intracellular vWF expression. The filled grey curve represents the isotype control whereas the empty curves are vWF stained cells (black line: static cells, grey line: cells exposed to shear stress). The isotype served as negative control. Appropriate mean fluorescence intensities are illustrated in the graph on the *right*. (B) Furthermore, static cells and cells exposed to shear stress (16 dyn/cm², 120 or 240 minutes) were analyzed for endothelial elastase (antibody No. 2 against neutrophil elastase) and vWF protein expression by western blot experiments. GAPDH was used as control for equal protein loading. A representative blot of three independent experiments is presented.

In order to prove release of vWF into the supernatant, western blot analysis was performed. Whereas the intracellular amount of vWF decreased (Figure III.8), the level of vWF increased in the extracellular compartment. After 120 and 240 minutes of stimulation with shear stress, vWF was detectable in cell supernatants, whereas no vWF band was detected in supernatants of static controls (Figure III.9A). To obtain quantitative data, an ELISA was performed. As this kit was not able to detect the porcine protein in PAEC supernatants, the assay was performed by using HUVEC. After 120 minutes of stimulation a 3 fold higher amount of vWF was detected in supernatants of cells exposed to shear stress than in untreated controls (static 2.0 mU/mg $\pm$ 0.7 vs. shear 6.1 mU/mg $\pm$ 1.9). After 240 minutes of treatment with shear stress, the concentration of vWF in the supernatant was even higher (static 3.4 $\pm$ 1.0 mU/mg vs. shear 9.1 $\pm$ 3.0 mU/mg) (Figure III.9B). As shown in chapter III.2.2, this increase coincided with an increase of elastase concentration in the supernatant.
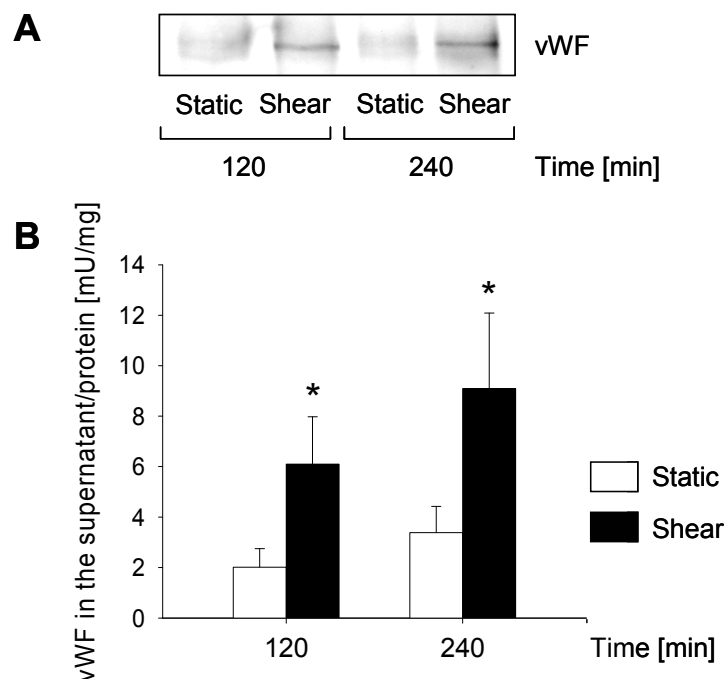
Figure III.9: Shear stress induces the release of vWF – extracellular analysis

PAEC or HUVEC were either kept as static controls or subjected to a shear stress of 16 dyn/cm² for 120 or 240 minutes. (A) PAEC supernatants were analyzed with western blots. One representative experiment out of three is shown. (B) Quantification of vWF in HUVEC supernatants was performed using an ELISA (n = 5, mean + SEM, * p < 0.05 vs. static, paired t-test).

5   EFFECTS OF EXOGENOUSLY APPLIED ELASTASE ON ENDOTHELIAL CELLS

5.1   ELASTASE TREATMENT INDUCES FGF-2 RELEASE

Since it was shown that shear stress induces the release of FGF-2, we investigated whether this release was also possible by exogenous application of elastase without shear stress. Therefore, cells were stimulated with porcine pancreatic elastase for 5, 10, 30 or 60 minutes. The concentration of FGF-2 in the supernatant increased in a time-dependent manner, reaching a significant difference to untreated controls after 60 minutes of stimulation (control 63.2 ± 12.0 pg/ml, elastase (60 min) 161.7 ± 21.4 pg/ml) (Figure III.10).

To test whether treatment with exogenously applied elastase induced the de novo synthesis of FGF-2, real time RT-PCR was performed. Neither after 8 nor after 16 hours FGF-2 mRNA expression was changed by elastase application (Figure III.11).

In order to check whether the source of the increased FGF-2 in the supernatant is either extracellular FGF-2, which was cut off from the matrix or cell surface proteoglycans, or intracellular FGF-2, being released from the cytosol, cells were treated with heparinase I. Heparinase I is an enzyme that cleaves heparan sulfate and heparin [122], which are major binding sites of FGF-2 on the cell surface. Incubation with heparinase for 60 minutes did not increase the concentration of FGF-2 in the supernatant, which was virtually identical with the concentration of FGF-2 in supernatants of untreated control cells (static 35.8 ± 5.3 pg/ml vs. heparinase 39.5 ± 5.8 pg/ml) (Figure III.12). Simultaneous application of elastase and heparinase did not further increase the FGF-2 concentration in the supernatant as compared to cells treated with elastase alone (elastase 124.3 ± 10.6 pg/ml vs. elastase + heparinase 128.7 ± 16.2 pg/ml).
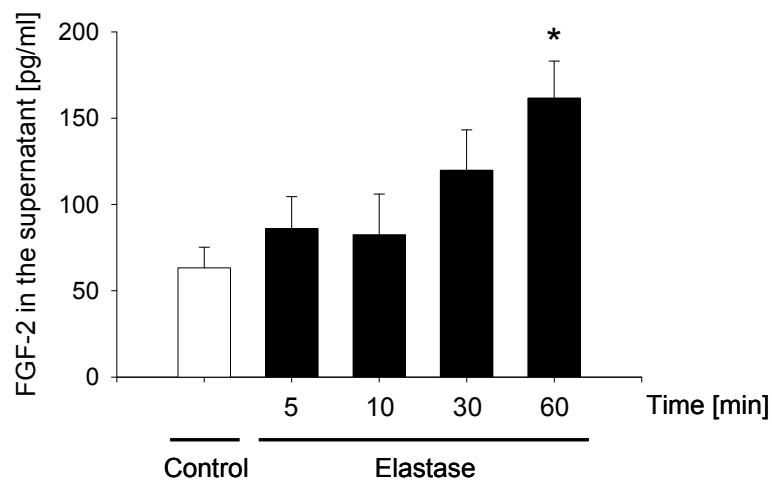
Figure III.10: Elastase induces the release of FGF-2 from endothelial cells

PAEC were stimulated for 5, 10, 30 and 60 minutes with porcine pancreatic elastase (0.5 U/ml). Supernatants were collected and analyzed quantitatively for FGF-2 concentration using an ELISA (n = 6, mean + SEM, * p < 0.05 vs. control, ANOVA RM, Student-Newman-Keuls).
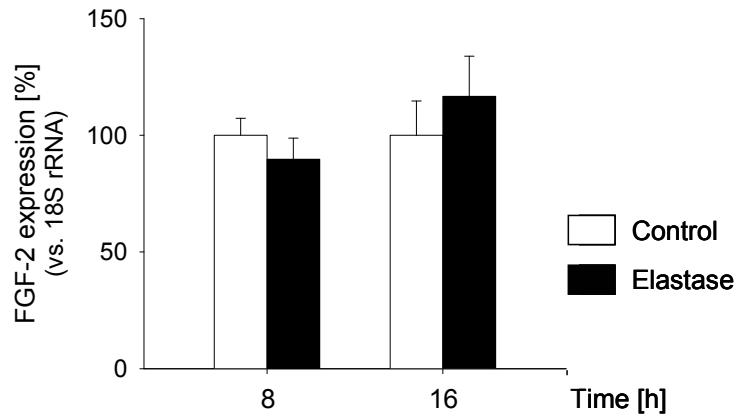
Figure III.11: Elastase has no influence on FGF-2 mRNA expression

PAEC were left untreated or incubated with porcine pancreatic elastase for about 8 or 16 hours. Expression of FGF-2 mRNA was measured by real-time RT-PCR. 18S rRNA was used as endogenous reference gene (n = 4, each in duplicate, mean + SEM, paired t-test).
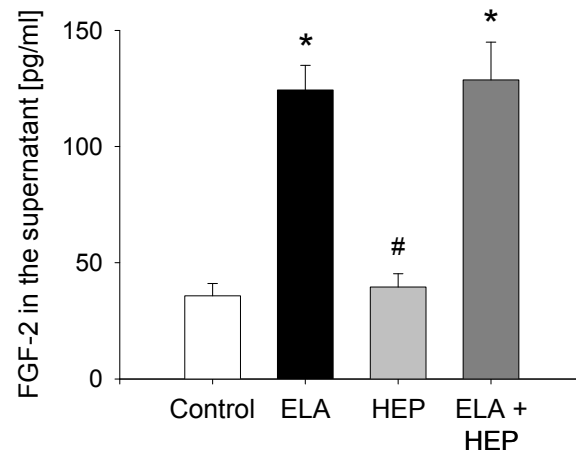
Figure III.12: Heparinase does not induce the release of FGF-2 from endothelial cells

PAEC were left untreated or stimulated with porcine pancreatic elastase (0.5 U/ml) (ELA), heparinase I (0.5 U/ml) (HEP) or both (ELA + HEP) for 60 minutes. Supernatants were collected and analyzed for FGF-2 concentration using a commercially available ELISA Kit (n = 12 and n = 6 for ELA + HEP, respectively, mean + SEM, * $p < 0.05$ vs. control, # $p < 0.05$ vs. ELA, ANOVA RM, Student-Newman-Keuls).

5.2   ELASTASE INDUCES INTEGRIN-DEPENDENT OUTSIDE-IN SIGNALING

5.2.1   Effects of elastase on extracellular matrix proteins

Extracellular matrix proteins act as ligands for integrins. In order to study the effect of elastase on ECM proteins, different matrix proteins were incubated with porcine pancreatic elastase for 60 minutes. To separate those proteins, a SDS-Page, which was run under reducing conditions, followed by coomassie staining was performed. Porcine pancreatic elastase did not show any influence on collagen type I and IV, whereas laminin, fibronectin and vitronectin were cleaved into fragments of smaller molecular weight (Figure III.13). Molecular masses of denatured but yet uncleaved matrix proteins are summarized in Table II.7. Laminin degradation produced new bands at 100 and 60 kDa. Proteolytic degradation of fibronectin resulted in fragments of approximately 160, 120, 70, 65, 60 and 45 kDa. Vitronectin degradation produced a fragment of 35 kDa and fragments in the dye front (< 20 kDa). The 27 kDa band represents pancreatic elastase, which was also loaded onto the gel in elastase treated samples.
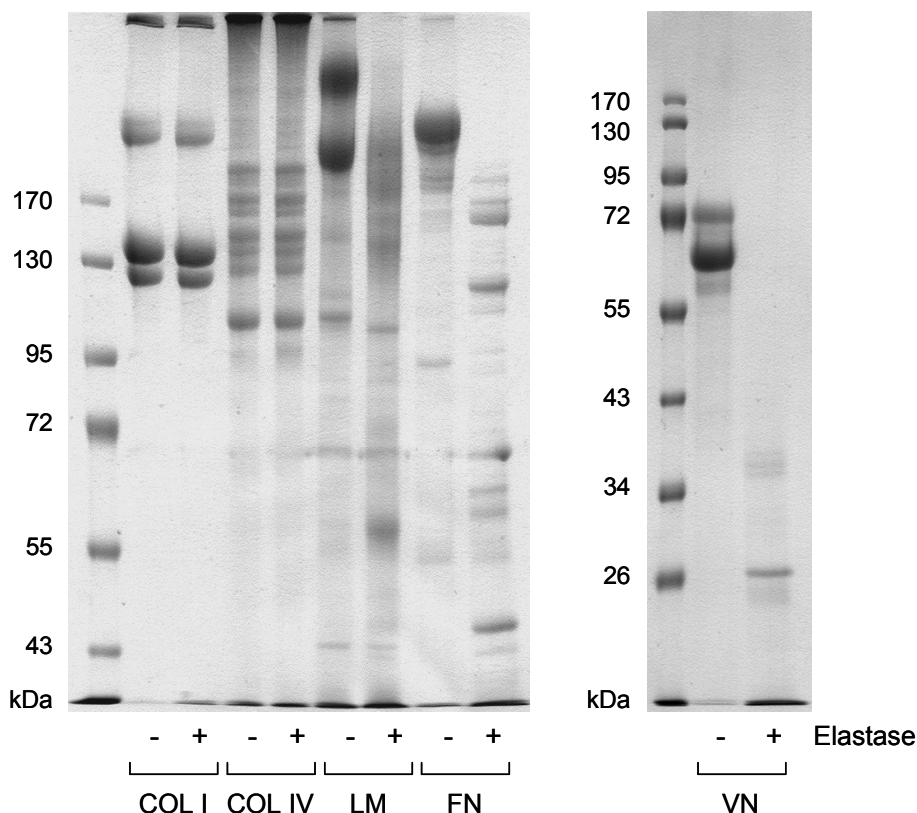
Figure III.13: Specific degradation of matrix proteins by elastase

SDS-Page and coomassie staining was performed to check the effect of elastase on different matrix proteins. Collagen type I (COL I, 300 µg/ml), collagen type IV (COL IV, 300 µg/ml), laminin (LM, 300 µg/ml), fibronectin (FN, 1 mg/ml) and vitronectin (VN, 150 µg/ml) were incubated for 60 minutes with 0.5 U/ml porcine pancreatic elastase (+), or just solvent (-) (n = 3). The same degradation profile was observed when treating the matrix proteins with a 5-fold higher concentration of elastase (2.5 U/ml).

To check the effect of elastase on endothelial cells and their extracellular matrix, PAEC grown on cell culture dishes for 24 hours were incubated with porcine pancreatic elastase. Cell supernatants, the cells and their extracellular matrix were separately isolated and analyzed for fibronectin, laminin and vitronectin by using western blots. Fibronectin, laminin and vitronectin were found to be degraded as compared to untreated controls (Figure III.14). However, the effect was less pronounced than observed after incubation of elastase with the isolated matrix components, the setup described above. Here, fibronectin fragments of approximately 160, 130, 120, 110 and 85 kDa and vitronectin fragments of 55, 43 and 35 kDa were detected. Whereas the protein fragments of laminin and vitronectin were found in the extracellular matrix layer, fibronectin fragments were detectable in the cell supernatant. By contrast, neither fragments of laminin nor vitronectin were found in supernatants (data not shown).
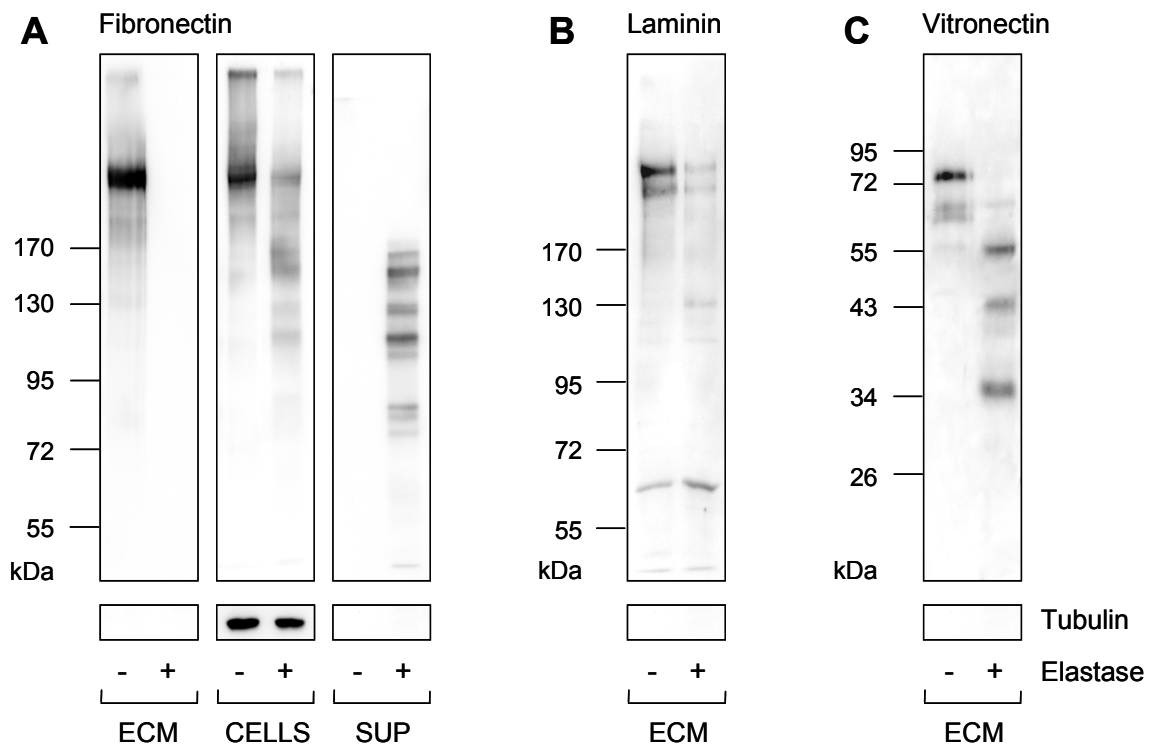
Figure III.14: Release of fibronectin fragments by elastase

The effect of porcine pancreatic elastase (0.5 U/ml) on (A) fibronectin, (B) laminin and (C) vitronectin was tested using western blot analysis. The isolated extracellular matrix (ECM), the cell lysate including intracellular and cell-associated protein (CELLS) and the cell supernatant (SUP) of PAEC were analyzed. β-tubulin was used as control for equal protein loading. One representative image out of 3 is shown.

As shown in Figure III.15 with immunofluorescence experiments, PAEC originally plated in collagen type I, form a compact network of fibronectin fibrils upon cultivation for 24 h. To compare effects of elastase and shear stress on the structure of this network, PAEC were alternatively incubated with porcine pancreatic elastase or were directly exposed to shear stress for 120 minutes. Additionally experiments with shear stress supernatants, that contain endothelial elastase, were performed. All treatments induced similar alterations in the fibronectin matrix. After incubation with pancreatic elastase, extracellular fibronectin was almost not detectable anymore. In cells treated with shear stress supernatants or with shear stress a similar, but less pronounced, change of the network appeared.

Compared to the pronounced changes in the fibronectin network, the structure of collagen type IV, laminin and vitronectin matrices were less affected by the application of pancreatic elastase (Figure III.16). The extra- and intracellular protein distribution of collagen type IV and vitronectin were not altered, while the laminin network appeared less dense than in untreated controls.
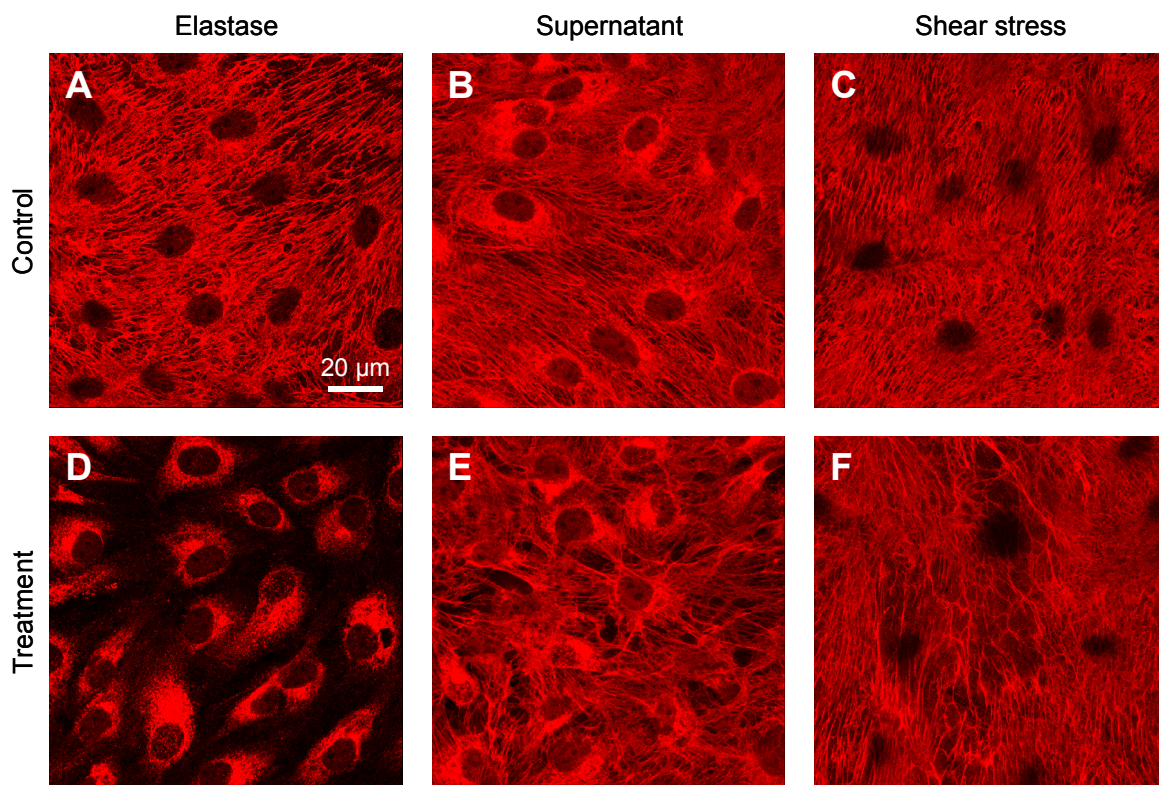
Figure III.15: Effects of elastase and shear stress on fibronectin macrostructure

The intra- and extracellular distribution of fibronectin in PAEC was analyzed after exposure to different treatments using confocal microscopy: *Upper panel* represents controls: (A) without elastase, (B) treatment with control supernatant of static cells or (C) without shear stress. *Lower panel*: treatment with (D) porcine pancreatic elastase (0.5 U/ml, 60 minutes), (E) supernatant of sheared cells (shear stress of 16 dyn/cm² (120 minutes) was applied, supernatant was collected and given on static cells were for 60 minutes) or (F) shear stress (16 dyn/cm², 6 h, applied with the parallel plate apparatus) (40x objective, pixel size: 0.12 x 0.12 µm, z-step size A,B: 0.5 µm, C,D,E and F: 0.25 µm, projection).
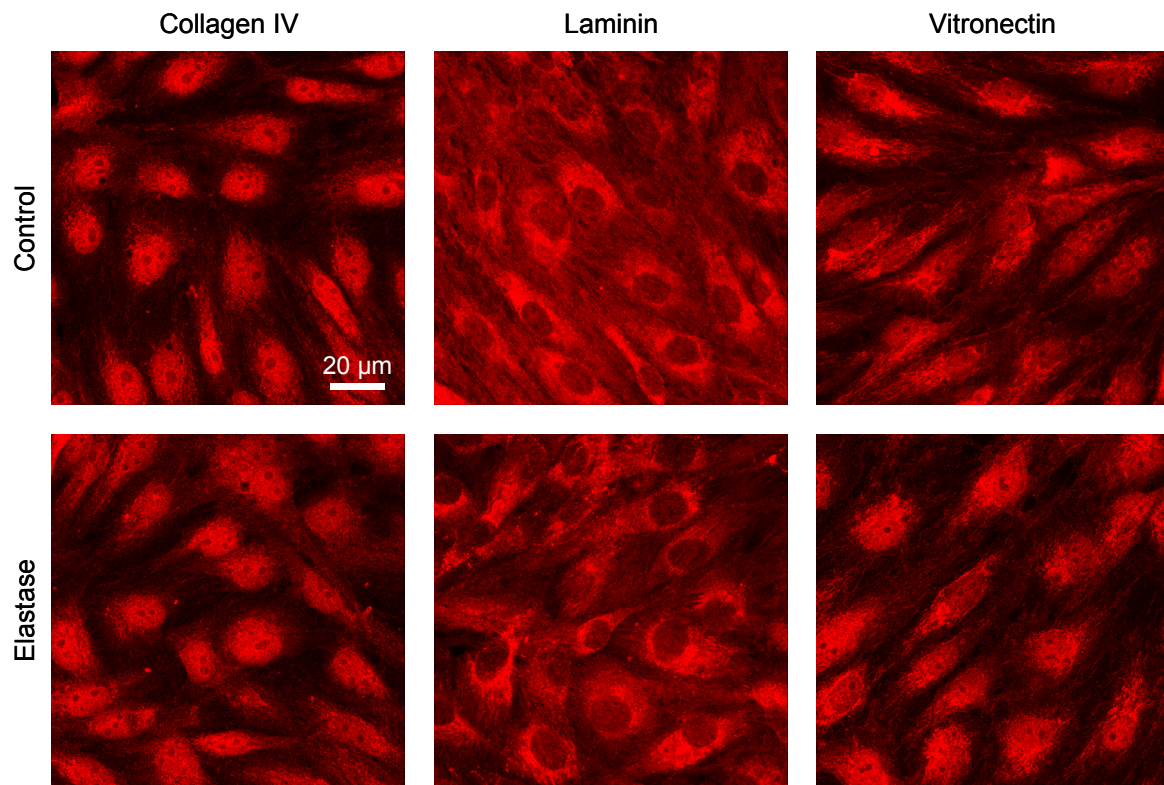
Figure III.16: Effects of elastase on collagen type IV, laminin, vitronectin macrostructure

Immunofluorescence images of collagen type IV, laminin and vitronectin in PAEC were taken using the confocal microscope. The *upper panel* shows the control cells, the *lower panel* the elastase treated cells (porcine pancreatic elastase, 0.5 U/ml, 60 minutes) (40x objective, pixel size: 0.12 x 0.12 µm, z-step size: 0.5 µm, projection).

5.2.2   Effects of elastase on integrin $\alpha_v\beta_3$

Activation of the integrin $\alpha_v\beta_3$ leads to its interaction with the adaptor protein Shc [36]. To check the effect of shear stress on this interaction, coimmunoprecipitation experiments were performed. Shear stress induced a significantly higher association of two out of three Shc isoforms (46 and 52 kDa) and the integrin $\alpha_v\beta_3$ as compared to static controls (shear: 46 kDa: 1.6 ± 0.3 and 52 kDa: 1.8 ± 0.3 fold over the static controls). The third Shc isoform of 66 kDa was not analyzed here as band density was too low in the western blots. Blocking of the elastase activity with the specific inhibitor MeOSuc-Ala-Ala-Pro-Val-chloromethylketone reduced the interaction of both Shc isoforms with the integrin (shear + MEO: 46 kDa: 1.3 ± 0.3 and 52 kDa: 1.3 ± 0.2 fold over the static controls). For the 52 kDa isoform this reduction was significant ($p < 0.05$), interaction of the 46 kDa form with integrin $\alpha_v\beta_3$ was lowered ($p = 0.062$) (Figure III.17A). The overall amount of Shc, which was analyzed to control equal protein loading, was not change by these treatments (Figure III.17B).
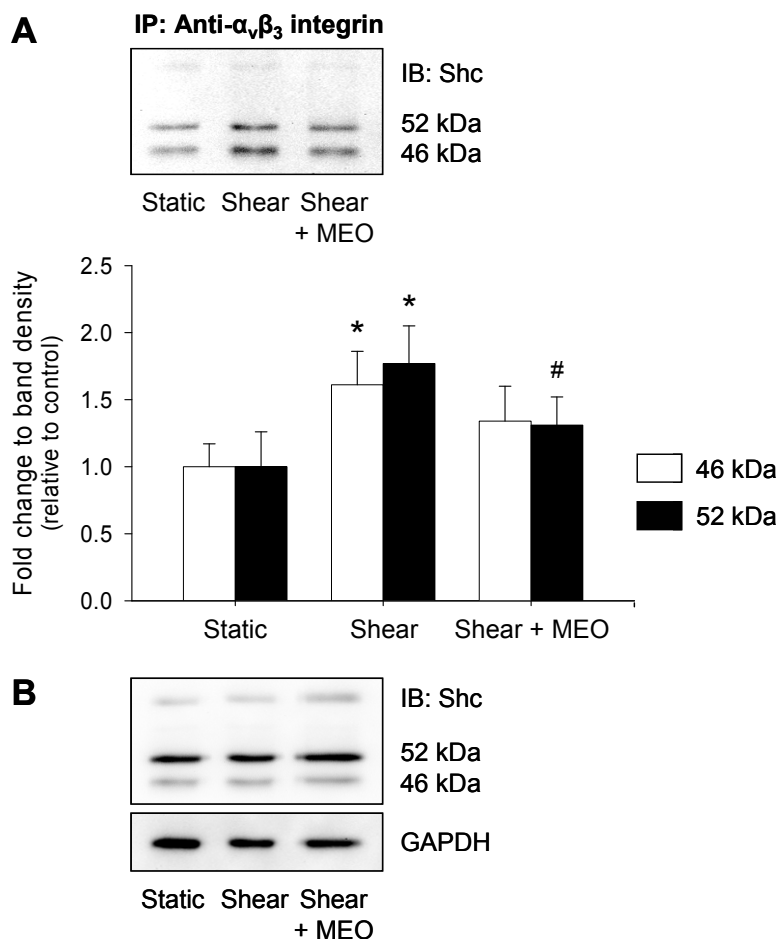
Figure III.17: Elastase inhibition decreases shear stress-induced integrin $\alpha_v\beta_3$ activation

(A) PAEC lysates of static cells, cells exposed to shear stress (16 dyn/cm², 60 minutes); cells exposed to shear stress with additional elastase inhibition (MEO: MeOSuc-Ala-Ala-Pro-Val-chloromethylketone, 50 µM) were analyzed via coimmunoprecipitation (IP: integrin $\alpha_v\beta_3$, IB: Shc) (n = 4, mean + SEM, * $p < 0.05$ vs. static, # $p < 0.05$ vs. shear, ANOVA RM, Student-Newman-Keuls) or (B) as input control immunoblotted against Shc (n = 4). GAPDH was used to check equal protein loading.

It was further investigated whether the same effects as observed after shear stress could also be induced by elastase treatment. After exposing PAEC to porcine pancreatic elastase for 10 minutes a significantly higher amount of all three Shc isoforms was associated with the integrin (elastase (10 min.) 44 kDa: 2.59 ± 0.61, 52 kDa: 1.71 ± 0.16 and 66 kDa: 3.28 ± 0.77 fold over controls). This interaction was also observed after treatment with elastase for 30 and 60 minutes (elastase (60 min): 46 kDa: 1.92 ± 0.52, 52 kDa: 1.61 ± 0.22 and 66 kDa: 3.88 ± 0.90 fold over controls) (Figure III.18A). To exclude a change in the overall cellular content of Shc during elastase treatment, cell lysates were immunoblotted for this protein. In cells treated with pancreatic elastase the amount of all the three Shc isoforms did not change in comparison to untreated controls (Figure III.18B).
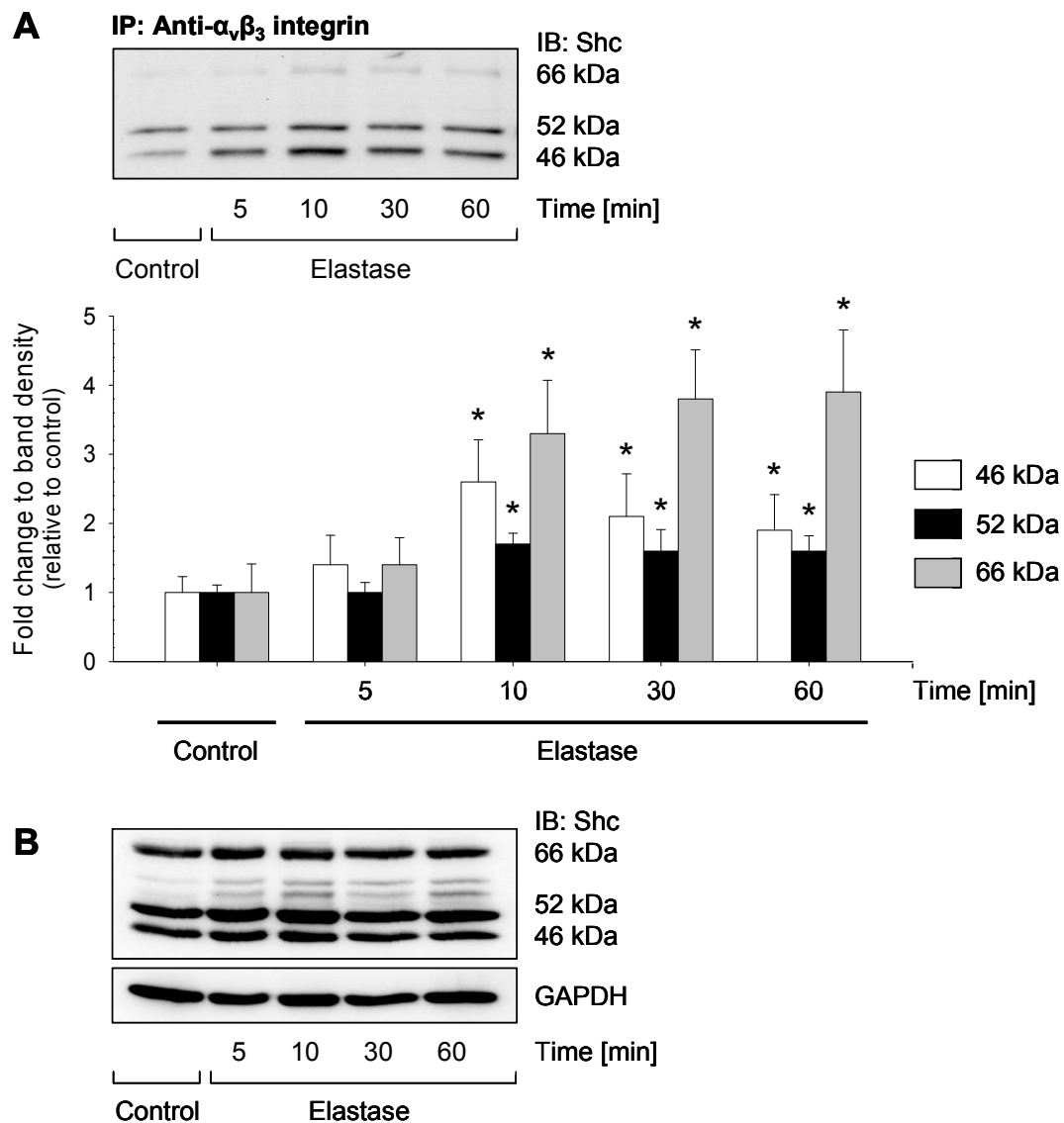
Figure III.18: Elastase induces the association of Shc and the integrin $\alpha_v\beta_3$

PAEC were treated with porcine pancreatic elastase (0.5 U/ml) for the time indicated. (A) Lysates were subjected to immunoprecipitation (IP) with an $\alpha_v\beta_3$ antibody and immunoblotted (IB) for Shc (n = 3, mean + SEM, * p < 0.05 vs. control, ANOVA RM, Student-Newman-Keuls) or (B) immunoblotted for the Shc protein (n = 6). GAPDH was used as loading control.

5.2.3   Effects on focal adhesion points

As integrins are directly linked to focal adhesions, the effect of porcine pancreatic elastase on focal adhesion kinase (FAK) and integrin-linked kinase (ILK), two prominent members of the focal contacts, was analyzed using confocal microscopy. In control cells both proteins were arranged as long thin fibers. Elastase caused the disappearance of these structures within 5 minutes of stimulation. The focal structures reappeared after 10 minutes and exhibited a "dot"-like conformation. At the end of the observation period, after 60 minutes of elastase treatment, these "dots" were detectable in high frequency in ILK as well as in FAK staining, indicating a colocalization of both proteins (Figure III.19). Same alterations were detected in cells plated on collagen type I and on fibronectin. For better visualization large-size images of FAK in control cells and cells exposed to 5 or 60 minutes of elastase treatment are shown in Figure III.20, illustrating the three different states of FAK appearance.
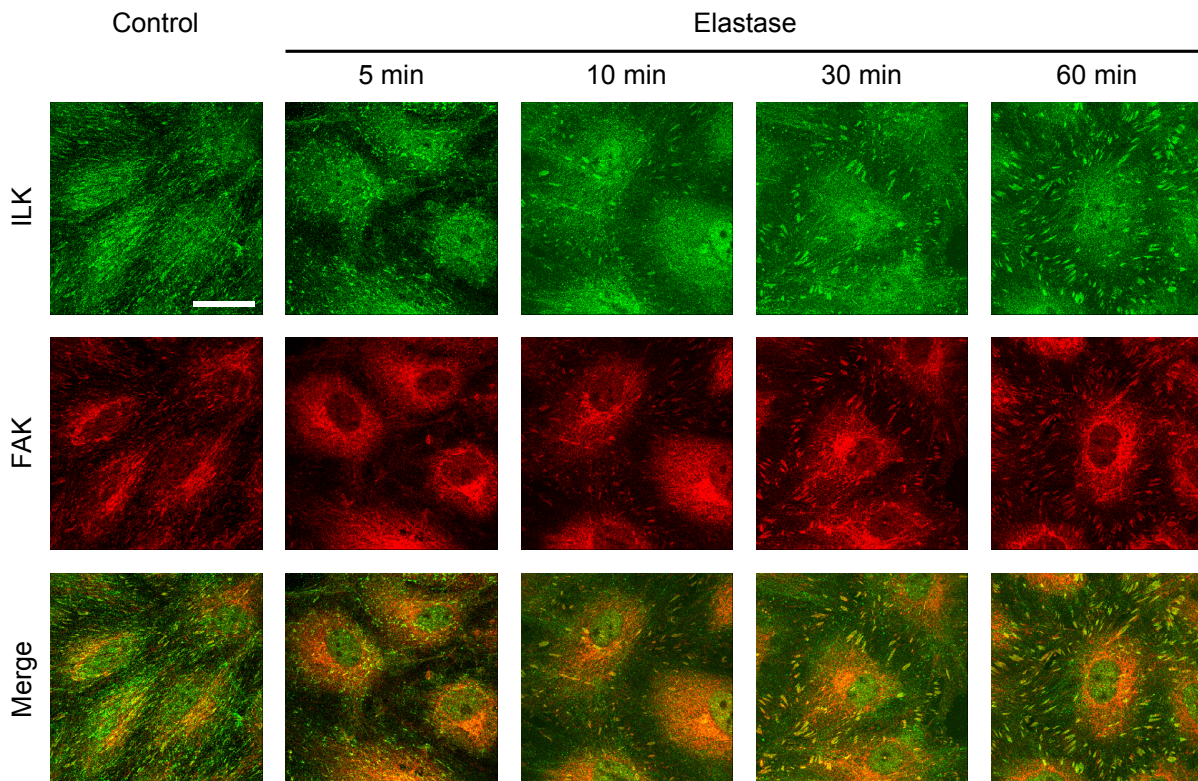
Figure III.19: Elastase induces a rearrangement of focal adhesion sites

Confocal microscope images of FAK and ILK in PAEC originally plated on collagen type I: Treatment with porcine pancreatic elastase (0.5 U/ml) induces a reorganization of focal adhesion points. The same effects and time course was observed in cells that were originally seeded onto fibronectin. Scale bar = 20 μm (63x objective, pixel size: 0.08 x 0.08 μm, z-step size: 0.25 μm, projection).
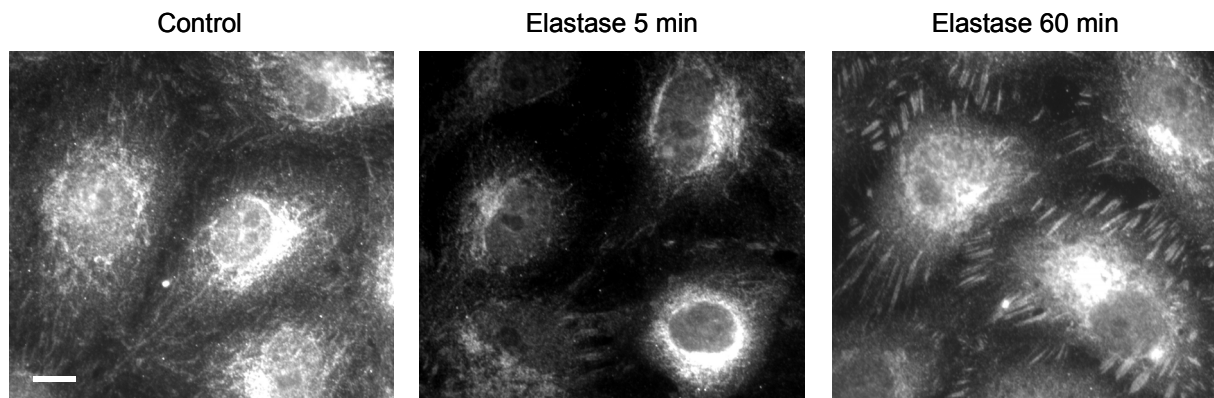
Figure III.20: FAK staining after elastase treatment

Immunofluorescence large size images of FAK illustrate the different states of FAK appearance without and with elastase (0.5 U/ml). Scale bar = 20 µm (100x objective, pixel size: 0.16 x 0.16 µm).

FAK is central regulator of integrin-mediated signaling. To check whether focal adhesion rearrangement was accompanied by changes in FAK activation, the tyrosine phosphorylation state of FAK was analyzed. In control cells Tyr397, Tyr576/577 and Tyr925 were phosphorylated. After 5 minutes of elastase treatment, these sites were, in comparison to control levels, dephosphorylated to a large extent and were rephosphorylated as analyzed between 10 to 60 minutes of ongoing elastase treatment (Figure III.21).
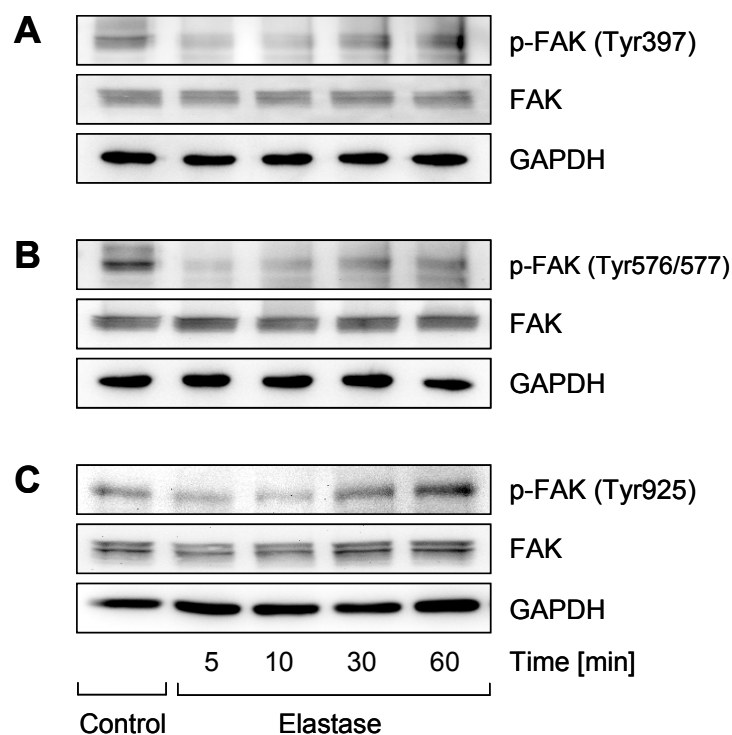
Figure III.21: Elastase alters FAK phosphorylation

PAEC treated with elastase (0.5 U/ml) were immunoblotted to check FAK tyrosine phosphorylation at three independent sites: (A) Tyr397, (B) Tyr576/577 and (C) Tyr925. GAPDH was used as control for equal protein loading. A blot representative for three independent experiments is presented.

5.2.4   Effects of elastase on the cell cytoskeleton

Focal adhesions directly link integrins to the cytoskeleton. Therefore we investigated the effects of porcine pancreatic elastase treatment on the cell cytoskeleton. The actin cytoskeleton was visualized using phalloidin (coupled to Alexa Fluor 488), a dye which labels F-actin. The integrin activation was indeed associated with cytoskeletal changes. Compared to control cells, cells treated with elastase showed a qualitatively higher density of stress fibers (see Figure III.22).
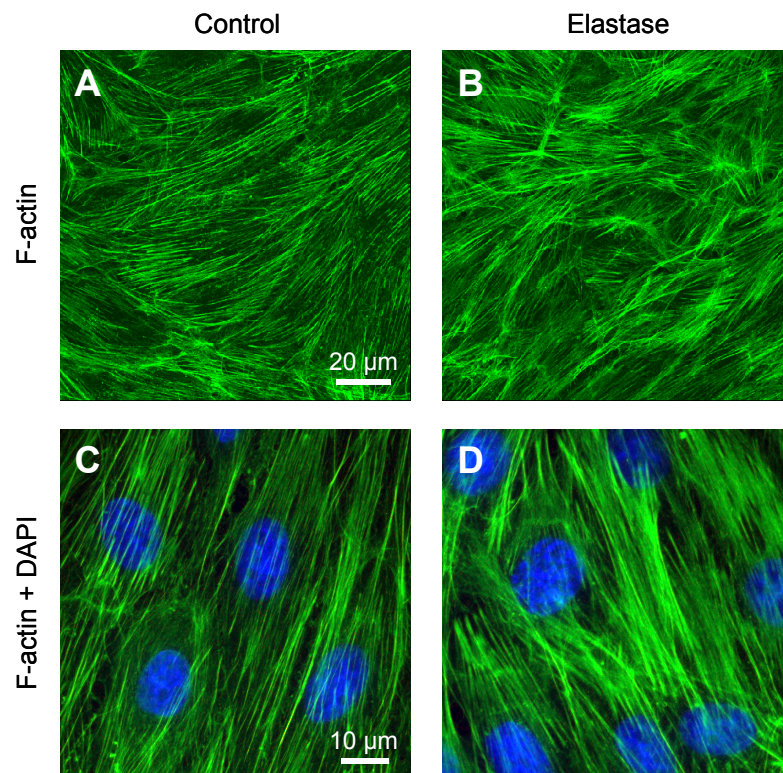
Figure III.22: Induction of stress fiber formation by elastase

Fluorescent phalloidin staining (green), a F-actin marker, in two magnifications without (*upper panel*) and with additionally DAPI staining (blue) (*lower panel*) was observed in control cells (A, C) and cells treated with porcine pancreatic elastase (0.5 U/ml) for 60 minutes (B, D). DAPI was used to stain the cell nuclei. Images in the upper panel were taken with the confocal microscope (40x objective, pixel size: 0.12 x 0.12 µm, z-step size: 0.5 µm, projection), whereas those in the lower panel were taken with the fluorescence microscope (63x objective, pixel size: 0.1 x 0.1 µm).

5.3   INTRACELLULAR SIGNALING PATHWAYS INVOLVED IN ELASTASE INDUCED FGF-2 RELEASE

5.3.1   Shear stress induces MAPK activation

It has been shown that in endothelial cells exposed to shear stress MAP kinases are activated [9]. In accordance with this, 120 minutes of shear stress application to PAEC resulted in an enhanced phosphorylation of p38, ERK1/2 and JNK1/2. This was observed in cells originally grown on collagen type I as well as on fibronectin. Under static conditions in cells seeded onto fibronectin MAPK were stronger phosphorylated than in cells seeded onto collagen type I, whereas after shear stress exposure the phosphorylation state was comparable for cells on both substrates (Figure III.23A).

Inhibition of elastase with the specific elastase inhibitor MeOSuc-Ala-Ala-Pro-Val-chloromethylketone or the unspecific elastase inhibitor chymostatin decreased the shear stress-induced p38 phosphorylation, whereas ERK1 and ERK2 activation was not reduced by elastase inhibition (Figure III.23B).
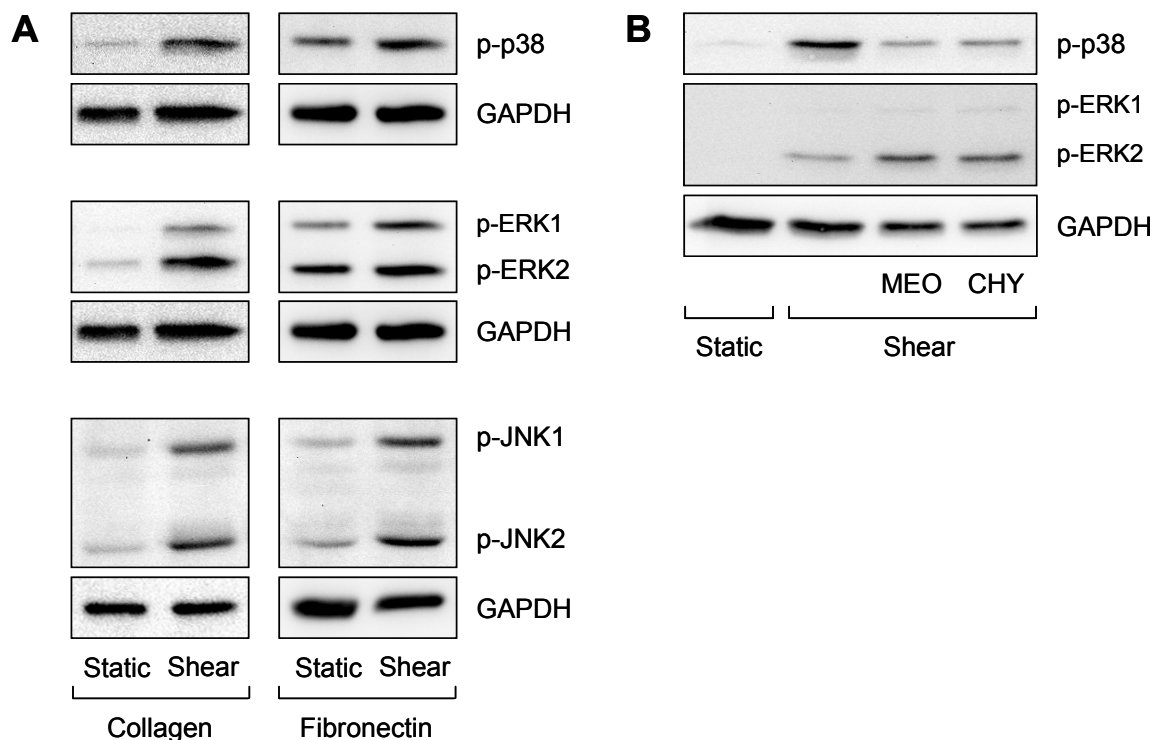
Figure III.23: MAPK are activated by shear stress

(A) Static cells and cells exposed to shear stress were analyzed by using western blot (16 dyn/cm², 120 minutes). Cells were originally seeded onto collagen type I (n = 6) or fibronectin (n = 3), respectively. (B) Elastase was inhibited using MeOSuc-Ala-Ala-Pro-Val-chloromethylketone (MEO, 50 µM) or chymostatin (CHY, 10 µg/ml) (n = 4, cells originally seeded onto collagen type I). GAPDH was used as control for equal protein loading.

5.3.2   Elastase induces MAPK activation

To investigate the effect of elastase on MAPK phosphorylation in detail, static cells were treated with porcine pancreatic elastase for different time periods and the cell lysates were analyzed by western blot. Elastase treatment activated all three MAPK. However, the extent of activation was dependent on the duration of exposure to elastase. The kinetics of phosphorylation differed between the different kinases: P38 and JNK phosphorylation increased throughout the observation period (after 60 minutes: p38: 4.2 ± 1.4, JNK1: 3.5 ± 0.7, JNK2: 3.3 ± 0.5 fold over controls). In contrast, ERK activation peaked at 10 to 30 minutes and almost returned to basal level after 60 minutes (after 10 minutes: ERK1: 2.0 ± 0.5, ERK2: 2.4 ± 0.6 fold over controls, after 60 minutes ERK1: 1.4 ± 0.3, ERK2 1.6 ± 0.4 fold over controls) (Figure III.24 and Figure III.25).
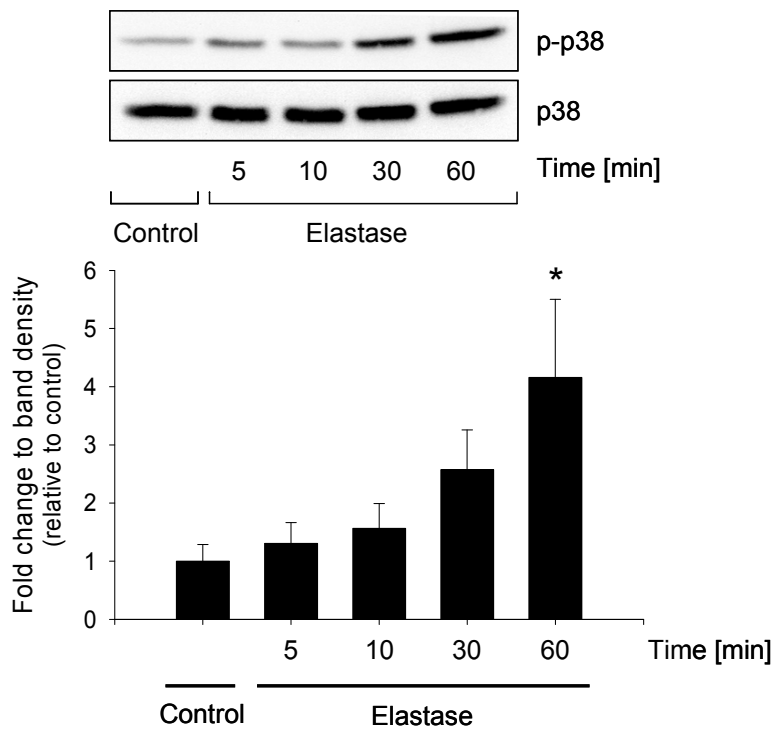
Figure III.24: Elastase causes activation of p38

Porcine pancreatic elastase treatment (0.5 U/ml) activates p38 (n = 6, mean + SEM, * p < 0.05 vs. control, 5 and 10 minutes elastase, ANOVA RM, Student-Newman-Keuls). Equal protein loading was controlled with p38. A representative blot of six separate experiments is presented.
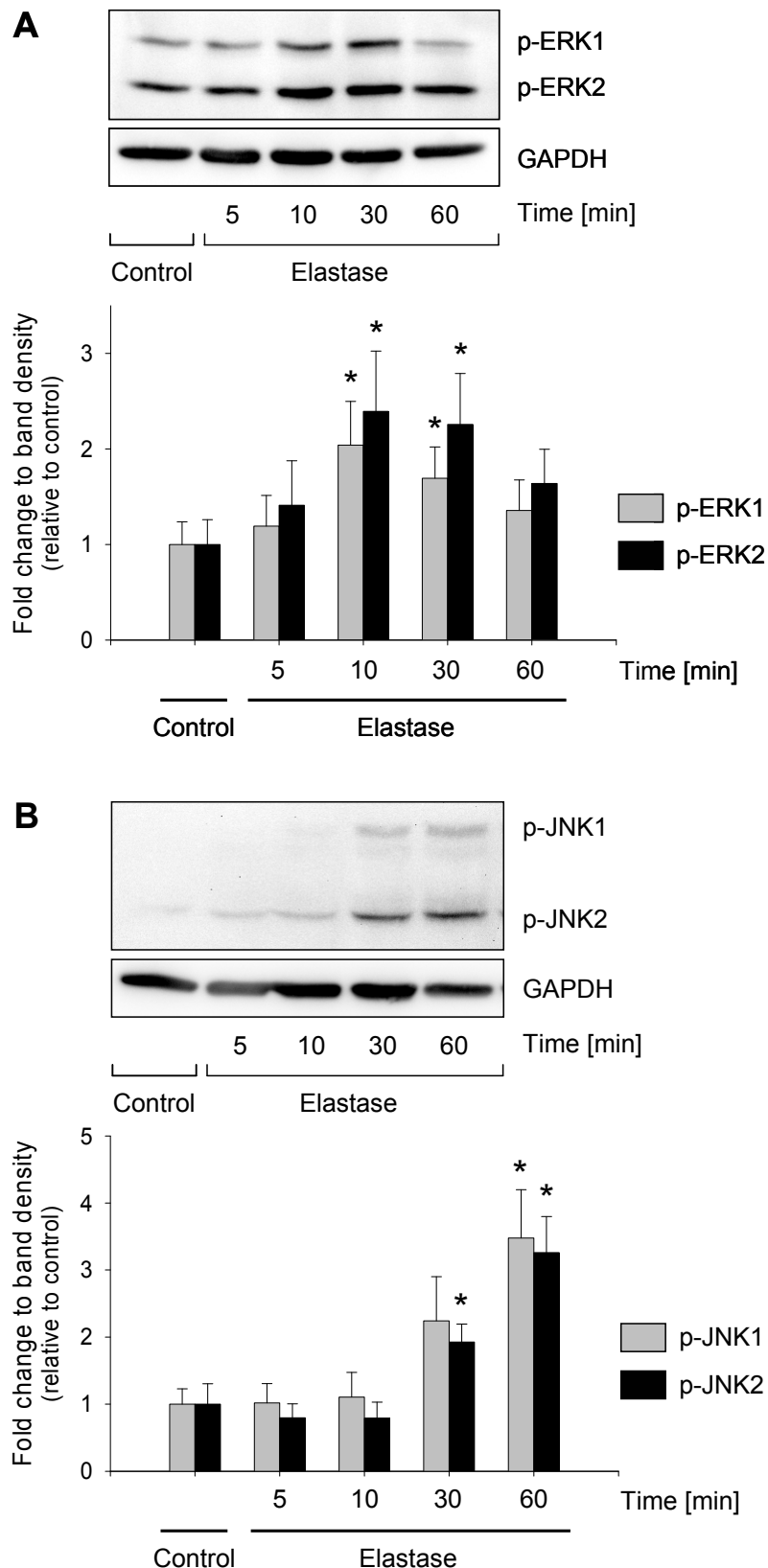
Figure III.25: Elastase causes activation of ERK and JNK

Porcine pancreatic elastase treatment (0.5 U/ml) activates (A) ERK1 (grey) and ERK2 (black) (n = 6, mean + SEM, * p < 0.05 vs. control, 5 and 60 minutes elastase) and (B) JNK1 (grey) and JNK2 (black) (n = 6, mean + SEM; * p < 0.05 vs. control, 5 and 10 minutes elastase, ANOVA RM, Student-Newman-Keuls). Equal protein loading was controlled with GAPDH. A representative blot of six separate experiments is presented.

To study whether the elastase-induced FGF-2 release was dependent on this MAP kinase activation, they were blocked using three specific inhibitors. Whereas p38 and JNK inhibition significantly decreased the FGF-2 release to $57 \pm 15\%$ and $63 \pm 17\%$ respectively, ERK inhibition had no influence on the elastase-induced release of this growth factor (Figure III.26).
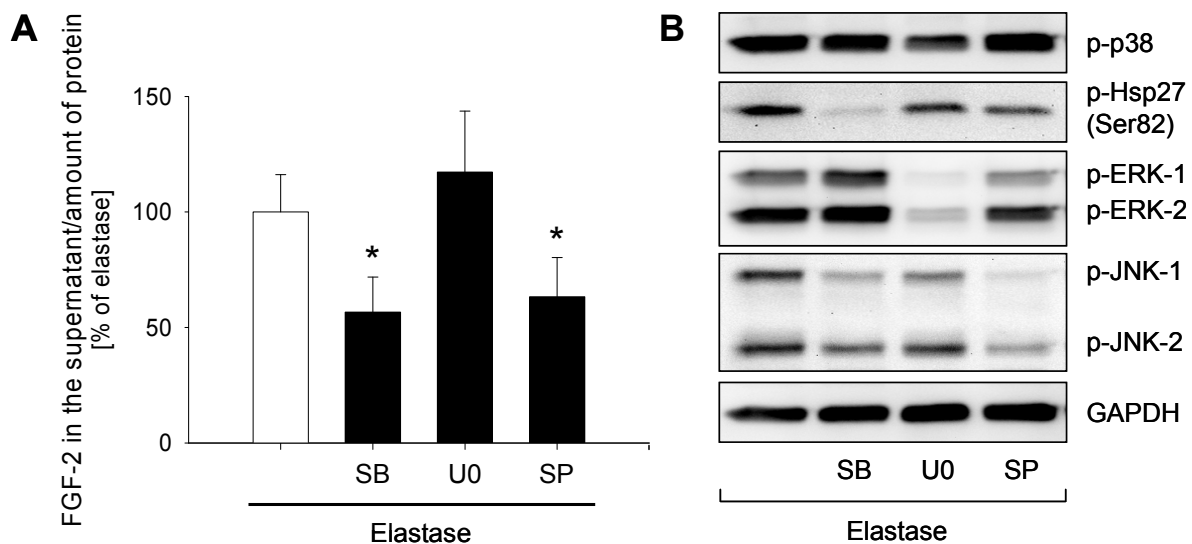
Figure III.26: P38 and JNK inhibition decrease elastase-induced FGF-2 release

Under elastase treatment (porcine pancreatic elastase, 0.5 U/ml, 60 minutes), the p38 inhibitor SB202190 (SB), the MEK1/2 inhibitor U0126 (U0) or the JNK1/2 inhibitor SP600125 (SP) (10 µM each) were used. (A) FGF-2 release in cell supernatants was analyzed using an ELISA system and normalized to protein concentration. (n = 12, mean + SEM, * p < 0.05 vs. elastase, ANOVA RM on Ranks, Student-Newman-Keuls). (B) Western blotting of cell lysates was performed to control inhibitory effects of the pharmacological substances used. Phospho-ERK and phospho-JNK levels were directly downregulated by U0126 and SP600125. Since SB202190 does not block p38 phosphorylation but its kinase activity, its downstream target Hsp27 was analyzed. Equal protein loading was controlled with GAPDH.

5.3.3   Role of Hsp27 in FGF-2 release

As shown before in our laboratory, elastase treatment induces the phosphorylation of Hsp27 and its translocation to the cell membrane [107]. To analyze a potential direct interaction of FGF-2 and Hsp27, coimmunoprecipitation experiments were performed. After 60 minutes of stimulation with porcine pancreatic elastase, a more than 3 fold higher amount of these two proteins was associated compared to untreated controls (3.3 ± 1.2 fold over control) (Figure III.27A). The overall amount of Hsp27 in these cell lysates was not affected by elastase treatment (Figure III.27B). Since the classical coimmunoprecipitation did not work reverse, sandwich ELISA experiments were performed, using the opposite order of the antibodies, namely an Hsp27 antibody as capturing and an FGF-2 antibody as detection antibody. Cells treated with 0.5 U/ml elastase showed a significantly increased interaction of FGF-2 and Hsp27 compared to controls (1.8 ± 0.1 fold over control) (Figure III.27C).

A

IP: Anti-FGF-2

IB: Hsp27

5   10   30   60   Time [min]

Control   Elastase

B

Hsp27

GAPDH

5   10   30   60   Time [min]

Control   Elastase

C
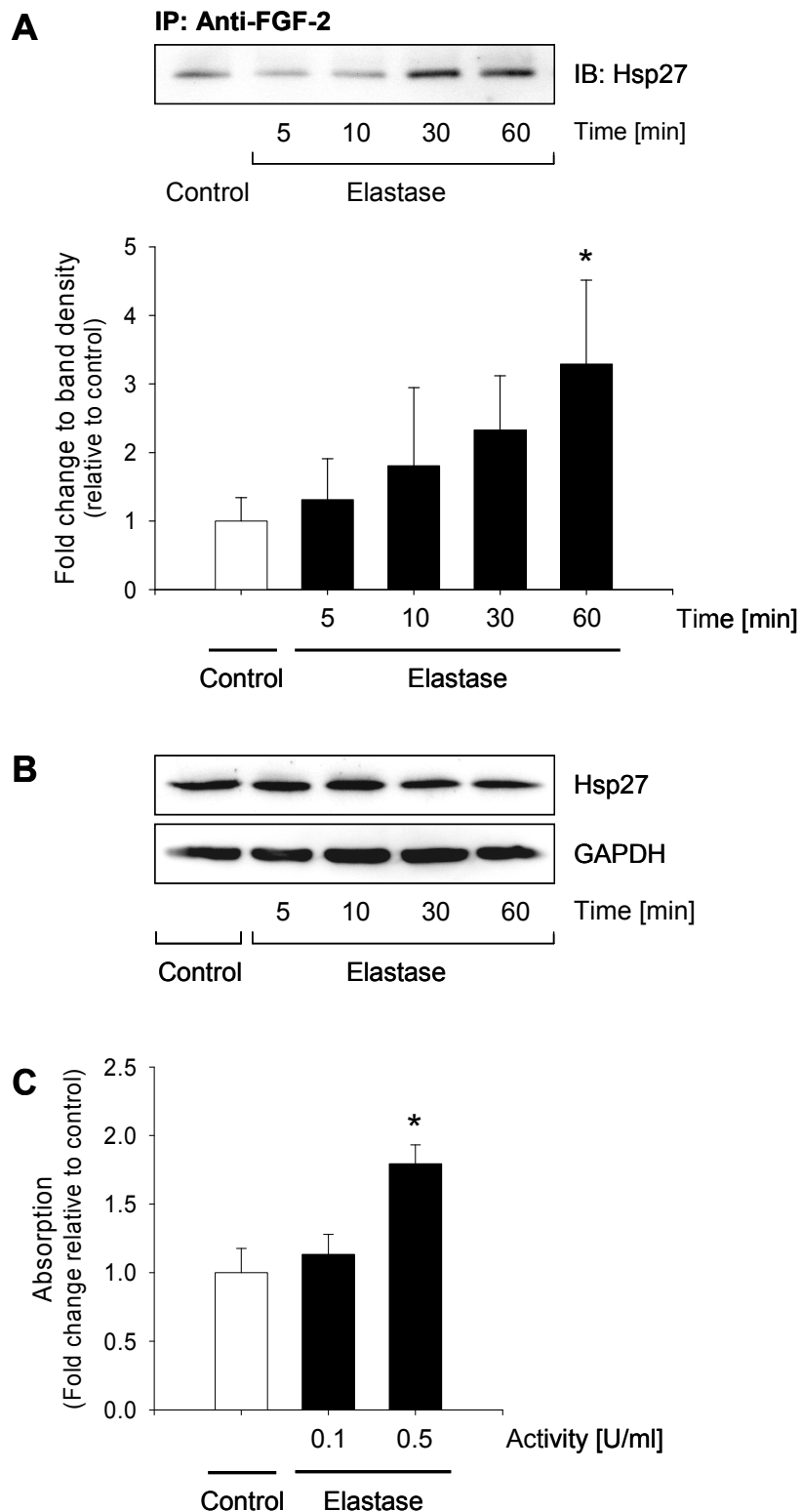
Figure III.27: Elastase induces an interaction of FGF-2 and Hsp27

(A) PAEC were treated with porcine pancreatic elastase (0.5 U/ml). To analyze the interaction of FGF-2 and Hsp27, coimmunoprecipitation experiments of FGF-2 (IP) and Hsp27 (IB) were performed (n = 4, mean + SEM, * p < 0.05 vs. control, ANOVA RM, Student-Newman-Keuls). (B) The overall amount of Hsp27 was not changed in cell lysates used for coimmunoprecipitation as shown in western blots. Equal protein loading was controlled by staining blots with GAPDH. (C) PAEC treated with porcine pancreatic elastase (0.1 U/ml and 0.5 U/ml for 60 minutes) were analyzed by a sandwich-ELISA using an Hsp27 antibody for capturing and an FGF-2 antibody for detection (n = 5, mean + SEM, * p < 0.05 vs. control, ANOVA RM on Ranks, Student-Newman-Keuls).

In order to study the direct involvement of Hsp27 in mediating the FGF-2 release, Hsp27 expression was reduced by using siRNA oligonucleotides. Protein expression analysis with western blots (Figure III.28A) revealed that after 48 hours of transfection 92% less Hsp27 protein was detected in these cells (data obtained by comparing band densities from 8 independent experiments). Knockdown of Hsp27 in PAEC lowered the elastase-induced FGF-2 release about 30% compared to cells transfected with control siRNA (Figure III.28B).
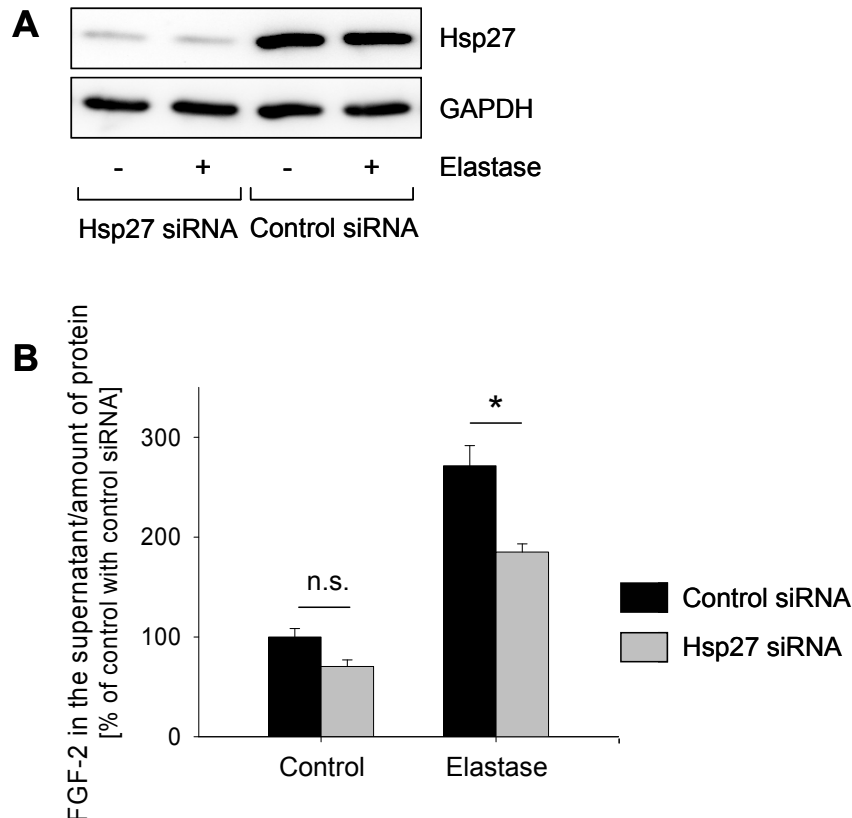
Figure III.28: Hsp27 knockdown decreases elastase-induced FGF-2 release

Cells were transfected either with control siRNA or Hsp27 siRNA (20 nM each). After 48 hours the medium was changed and cells were treated with porcine pancreatic elastase (0.5 U/ml) for 60 minutes. (A) Hsp27 knockdown efficacy was controlled using western blots (n = 4). Equal protein loading was controlled by staining blots with GAPDH. (B) The quantity of FGF-2 released to the supernatant was measured by ELISA and normalized to the protein concentrations which were determined in the appropriate cell lysate (n = 24, mean + SEM, * $p < 0.001$, n.s. = not significant, ANOVA RM, Student-Newman-Keuls).

DISCUSSION

IV DISCUSSION

The vasculature continuously undergoes remodeling not only in the embryo but throughout adult life. Vascular remodeling requires the formation of new vessels but also a permanent adjustment of existing vessels in response to functional needs. In the adult circulation, remodeling adapts vessels especially to changes in hemodynamic forces. Chronic changes in blood flow velocity and thus alterations in shear stress are one main stimulus for vessel remodeling and adaptation [41,206].

1   AN ENDOTHELIAL ELASTASE AS MEDIATOR IN MECHANOTRANSDUCTION

The present study extends previous work from our laboratory published by Gloe et al. and presented in the thesis of Christina Klarskov Mogensen. In 2002 Gloe et al. demonstrated that shear stress induces the release of FGF-2 from endothelial cells. This process was found to be specifically dependent on the integrin $\alpha_v\beta_3$ because inhibition of this integrin with RGD peptides or antibodies blocked the shear stress induced FGF-2 release, whereas inhibition of the integrin $\alpha_5\beta_1$ had no effect on this process [75]. In a follow up study, Klarskov Mogensen found a serine protease with elastase activity to be involved in the shear stress-induced FGF-2 release [107].

The current study extends these previous findings and identifies specific steps in the signaling cascade leading to shear stress-induced FGF-2 release. The main finding is that a not yet described elastase is released by shear stress leading to activation of the integrin $\alpha_v\beta_3$. Though it was not yet possible to identify the elastase, experiments with another isoform of the elastase family confirmed the specific role in the signaling process.

The involvement of proteases in angiogenesis and vascular remodeling is well established. Protease inhibitors like α1-antitrypsin have been shown to inhibit angiogenesis [94]. Marimastat was the first orally bioavailable MMP-inhibitor to have entered clinical trials in the field of oncology [160]. MMP- and specific elastase inhibitors may also be effective in the remodeling of larger vessels as they were shown to induce a regression of pulmonary artery thickening in vivo [42].

Few publications exist showing an influence of shear stress on protease activity. Those particularly examined the activity of MMPs and cathepsins. It was demonstrated that laminar shear stress increased MMP-2 and MMP-9 activity in porcine aortic valves whereas the activity and expression of cathepsin L was reduced in these valves as well as in endothelial cells [152,154]. On the other hand, oscillatory shear stress was found to increase the release of cathepsin K from endothelial cells [153]. These publications demonstrate that in principle, shear

forces can give rise to protease activity in the vascular wall in a rather specific manner and therefore might play a role in the mechanotransduction of shear stress.

The current study demonstrates that the shear stress-induced endothelial FGF-2 release was reduced by specific elastase inhibition with MeOSuc-Ala-Ala-Pro-Val-chloromethylketone. Besides, a higher elastase activity was detected in shear stress supernatants using the specific substrate MeOSuc-Ala-Ala-Pro-Val-p-nitroaniline, which is cleaved by neutrophil and pancreatic elastase [32,134], but not by other proteases, like cathepsins or matrix metalloproteinases (MMPs), which as described above were found to be released from endothelial cells as well. Thus, the involvement of other proteases from the cathepsin- or MMP-family was excluded. Since the shear stress-induced FGF-2 release was also dependent on the integrin $\alpha_v\beta_3$ which, due to its interaction with the matrix and the cytoskeleton might act as a mechanosensor of shear stress, it was conceivable that the release of the elastase occurred as a result of the integrin activation. However, since the inhibition of the integrin by abciximab had no influence on the release of elastase, activation of the integrin $\alpha_v\beta_3$ is not a necessary step for the release of elastase. Rather, our findings suggest that an enzyme with elastase activity mediates the shear stress-induced integrin $\alpha_v\beta_3$ activation.

In order to prove this hypothesis, cells were incubated with pancreatic elastase. Going in line with the shear stress experiments, the treatment with this exogenously applied elastase induced activation of the integrin $\alpha_v\beta_3$ and, probably as a consequence, release of FGF-2. This finding furthermore supported the idea of an elastase mediating the shear stress induced effects.

The presence of enzymes with an elastolytic activity in the vessel wall has previously been reported: Endothelial cells as well as smooth muscle cells and fibroblasts were shown to synthesize elastolytic enzymes [113,129]. Hornebeck et al. described an aortic elastase which exhibits an elastolytic activity similar to pancreatic elastase [92]. None of these publications analyzed which particular enzyme was responsible for the activity measured. In this thesis we show that neither mRNA nor protein of neutrophil and pancreatic elastase is expressed in human and porcine endothelial cells. However, an antibody raised against neutrophil elastase was able to detect the endothelial elastase in western blot and immunofluorescence staining, suggesting that neutrophil and endothelial elastase possess structural similarities. The protein band that was observed in western blot exhibited a molecular weight in the range of 26 to 29 kDa, similar to pancreatic and neutrophil elastase (pancreatic elastase: 27.8 kDa [Homo sapiens], 28.8 kDa [Sus scrofa], neutrophil elastase: 28.5 kDa [Homo sapiens] [171]). We propose that a vascular elastase, a serine protease with elastase activity different from neutrophil and pancreatic elastase, but with homologies to neutrophil elastase, is expressed by and released from endothelial cells. The major evidence for this conclusion is the following: (1) susceptibility to specific elastase inhibitors, (2) cleavage of the specific elastase substrate and (3) appropriate molecular weight.

1.1   ELASTASE INDUCES AN ACTIVE RELEASE OF FGF-2

As mentioned above, treatment of endothelial cells with pancreatic elastase led to a time-dependent release of FGF-2. A similar pancreatic elastase-mediated release of FGF-2 was described by Buczek-Thomas. Based on their experiments in pulmonary fibroblasts, the authors postulated that FGF-2 is released by proteolytic digestion from proteoglycan storage sites in the extracellular matrix [22,23]. They further demonstrated that the FGF-2 release correlated with the liberation of sulfated glycosaminoglycans and thereby concluded that elastase induces the release of extracellularly bound FGF-2 through disruption of matrix proteoglycans. In another study, Thompson and colleagues showed that neutrophil elastase releases FGF-2 from extracellular matrix storage sites of pulmonary smooth muscle cells [190]. In contrast to these findings, Gloe et al. demonstrated that in response to shear stress FGF-2 was released from the cytosolic pool of endothelial cells. At present it is difficult to reconcile these apparently contradictory findings. It is possible, that the amount of bound FGF-2 is much higher in the extracellular matrix and on the surface of fibroblasts and smooth muscle cells especially from the lung than in endothelial cells. In such a case, an additional release from inside the cells may be quantitatively smaller and therefore be overlooked. In the original experiments described by Gloe et al., a clear reduction of intracellular FGF-2 in response to shear stress was detected, indicating FGF-2 release from the cytosol [75]. Moreover, if FGF-2 was only released from extracellular matrix storage sites it would be difficult to explain why this purely extracellular liberation process should be stopped by inhibition of the integrin $\alpha_v\beta_3$, by MAPK inhibition or by knockdown of Hsp27. The present thesis furthermore demonstrated that application of heparinase I, an enzyme that cleaves heparin and heparan sulfate proteoglycans [122] and has been shown to release extracellular matrix bound FGF-2 [14,106], was not able to release FGF-2 in our setting. Therefore, the present data suggest that cytosolic FGF-2 is released by endothelial cells as a consequence of the complex signaling cascade described in this work.

Engling et al. demonstrated that chinese hamster ovary (CHO) cells transfected with FGF-2 release the growth factor continuously [56]. The present study also reveals that a basal amount of FGF-2 at low levels is released under static conditions. In contrast to the findings in CHO cells, in our endothelial cells, the release of FGF-2 strongly increased after exposure to shear stress or external application of pancreatic elastase. This may be due to the different cell types used. While Engling et al. used CHO cells that are subcultivated for a long period of time, we used freshly isolated, primary endothelial cells. Moreover, cells transfected with FGF-2 may respond differently as cells that naturally express the protein. In our view, primary endothelial cells were a valid model to investigate conditions appearing in the intact vessel.

As shear stress exerts a force on the cells, one can furthermore argue that cytosolic FGF-2 is set free as a result of cell damage, a mechanism that was suggested by several groups. This

can be excluded in the present setting, because experiments of Gloe et al. showed that shear stress of the magnitude and duration applied here did not result in membrane damage [75]. Additionally, integrin inhibition would not block FGF-2 release if it was set free as a result of cell damage.

Also, cells treated with elastase in a concentration of 0.5 U per ml, as used in the experiments performed here, did not show any sign of membrane damage. As demonstrated by Klarskov Mogensen, elastase treated cells were viable with intact cell membranes which was shown by negative staining for propidium iodide [107]. Moreover, experiments performed in this study revealed no measurable release of lactate dehydrogenase after elastase treatment (data not shown). Thus, the release of FGF-2 must be a regulated and active process.

We investigating whether elastase affects the de novo synthesis of FGF-2 and demonstrated that exposure of endothelial cells to pancreatic elastase had no effect on FGF-2 mRNA expression as assessed after 8 and 16 hours of elastase treatment.

Comparing these results with data from the literature that analyzed the de novo synthesis of FGF-2 after shear stress, controversial results have been found. Application of shear stress of 20 dyn/cm² increased FGF-2 expression as shown in porcine aortic endothelial and smooth muscle cells after 24 hours of stimulation [201]. Investigating bovine aortic endothelial cells Malek et al. described only a mild but transient increase in FGF-2 mRNA levels at shear forces of 15 dyn/cm², whereas higher flow velocities of 32 dyn/cm² induced a significant increase after 6 hours [125].

In vivo physical exercise, which is linked to increasing shear levels, was shown to increase FGF-2 expression in the hippocampus of rats after the fourth night of wheel running [76]. By contrast, only 45 minutes of one-legged exercise in humans had no effect on FGF-2 mRNA levels [83]. Finally, Deindl et al. demonstrated that, in arteriogenesis, a process with strongly increased shear levels, FGF receptor 1 expression levels increased in growing collateral arteries. However FGF-2 mRNA was not upregulated [49].

1.2   INTRACELLULAR STORAGE OF ENDOTHELIAL ELASTASE

As it was shown that an elastase mediates the shear stress-induced release of FGF-2, the intracellular storage sites of this enzyme in endothelial cells were further examined. In microglia an elastase or elastase-like protein was described which is secreted and detectable in the conditioned medium [135]. For neutrophils it is well known that their elastase content is stored in intracellular azurophilic granules and liberated after activation of the cells.

In endothelial cells, Weibel-Palade bodies, which allow for fast protein secretion in relative high amounts, are the main storage bodies. Previously it was demonstrated that shear stress induces the exocytosis of these Weibel-Palade bodies [67]. The experiments presented here showed that vWF, the main content of these vesicles, colocalizes with elastase within the cell.

Furthermore, similar release kinetics of both these proteins were observed. Whereas the intracellular contents of vWF and elastase decreased after 240 minutes of shear stress application, the secreted amount increased. Therefore, the here presented observations are consistent with the hypothesis that both proteins are stored together in Weibel-Palade bodies and are released together in response to mechanical stimulation of endothelial cells by shear stress.

It has to be mentioned that after 120 minutes of shear stress stimulation vWF and elastase were detectable outside the cells, whereas inside these cells no decrease in the amount of both proteins was measurable with western blots at this time point. This was probably due to the fact that only a small fraction of the overall protein content is released. The supernatant fraction was concentrated and therefore these amounts of protein were easier to measure. After 240 minutes of shear stress application the intracellular content of vWF and elastase measurably decreased compared to static cells. The parallel time dependencies in vWF and elastase release furthermore supported the idea of both proteins being released together.

2   ELASTASE INDUCES INTEGRIN OUTSIDE-IN SIGNALING

In 2002, Gloe et al. showed that integrin $\alpha_v\beta_3$ is strongly involved in the signaling process linking shear stress to FGF-2 release, since inhibition of the integrin $\alpha_v\beta_3$ blocked the shear stress induced release of FGF-2 [75].

The current study demonstrates that shear stress indeed induces integrin $\alpha_v\beta_3$ activation as assessed by the enhanced interaction of the integrin $\alpha_v\beta_3$ and its adaptor protein Shc. This association was reduced when incubating the cells with a specific elastase inhibitor, indicating that elastase is mediating the shear stress-induced integrin activation and again confirming that the integrin is located downstream of elastase in the signaling cascade. Furthermore, we showed that exogenously applied pancreatic elastase increased the interaction of the integrin $\alpha_v\beta_3$ and Shc as well. The time course observed here (significant activation after 10 minutes, that last till 60 minutes of stimulation) agreed with the one observed by Chen and colleagues after shear stress administration [36]. In 2001, Jalali and coworkers already demonstrated that shear stress increased the association of the integrin $\alpha_v\beta_3$ and Shc in endothelial cells. Consistent with the role of elastase, cells plated on fibronectin and vitronectin for 2 hours showed integrin $\alpha_v\beta_3$ activation but not those grown on collagen type I or laminin [98]. Tzima et al. also demonstrated that shear stress activates the integrin $\alpha_v\beta_3$ in endothelial cells using an independent method i.e. an antibody that selectively detects the activated integrin $\alpha_v\beta_3$ called WOW-1 [194].

Integrins can be principally activated by extracellular cleavage [178], phosphorylation, conformational changes, clustering or the exposure of new binding sites in the extracellular matrix. Integrin activation by direct proteolytic cleavage was excluded in our system, because

exposure to elastase did not alter the size of the integrin α_v subunit, and therefore did not cleave the integrin (Gloe, unpublished data). Moreover elastase had no effect on FGF-2 release when acting on endothelial cells in suspension [107].

The ability of proteases to generate integrin-mediated intracellular signals by remodeling the matrix has previously been demonstrated [57]. To investigate the effect of elastase on the macrostructure of the extracellular matrix, different matrix proteins were incubated with pancreatic elastase. Since the capability of elastases to degrade elastin is well known, this was not investigated in this study. Pancreatic elastase was found to degrade fibronectin, laminin and vitronectin, whereas collagen type I and IV were not affected. Data from the literature showed a comparable but slightly different activity for neutrophil elastase: It cleaves fibronectin and laminin but also collagen type IV [51,86,127,200]. In the case of collagen type I contradictory results exist. Whereas Kafienah proposed neutrophil elastase to be capable of degrading this collagen [102], the group around Dunsmore showed that total lung collagen was not increased in neutrophil elastase-deficient mice [52]. Therefore the degradation profile of the two elastolytic enzymes seems to differ especially in their effect on collagens. Since human neutrophil elastase and porcine pancreatic elastase are 43% homologue, these different degradation properties may be explained by changes in several residues [179].

Since in our study the activation of the integrin $\alpha_v\beta_3$ was investigated, the influence of elastase on major integrin $\alpha_v\beta_3$ ligands was most interesting. The integrin serves as receptor for RGD-containing proteins, predominantly vitronectin, fibronectin, laminin and fibrinogen [37,93]. By contrast, attachment of this integrin to collagens has not been described. Orr et al. demonstrated that flow induced the activation of the integrin $\alpha_v\beta_3$ only in cells grown on fibronectin or fibrinogen, but not on collagen type I [142]. Moreover, Cai and colleagues demonstrated that cells grown on fibronectin expressed high levels of integrin $\alpha_v\beta_3$ and $\alpha_5\beta_1$ as well as FAK and phospho-FAK (Tyr397), whereas cells cultured on laminin express lower levels of FAK and the integrins [28]. Thus, we suggest that the integrin $\alpha_v\beta_3$ is activated by only a few matrix components including fibronectin.

Immunofluorescence experiments revealed that the effect of pancreatic elastase on fibronectin was most prominent, compared to other extracellular matrix components. Whereas the macrostructure of vitronectin and laminin matrices was only slightly changed, the extracellular fibronectin network almost completely disappeared after elastase treatment. Similar, but less pronounced effects were detected after the application of shear stress supernatant containing endothelial elastase, or direct exposure to shear stress. Other groups showed that after 12 hours of shear stress exposure, using 24 or 30 dyn/cm², respectively, fibronectin levels in the extracellular matrix were lower than in static controls [82,191]. This may also be explained by the mechanisms described here i.e. due to proteolytic degradation of matrix fibronectin by elastase.

Furthermore it was shown here that fibronectin fragments are released to the supernatant by pancreatic elastase stimulation. For neutrophil elastase McDonald et al. demonstrated that

incubation of fibronectin with this enzyme produced biologically active fragments with cell-adhesive and gelatin-binding activity [127]. Moreover, Loeser et al. demonstrated in chondrocytes that a 120 kDa fibronectin, a chymotryptic fragment, as well as a 110 kDa fibronectin fragment are able to activate the ERK1/2, JNK and p38 MAP kinase [63,124]. Henriksen and coworkers provided evidence that the action of neutrophil elastase on elastin, collagen, fibronectin and proteoglycans exposes new recognition sites that bind integrins [89].

In the current study three different modes of integrin $\alpha_v\beta_3$ activation have to be considered: (1) direct integrin activation by fibronectin fragments, (2) exposure of new laminin, vitronectin or fibronectin binding sites that directly activate integrins or (3) alterations of the macrostructure of the matrix that may provoke integrin (re-)clustering or conformational changes and thereby, indirectly, their activation.

Girard and colleagues demonstrated that the integrin $\alpha_v\beta_3$ is present in focal contacts [73]. Focal adhesion activation provides a mechanism for integrins to transduce signals from the extracellular matrix into the cell. The most definitive evidence that FAK, the most prominent member of focal adhesions, is directly downstream of signals initiated by the extracellular matrix is the finding, that the phenotype of FAK null-embryos strongly resembles that of fibronectin deficient mice. They both display almost identical vascular defects [96]. These similarities supported the idea that FAK and fibronectin are part of the same signaling pathway.

Several reports demonstrated that shear stress influences the arrangement of focal adhesions [47,73,176]. Shikata and colleagues showed that in endothelial cells exposed to shear stress, focal adhesions are redistributed and accumulate in the cell periphery [176]. Galbraith and coworkers furthermore demonstrated that this redistribution allows the endothelial cells to remain attached in the face of the fluid force [66].

To further evaluate the role of focal contacts in our setting, the effect of elastase on these adhesion points was investigated. Own experiments with pancreatic elastase demonstrate that focal contacts, as assessed by ILK and FAK staining, were reorganized after treatment with pancreatic elastase. Under basal conditions focal contacts appeared as thin fibers whereas after 60 minutes of elastase stimulation the spatial structure of these focal adhesions appeared completely different. They now appeared as big pronounced dots which were situated mainly in the cell periphery. In between these two events, after 5 minutes of stimulation, the FAK and ILK staining in the cell periphery vanished almost completely. The different appearance of the focal contacts before and after stimulation may be due to different matrix-integrin interactions. This conclusion is consistent with findings of Honore et al., who showed that, depending on the matrix composition and the specific integrin, focal points appear quite different [90]. When examining FAK phosphorylation, we observed a time-course similar to that in immunofluorescence experiments on focal adhesion changes. The basal as well as the activated state were characterized by FAK phosphorylation, whereas in the meantime the protein was dephosphorylated.

Based on these findings the following model of focal adhesion activation is proposed. In untreated controls FAK has a constitutive basal activity, which may allow for the association to integrins and therefore their anchoring to the extracellular matrix, providing cell adhesion. Direct elastase stimulation leads to changes in the matrix and activates the integrin $\alpha_v\beta_3$, which results in FAK activation, focal adhesion assembly and reorganization. This may on the one hand increase cell matrix adhesion which stabilize the cells and on the other hand induce intracellular signaling. As already mentioned, in between the basal and activated state FAK was dephosphorylated. By investigating this state with immunofluorescence experiments we found that the FAK/ILK focal contacts were disappeared in the cell periphery. However, cells stayed attached, indicating that at this point cells may be connected to the matrix via other structures than FAK and ILK composing focal adhesions.

Tzima et al. showed a similar biphasic regulation of Rho activity after shear stress treatment. They observed a decrease in Rho activity after 5 to 15 minutes of shear stress that was followed by an increase which peaked at 60 minutes [194]. This is interesting since Rho is a key regulator of the actin cytoskeleton and strongly implicated in the formation of stress fibers [6,85]. This protein can be activated by integrins inducing maturation of cell contacts to form actin stress fibers, with associated increases in FAK activity [173]. Therefore Rho and FAK activity might be linked together, explaining the identical activation profile after shear stress or elastase application, respectively.

Focal adhesions are directly connected to the actin cytoskeleton. Activation of FAK can lead to actin remodeling and stress fiber formation [71]. The development of stress fibers in cultured endothelial cells exposed to shear stress has been demonstrated by several groups [65,126,138]. That is why we investigated the effect of elastase on F-actin. Endothelial cell stimulation with pancreatic elastase induced the formation of stress fibers. It remains elusive, however, by which signaling pathway this may be transduced. As Rho activation has been directly linked to stress fiber formation, the effect could be directly induced by Rho activation. Alternatively, as has been published before, p38 and Hsp27 could be involved in actin polymerization and cytoskeletal remodeling [149], both proteins being activated after elastase treatment in our experiments. Therefore stress fiber formation may alternatively, or in addition, be a consequence of MAPK and Hsp27 activation.

3   INTRACELLULAR SIGNALING CASCADES INVOLVED IN FGF-2 RELEASE

Whereas the biological functions of FGF-2 are well characterized [139], the mechanisms leading to its release remain elusive. Also, the release mechanism itself is unclear, since FGF-2 lacks a signal sequence needed for classical protein secretion via the endoplasmic reticulum and Golgi apparatus. The following chapter will focus on some of the intracellular mechanisms involved in FGF-release as assessed in this work.

3.1   MAPK PATHWAYS INVOLVED IN FGF-2 RELEASE

In this study, we demonstrate that shear stress exposure activates all three main MAPK, which are p38, ERK and JNK. Furthermore, it was demonstrated that elastase inhibition reduced the shear stress-induced p38 activation, whereas ERK activation was not inhibited.

Christina Klarskov Mogensen showed that cell stimulation with pancreatic elastase for about 60 minutes induced p38 activation whereas ERK phosphorylation was not affected at this time [107]. The experiments performed in this study extended these data analyzing the time course of MAPK activation after 5, 10, 30 and 60 minutes of elastase stimulation. These experiments show that not only p38 but also ERK and JNK are activated by elastase although they exhibit different activation kinetics. Whereas p38 and JNK were maximally activated after 60 minutes; ERK activation peaked already at 10 to 30 minutes to reach control levels again after 60 minutes of stimulation, which explains why Klarskov Mogensen did not detect ERK activation. Data from the literature revealed similar time courses of MAPK activation after shear stress application. Li and coworkers demonstrated that maximal ERK phosphorylation is reached earlier than p38 and JNK activation, which peaked around 20 minutes later [120].

To test which of these kinases is involved in FGF-2 release, inhibitors were used that specifically block each MAPK pathway (see Figure I.13). While inhibiting p38 and JNK significantly reduced FGF-2 release, blocking ERK did not alter the amount of FGF-2 secreted in response to elastase treatment. Thus the experiments presented here, demonstrated that only p38 and JNK play a role in the process of shear stress-induced FGF-2 release.

As it was shown by several groups that inhibition of the integrin $\alpha_v\beta_3$ blocked the shear stress-induced activation of p38, ERK and JNK [98,114,118], it is reasonable to argue that flow-induced MAPK phosphorylation is mediated via this integrin. This is further supported by previous findings of our laboratory, which demonstrated that elastase-induced p38 activation can be blocked with the integrin $\alpha_v\beta_3$ blocker abciximab [107]. This is also in accordance with results reported by Chen et al. showing that inhibition of α_v integrins or downregulation of their expression decreased active levels of p38 [35]. The precise signaling pathway connecting the integrin and MAP kinase activation is still elusive in our setting. However, since shear stress and elastase stimulation induced the association of the integrin $\alpha_v\beta_3$ with its adaptor protein

Shc and, in addition to that, the formation of new focal adhesion points, downstream signaling may be transduced via Shc or focal contact proteins like FAK (see Figure I.11).

3.2   INVOLVEMENT OF HSP27 IN FGF-2 RELEASE

Heat shock proteins are molecular chaperones that are required for protein folding. Wesche et al. provided evidence that the Hsp90 molecule is crucial for the translocation of FGF-1 and FGF-2 from endosomes into the cytosol [202], indicating that this class of proteins may be involved in protein translocation. Piotrowicz and colleagues proposed that the Hsp27 protein facilitates the release of FGF-2 from bovine aortic endothelial cells by interacting with it. They demonstrated that the expression of Hsp27 doubled the rate of FGF-2 secretion, whereas a decrease in the endogenous Hsp27 level decreased FGF-2 release [150]. Morover, Cao et al. showed that the thrombin-induced release of FGF-2 is reduced by Hsp27 knockdown [30]. Therefore the role of Hsp27 in elastase-induced FGF-2 release was further examined.

In the present work the association of FGF-2 and Hsp27 was investigated after elastase stimulation using two different approaches, on the one hand a coimmunoprecipitation assay and on the other hand an ELISA. It was shown that after 60 minutes of elastase treatment the association of the two proteins was significantly increased compared to untreated controls. In addition, to clarify whether Hsp27 is necessary for the release of FGF-2, Hsp27 knockdown experiments were performed. This knockdown reduced FGF-2 release by 30%. Therefore Hsp27 has been shown to play a significant role in FGF-2 release, but the reduction of FGF-2 release was limited. Two explanations come into consideration to account for the incomplete reduction of FGF-2 release. Firstly, the release of FGF-2 via Hsp27 may not be the only pathway and other mechanisms or molecules additionally or alternatively facilitate the release. Secondly, as the knockdown experiments did not totally eliminate Hsp27 expression (about 8% of the Hsp27 protein were still expressed), the small amount left may be sufficient to allow for the remaining release of FGF-2.

The involvement of Hsp27 in FGF-2 release has already been investigated by Christina Klarskov Mogensen in our laboratory. She demonstrated that shear stress exposure as well as treatment with pancreatic elastase induced a translocation of FGF-2 and Hsp27 to the cell membrane with similar time courses. Furthermore, she showed that both kinds of treatment led to Hsp27 phosphorylation. This happened in an integrin $\alpha_v\beta_3$ and p38 dependent manner, because pretreatment with abciximab or SB202190 blocked Hsp27 phosphorylation under these conditions [107].

Summarizing the here presented novel data and previous findings from Klarskov Mogensen, it can be concluded that elastase stimulation induces the formation of a complex of FGF-2 and Hsp27 that translocates to the membrane. Therefore we propose that the Hsp27 molecule

assists the cellular transport of FGF-2 towards the membrane and therefore is one important factor facilitating the release of FGF-2.

These findings were supported by data from the literature showing that the same stimuli that lead to a release of FGF-2 also lead to Hsp27 phosphorylation (see chapter I.3.4.1 and I.4.2), indicating that Hsp27 is not only required for the release of FGF-2 during shear stress but for multiple other stimuli. Whether the heat shock protein is also required for the passage of FGF-2 through the membrane is still unclear.

4   IMPLICATIONS OF FGF-2 ON VASCULAR REMODELING

Application of recombinant FGF-2 has been shown to increase angiogenesis and arteriogenesis in experimental in vivo models [11]. Factors that lead to the release of FGF-2 may therefore facilitate developmental processes, angiogenesis or vascular remodeling. Shear stress induces the release of FGF-2 from endothelial cells as shown by Gloe et al. in vitro and by Lepidi et al. from veins in vivo [75,115].

Exercise training is a physiological situation with at least temporarily elevated shear levels. Accordingly, it was demonstrated that circulating FGF-2 is enhanced acutely after maximal exercise [29] and chronically after 6 months of exercise training [174]. Jensen el al. showed that exercise training induces capillary growth and a transient proliferation of endothelial cells within 4 weeks, and therefore stimulates angiogenesis, but they did not relate their findings to FGF-2 release [100]. However, the findings of enhanced FGF-2 release are not conclusive since other groups reported no change [79] or even a decrease in FGF-2 levels [54] after exercise.

FGF-2 does not only support angiogenesis but also vascular remodeling in arteriogenesis. It is proposed that FGF-2 released from cells of the vessel wall attracts and activates monocytes, which then in turn supply FGFs to the growing collateral arteries and thereby promote arteriogenesis in a paracrine manner [49]. Bryant et al. identified FGF-2 as an important factor in vascular remodeling, not only regulating vascular tone but also inward remodeling, as antibodies against FGF-2 attenuated inward remodeling in a mouse model of carotid artery flow cessation [21]. However, lack of FGF-2 in mice did not affect structural remodeling of large arteries in response to chronically altered blood flows and had furthermore no effect on angiogenesis and arteriogenesis after femoral artery ligation [183,184].

The results of the presented study implicate that higher levels of shear forces caused by exercise training or in arteriogenesis may be linked to increasing levels of FGF-2 in the vessel. Thus, FGF-2 signaling is induced, which increases cell proliferation, migration and differentiation and thereby contributes to vascular remodeling processes.

5   LIMITATIONS OF THE STUDY

All experiments presented here were performed using primary endothelial cells, most assays with porcine endothelial cells (PAEC) and some using human endothelial cells (HUVEC). Usage of human cells throughout the whole study was impractical due to limited access to umbilical cords and slow growing properties of these cells. By contrast, PAEC were available in higher quantity, easier to handle, less susceptible and growing much faster. Moreover, arterial endothelial cells corresponded better to our model than venous cells. Due to high protein sequence homologies between human and pig, most antibodies raised against the protein of human origin also detected the porcine one. Only the vWF ELISA did not work with porcine cells, therefore the assay was performed using HUVEC.

As mentioned before, the two types of endothelial cells used here differ in their vessel origin: PAEC are arterial endothelial cells, HUVEC are venous endothelial cells. The data from Gloe et al. were obtained using HUVEC [75]. In contrast, Klarskov Mogensen's data and the data presented here were obtained mainly studying PAEC [107]. As experiments with the two cell types, produced comparable results, we would suggested that the mechanisms for FGF-2 release proposed here can be found in arterial and venous vessels to the extent that cultured cells represent their tissue of origin. However, as arteries and veins do not only vary in diameter and structure, but also in their function, it is hard to compare them, especially due to the fact that venous endothelial cells under physiological circumstances are hardly exposed to shear stresses exceeding 6 dyn per cm² and were therefore exposed to "non-physiological" levels in this case.

The shear stress applied here was within a range that can be observed in small arteries and therefore reflects a relevant physiological level especially with respect to arteriogenesis. However, it must be stated that only short-term effects of elevated shear stress were analyzed here. Therefore it is not possible to conclude that chronic shear stress still maintains a chronic level of elastase release and the subsequent signaling cascade or whether the cascade of events described here always requires a major change of the actual shear stress.

The use of static endothelial cells as controls does not reflect a physiological situation, because in vivo endothelial cells are continuously exposed to blood flow. However, a system which allows the long-term application of shear stress limits the experimental capacity considerably and was, therefore, not available for this study. Therefore, we cannot exclude that comparing different levels of shear stress would yield the same results as comparing no shear stress with arterial shear stress.

Although this study showed that a new type of elastase is expressed in endothelial cells, its identity and therefore its structure is not yet known. With one of the antibodies the enzyme was detected in western blot. Moreover, immunofluorescence experiments and electron microscopy were performed in search of intracellular localization. Protein purification

techniques such as immunoprecipitation followed by mass spectrometry are going to be applied but will not contribute to the results of the present manuscript due to time constraints. Since the endothelial elastase was not identified here, we were forced to use another enzyme that also exerts an elastolytic activity for experiments with elastase stimulation. Therefore we used porcine pancreatic elastase. Although this enzyme might not have a completely identical substrate spectrum, we obtained comparable results when using shear stress and exogenously applied pancreatic elastase (see Table IV.1). Overall the same signaling cascades were activated by both stimuli. Therefore we propose that the activities of endothelial elastase and pancreatic elastase are comparable with regard to our model.

Regarding the specificity of elastase, it seemed an obvious approach, to investigate whether the shear dependent activation of the intracellular signaling cascades depends on various specific protein matrices. Since, as mentioned before, fibronectin but not collagen type I is a ligand of integrin $\alpha_v\beta_3$ and a substrate for pancreatic elastase, cells were grown on glass plates coated with either collagen type I or fibronectin for 24 hours. However, cells originally seeded on collagen type I had secreted significant amounts of fibronectin within this time period, thereby changing the composition of the extracellular matrix. Thus, all effects which were observed in cells originally grown on collagen type I, may as well be a consequence of fibronectin signaling.

However, our idea of shear stress being mediated via fibronectin, was recently supported by Hahn et al., who demonstrated that cells seeded onto fibronectin showed a marked increase in JNK phosphorylation in response to flow, whereas cells on collagen type I showed no activation compared to static controls [84]. They, in contrast to us, performed their experiments after 4 hours of seeding time. Indeed, cells in our system had not been highly adherently and confluent after 4 hours of seeding time, which is why we performed shear stress experiments later.

Lastly, for a more accurate prediction of the results obtained in endothelial cell cultures in vitro, they need to be verified with an in vivo model, for example using an exercise or an arteriogenesis model, processes that involve increasing blood velocities.

Table IV.1: Comparison of results obtained after shear stress exposure and application of pancreatic elastase including the specific reference

Treatment Effect	Shear stress exposure (16 dyn/cm²)		Elastase treatment (0.5 U/ml)	
	Result	Figure/ Reference	Result	Figure/ Reference
FGF-2 release + elastase inhibition + integrin $\alpha_v\beta_3$ inhibition	Increase Reduction Reduction	Figure III.2 Figure III.2 Figure III.2	Increase ----------- Reduction	Figure III.10 Klarskov, 2006
FGF-2 cell surface localization + integrin $\alpha_v\beta_3$ inhibition	Increase Not tested	Klarskov, 2006	Increase Reduction	Klarskov, 2006 Klarskov, 2006
FGF-2 expression	Slight increase	Chien, 1998	No effect	Figure III.11
Fibronectin degradation	Slight restructuring	Figure III.15 Orr, 2006	Degradation	Figure III.14 Figure III.15
Interaction of integrin $\alpha_v\beta_3$ and Shc + elastase inhibition	Increased interaction Reduction	Figure III.17 Figure III.17	Increased interaction ----------	Figure III.18
Focal adhesion rearrangement	Rearrangement	Davies, 1994 Girard, 1995 Shikata, 2005	Rearrangement	Figure III.19 Figure III.20 Figure III.21
Stress fiber formation	Increase	Franke, 1984 Malek, 1996 Noria, 2004	Increase	Figure III.22
p38 phosphorylation + elastase inhibition + integrin $\alpha_v\beta_3$ inhibition	Increase Reduction Not tested	Figure III.23A Figure III.23B	Increase ---------- Reduction	Figure III.24 Klarskov, 2006
ERK phosphorylation	Increase	Figure III.23A	Increase	Figure III.25A
JNK phosphorylation	Increase	Figure III.23A	Increase	Figure III.25B
Hsp27 in membrane fraction (translocation) + integrin $\alpha_v\beta_3$ inhibition + p38 inhibition	Increase Not tested Not tested	Klarskov, 2006	Increase Reduction Reduction	Klarskov, 2006 Klarskov, 2006 Klarskov, 2006
Hsp27 phosphorylation + integrin $\alpha_v\beta_3$ inhibition + p38 inhibition	Increase Not tested Reduction	Klarskov, 2006 Azuma, 2001	Increase Reduction Reduction	Klarskov, 2006 Klarskov, 2006 Klarskov, 2006
Interaction of Hsp27 and FGF-2	Not tested		Increased interaction	Figure III.27
Hsp27 Knockdown	Not tested		Reduction of FGF-2 release	Figure III.28

SUMMARY

V SUMMARY

Chronic elevation of shear stress is considered to be one of the most powerful stimuli for vascular remodeling, which requires control of cell proliferation, migration and differentiation, events that are known to be regulated by growth factors. Fibroblast growth factor-2 (FGF-2) which is stored within the endothelium has been shown to be released from cells exposed to shear stress.

The objective of the present study was to identify and characterize the mechanisms of shear stress-induced FGF-2 release in endothelial cells, regarding integrin outside-in signaling and intracellular signaling pathways.

Using cultured porcine aortic endothelial cells (PAEC), which were exposed to arterial levels of laminar shear stress, we showed that shear stress was associated with the appearance of an elastase activity in the supernatant. Activation of the integrin $\alpha_v\beta_3$ was not necessary for the release of elastase; however, the integrin was indispensable for the shear stress-mediated FGF-2 release, suggesting that the integrin $\alpha_v\beta_3$ activation is downstream of the elastase release. As specific inhibition of elastase activity prevented FGF-2 release, we propose that an elastase mediates the shear stress-induced FGF-2 release. This endothelial elastase, a serine protease with elastase activity, differs from the hitherto described elastases – neutrophil and pancreatic elastase – since both elastases could not be detected by RT-PCR in PAEC. The enzyme colocalized with von Willebrand factor, indicating that endothelial elastase is stored in the Weibel-Palade bodies. As the molecular structure of this enzyme is still not known, knockdown experiments were not possible. Instead, we studied the effect of exogenously-applied pancreatic elastase to further clarify the effects of an elastase on FGF-2 release. In fact, treatment with porcine pancreatic elastase resulted in a FGF-2 release from static cells similar to that induced by shear stress. Pancreatic elastase induced extracellular matrix alterations, thereby affecting vitronectin, laminin and especially the extracellular macrostructure of fibronectin. Similar effects were observed after exposing matrix layers to the elastase-containing supernatant of PAEC exposed to shear stress. Elastase treatment further resulted in activation of the integrin $\alpha_v\beta_3$ and reorganization of focal adhesion sites, indicating an active outside-in signaling. The latter could be linked to activation of the MAP kinases p38 and JNK as well as the downstream p38 target Hsp27.

Since we could show that both stimuli – shear stress and exogenously applied elastase – activate the same signaling pathway, the following model is proposed: Elastase, which is released from the endothelium as a consequence of shear stress exposure, alters extracellular matrix components, among them fibronectin, a ligand for $\alpha_v\beta_3$, thereby inducing a remodeling of the matrix's macrostructure. As a consequence, the integrin $\alpha_v\beta_3$ is activated, and focal adhesions rearrange to build newly organized focal contacts. This is a signal to activate the MAP kinases p38, ERK and JNK. However, only p38 and JNK phosphorylation is necessary

for the release process of FGF-2. This cascade ultimately leads to the interaction of Hsp27 with FGF-2, thereby facilitating the release of the growth factor (see Figure V.1).

In summary, we present a new model for the transduction of shear stress into extracellular matrix-dependent signals, integrin outside-in signaling and FGF-2 release via a novel endothelial elastase. The cascade presented here may represent a necessary initial step in the adaptive remodeling process induced by shear stress.
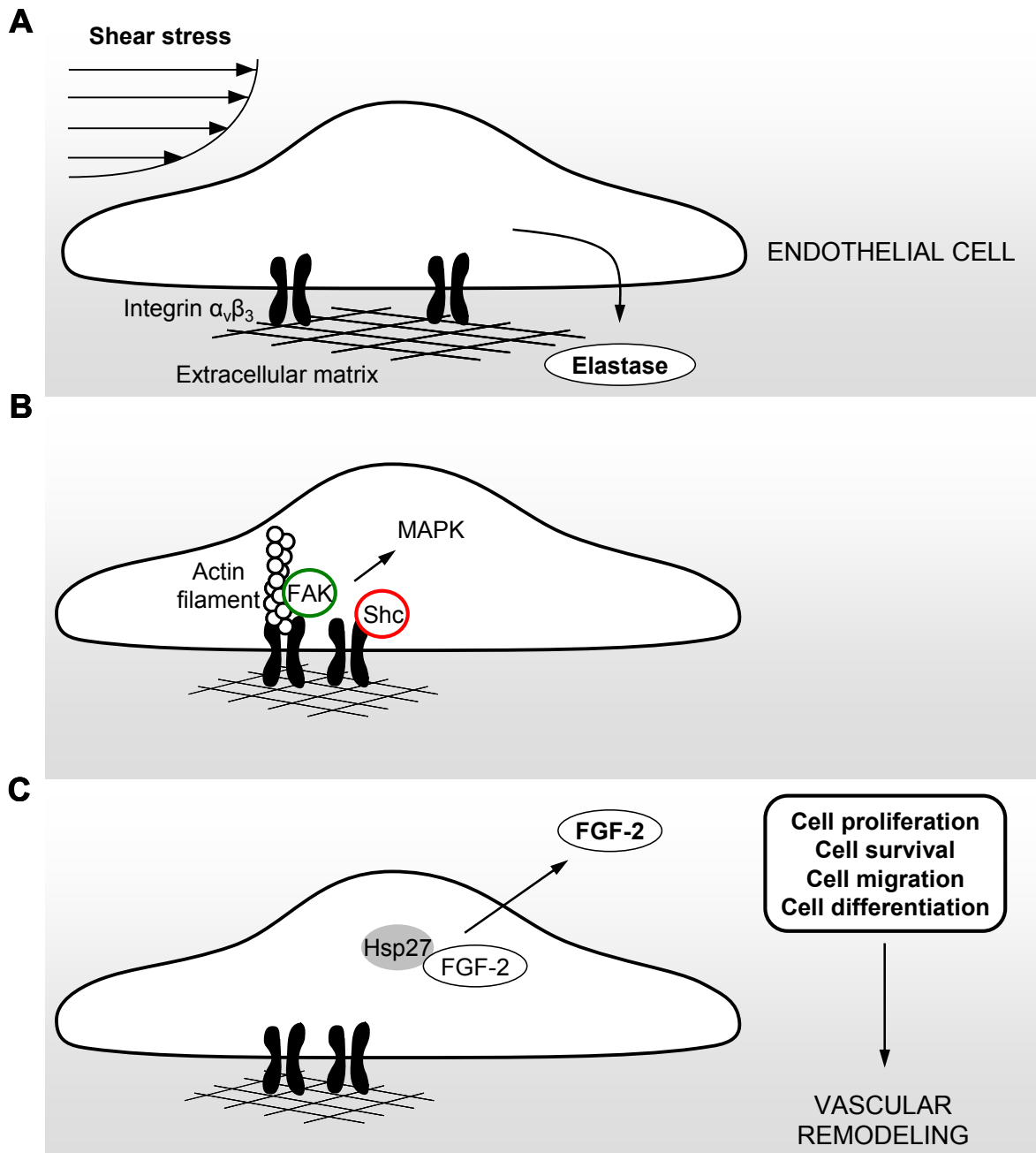

Figure V.1: The model for shear stress-induced FGF-2 release

(A) Step 1: Shear stress induces the release of endothelial elastase, which induces structural changes in the ECM. (B) Step 2: Integrin outside-in signaling is induced and intracellular signaling cascades are activated. (C) Step 3: FGF-2 is released. Hsp27 facilitates this process.

REFERENCES

VI   REFERENCES

1   Abraham, J.A., Whang, J.L., Tumolo, A., Mergia, A. *et al.*, Human basic fibroblast growth factor: nucleotide sequence and genomic organization. *EMBO J.* (1986), 5 (10), 2523-2528.

2   Acevedo, A.D., Bowser, S.S., Gerritsen, M.E. and Bizios, R., Morphological and proliferative responses of endothelial cells to hydrostatic pressure: role of fibroblast growth factor. *J Cell Physiol.* (1993), 157 (3), 603-614.

3   Aikawa, R., Nagai, T., Kudoh, S., Zou, Y. *et al.*, Integrins play a critical role in mechanical stress-induced p38 MAPK activation. *Hypertension.* (2002), 39 (2), 233-238.

4   Alberts, B., Molecular biology of the cell. 4. ed. Garland, New York (2002).

5   Albuquerque, M.L., Akiyama, S.K. and Schnaper, H.W., Basic fibroblast growth factor release by human coronary artery endothelial cells is enhanced by matrix proteins, 17beta-estradiol, and a PKC signaling pathway. *Exp Cell Res.* (1998), 245 (1), 163-169.

6   Amano, M., Chihara, K., Kimura, K., Fukata, Y. *et al.*, Formation of actin stress fibers and focal adhesions enhanced by Rho-kinase. *Science.* (1997), 275 (5304), 1308-1311.

7   Aumailley, M. and Gayraud, B., Structure and biological activity of the extracellular matrix. *J Mol Med.* (1998), 76 (3-4), 253-265.

8   Azuma, N., Akasaka, N., Kito, H., Ikeda, M. *et al.*, Role of p38 MAP kinase in endothelial cell alignment induced by fluid shear stress. *Am J Physiol Heart Circ Physiol.* (2001), 280 (1), H189-197.

9   Azuma, N., Duzgun, S.A., Ikeda, M., Kito, H. *et al.*, Endothelial cell response to different mechanical forces. *J Vasc Surg.* (2000), 32 (4), 789-794.

10   Backhaus, R., Zehe, C., Wegehingel, S., Kehlenbach, A. *et al.*, Unconventional protein secretion: membrane translocation of FGF-2 does not require protein unfolding. *J Cell Sci.* (2004), 117 (Pt 9), 1727-1736.

11   Baffour, R., Berman, J., Garb, J.L., Rhee, S.W. *et al.*, Enhanced angiogenesis and growth of collaterals by in vivo administration of recombinant basic fibroblast growth factor in a rabbit model of acute lower limb ischemia: dose-response effect of basic fibroblast growth factor. *J Vasc Surg.* (1992), 16 (2), 181-191.

12   Ballermann, B.J., Dardik, A., Eng, E. and Liu, A., Shear stress and the endothelium. *Kidney Int Suppl.* (1998), 67, S100-108.

13   Barchowsky, A., Williams, M.E., Benz, C.C. and Chepenik, K.P., Oxidant-sensitive protein phosphorylation in endothelial cells. *Free Radic Biol Med.* (1994), 16 (6), 771-777.

14 Bashkin, P., Doctrow, S., Klagsbrun, M., Svahn, C.M. *et al.*, Basic Fibroblast Growth-Factor Binds to Subendothelial Extracellular-Matrix and Is Released by Heparitinase and Heparin-Like Molecules. *Biochemistry.* (1989), 28 (4), 1737-1743.

15 Benndorf, R., Hayess, K., Ryazantsev, S., Wieske, M. *et al.*, Phosphorylation and supramolecular organization of murine small heat shock protein HSP25 abolish its actin polymerization-inhibiting activity. *J Biol Chem.* (1994), 269 (32), 20780-20784.

16 Bergers, G. and Benjamin, L.E., Tumorigenesis and the angiogenic switch. *Nat Rev Cancer.* (2003), 3 (6), 401-410.

17 Bode, W., Meyer, E., Jr. and Powers, J.C., Human leukocyte and porcine pancreatic elastase: X-ray crystal structures, mechanism, substrate specificity, and mechanism-based inhibitors. *Biochemistry.* (1989), 28 (5), 1951-1963.

18 Bonnefoy, A. and Legrand, C., Proteolysis of subendothelial adhesive glycoproteins (fibronectin, thrombospondin, and von Willebrand factor) by plasmin, leukocyte cathepsin G, and elastase. *Thromb Res.* (2000), 98 (4), 323-332.

19 Brooks, P.C., Clark, R.A. and Cheresh, D.A., Requirement of vascular integrin alpha v beta 3 for angiogenesis. *Science.* (1994), 264 (5158), 569-571.

20 Brooks, P.C., Montgomery, A.M.P., Rosenfeld, M., Reisfeld, R.A. *et al.*, Integrin Alpha(V)Beta(3) Antagonists Promote Tumor-Regression by Inducing Apoptosis of Angiogenic Blood-Vessels. *Cell.* (1994), 79 (7), 1157-1164.

21 Bryant, S.R., Bjercke, R.J., Erichsen, D.A., Rege, A. *et al.*, Vascular remodeling in response to altered blood flow is mediated by fibroblast growth factor-2. *Circ Res.* (1999), 84 (3), 323-328.

22 Buczek-Thomas, J.A., Lucey, E.C., Stone, P.J., Chu, C.L. *et al.*, Elastase mediates the release of growth factors from lung in vivo. *Am J Respir Cell Mol Biol.* (2004), 31 (3), 344-350.

23 Buczek-Thomas, J.A. and Nugent, M.A., Elastase-mediated release of heparan sulfate proteoglycans from pulmonary fibroblast cultures. A mechanism for basic fibroblast growth factor (bFGF) release and attenuation of bfgf binding following elastase-induced injury. *J Biol Chem.* (1999), 274 (35), 25167-25172.

24 Burke, D., Wilkes, D., Blundell, T.L. and Malcolm, S., Fibroblast growth factor receptors: lessons from the genes. *Trends Biochem Sci.* (1998), 23 (2), 59-62.

25 Buschmann, I. and Schaper, W., Arteriogenesis Versus Angiogenesis: Two Mechanisms of Vessel Growth. *News Physiol Sci.* (1999), 14, 121-125.

26 Buschmann, I.R., Lehmann, K. and Le Noble, F., Physics meets molecules: is modulation of shear stress the link to vascular prevention? *Circ Res.* (2008), 102 (5), 510-512.

27 Busse, R. and Fleming, I., Regulation of endothelium-derived vasoactive autacoid production by hemodynamic forces. *Trends Pharmacol Sci.* (2003), 24 (1), 24-29.

28   Cai, W.J., Li, M.B., Wu, X., Wu, S. *et al.*, Activation of the integrins alpha5beta1 and alphavbeta3 and focal adhesion kinase (FAK) during arteriogenesis. *Mol Cell Biochem.* (2009), 322 (1-2), 161-169.

29   Campuzano, R., Barrios, V., Cuevas, B., Asin-Cardiel, E. *et al.*, Serum basic fibroblast growth factor levels in exercise-induced myocardial ischemia more likely a marker of endothelial dysfunction than a marker of ischemia? *Eur J Med Res.* (2002), 7 (3), 93-97.

30   Cao, H., Dronadula, N., Rizvi, F., Li, Q. *et al.*, Novel role for STAT-5B in the regulation of Hsp27-FGF-2 axis facilitating thrombin-induced vascular smooth muscle cell growth and motility. *Circ Res.* (2006), 98 (7), 913-922.

31   Carmeliet, P., Angiogenesis in health and disease. *Nat Med.* (2003), 9 (6), 653-660.

32   Castillo, M.J., Nakajima, K., Zimmerman, M. and Powers, J.C., Sensitive substrates for human leukocyte and porcine pancreatic elastase: a study of the merits of various chromophoric and fluorogenic leaving groups in assays for serine proteases. *Anal Biochem.* (1979), 99 (1), 53-64.

33   Ceccarelli, S., Visco, V., Raffa, S., Wakisaka, N. *et al.*, Epstein-Barr virus latent membrane protein 1 promotes concentration in multivesicular bodies of fibroblast growth factor 2 and its release through exosomes. *Int J Cancer.* (2007), 121 (7), 1494-1506.

34   Chatzizisis, Y.S., Coskun, A.U., Jonas, M., Edelman, E.R. *et al.*, Role of endothelial shear stress in the natural history of coronary atherosclerosis and vascular remodeling: molecular, cellular, and vascular behavior. *J Am Coll Cardiol.* (2007), 49 (25), 2379-2393.

35   Chen, J., Baskerville, C., Han, Q., Pan, Z.K. *et al.*, Alpha(v) integrin, p38 mitogen-activated protein kinase, and urokinase plasminogen activator are functionally linked in invasive breast cancer cells. *J Biol Chem.* (2001), 276 (51), 47901-47905.

36   Chen, K.D., Li, Y.S., Kim, M., Li, S. *et al.*, Mechanotransduction in response to shear stress. Roles of receptor tyrosine kinases, integrins, and Shc. *J Biol Chem.* (1999), 274 (26), 18393-18400.

37   Cheresh, D.A., Structure, function and biological properties of integrin alpha v beta 3 on human melanoma cells. *Cancer Metastasis Rev.* (1991), 10 (1), 3-10.

38   Cobb, M.H., MAP kinase pathways. *Progress in Biophysics & Molecular Biology.* (1999), 71 (3-4), 479-500.

39   Concannon, C.G., Gorman, A.M. and Samali, A., On the role of Hsp27 in regulating apoptosis. *Apoptosis.* (2003), 8 (1), 61-70.

40   Conrad, H.E., Heparin-binding proteins. Academic Press, (1998).

41   Cowan, D.B. and Langille, B.L., Cellular and molecular biology of vascular remodeling. *Current Opinion in Lipidology.* (1996), 7 (2), 94-100.

42   Cowan, K.N., Jones, P.L. and Rabinovitch, M., Elastase and matrix metalloproteinase inhibitors induce regression, and tenascin-C antisense prevents progression, of vascular disease. *J Clin Invest.* (2000), 105 (1), 21-34.

43   Cucina, A., Borrelli, V., Di Carlo, A., Pagliei, S. *et al.*, Thrombin induces production of growth factors from aortic smooth muscle cells. *J Surg Res.* (1999), 82 (1), 61-66.

44   Cucina, A., Corvino, V., Sapienza, P., Borrelli, V. *et al.*, Nicotine regulates basic fibroblastic growth factor and transforming growth factor beta1 production in endothelial cells. *Biochem Biophys Res Commun.* (1999), 257 (2), 306-312.

45   D'Amore, P.A., Modes of FGF release in vivo and in vitro. *Cancer Metastasis Rev.* (1990), 9 (3), 227-238.

46   Datta, Y.H. and Ewenstein, B.M., Regulated secretion in endothelial cells: biology and clinical implications. *Thromb Haemost.* (2001), 86 (5), 1148-1155.

47   Davies, P.F., Robotewskyj, A. and Griem, M.L., Quantitative studies of endothelial cell adhesion. Directional remodeling of focal adhesion sites in response to flow forces. *J Clin Invest.* (1994), 93 (5), 2031-2038.

48   Dawson, J.M. and Hudlicka, O., The effects of long term administration of prazosin on the microcirculation in skeletal muscles. *Cardiovasc Res.* (1989), 23 (11), 913-920.

49   Deindl, E., Hoefer, I.E., Fernandez, B., Barancik, M. *et al.*, Involvement of the fibroblast growth factor system in adaptive and chemokine-induced arteriogenesis. *Circ Res.* (2003), 92 (5), 561-568.

50   Dono, R., Texido, G., Dussel, R., Ehmke, H. *et al.*, Impaired cerebral cortex development and blood pressure regulation in FGF-2-deficient mice. *EMBO J.* (1998), 17 (15), 4213-4225.

51   Dubaybo, B.A., Crowell, L.A. and Thet, L.A., Changes in tissue fibronectin in elastase induced lung injury. *Cell Biol Int Rep.* (1991), 15 (8), 675-686.

52   Dunsmore, S.E., Roes, J., Chua, F.J., Segal, A.W. *et al.*, Evidence that neutrophil elastase-deficient mice are resistant to bleomycin-induced fibrosis. *Chest.* (2001), 120 (1 Suppl), 35S-36S.

53   Egginton, S., Zhou, A.L., Brown, M.D. and Hudlicka, O., Unorthodox angiogenesis in skeletal muscle. *Cardiovasc Res.* (2001), 49 (3), 634-646.

54   Eliakim, A., Oh, Y. and Cooper, D.M., Effect of single wrist exercise on fibroblast growth factor-2, insulin-like growth factor, and growth hormone. *Am J Physiol Regul Integr Comp Physiol.* (2000), 279 (2), R548-553.

55   Eliceiri, B.P. and Cheresh, D.A., The role of alpha v integrins during angiogenesis. *Molecular Medicine.* (1998), 4 (12), 741-750.

56   Engling, A., Backhaus, R., Stegmayer, C., Zehe, C. *et al.*, Biosynthetic FGF-2 is targeted to non-lipid raft microdomains following translocation to the extracellular surface of CHO cells. *J Cell Sci.* (2002), 115 (Pt 18), 3619-3631.

57   Faisal Khan, K.M., Laurie, G.W., McCaffrey, T.A. and Falcone, D.J., Exposure of cryptic domains in the alpha 1-chain of laminin-1 by elastase stimulates macrophages urokinase and matrix metalloproteinase-9 expression. *J Biol Chem.* (2002), 277 (16), 13778-13786.

58   Fan, T.P., Yeh, J.C., Leung, K.W., Yue, P.Y. *et al.*, Angiogenesis: from plants to blood vessels. *Trends Pharmacol Sci.* (2006), 27 (6), 297-309.

59   Felmeden, D.C., Blann, A.D. and Lip, G.Y., Angiogenesis: basic pathophysiology and implications for disease. *Eur Heart J.* (2003), 24 (7), 586-603.

60   Ferns, G., Shams, S. and Shafi, S., Heat shock protein 27: its potential role in vascular disease. *Int J Exp Pathol.* (2006), 87 (4), 253-274.

61   Fire, A., Xu, S., Montgomery, M.K., Kostas, S.A. *et al.*, Potent and specific genetic interference by double-stranded RNA in Caenorhabditis elegans. *Nature.* (1998), 391 (6669), 806-811.

62   Florkiewicz, R.Z., Majack, R.A., Buechler, R.D. and Florkiewicz, E., Quantitative export of FGF-2 occurs through an alternative, energy-dependent, non-ER/Golgi pathway. *J Cell Physiol.* (1995), 162 (3), 388-399.

63   Forsyth, C.B., Pulai, J. and Loeser, R.F., Fibronectin fragments and blocking antibodies to alpha2beta1 and alpha5beta1 integrins stimulate mitogen-activated protein kinase signaling and increase collagenase 3 (matrix metalloproteinase 13) production by human articular chondrocytes. *Arthritis Rheum.* (2002), 46 (9), 2368-2376.

64   Frangos, J.A., McIntire, L.V. and Eskin, S.G., Shear stress induced stimulation of mammalian cell metabolism. *Biotechnol Bioeng.* (1988), 32 (8), 1053-1060.

65   Franke, R.P., Grafe, M., Schnittler, H., Seiffge, D. *et al.*, Induction of human vascular endothelial stress fibres by fluid shear stress. *Nature.* (1984), 307 (5952), 648-649.

66   Galbraith, C.G., Skalak, R. and Chien, S., Shear stress induces spatial reorganization of the endothelial cell cytoskeleton. *Cell Motil Cytoskeleton.* (1998), 40 (4), 317-330.

67   Galbusera, M., Zoja, C., Donadelli, R., Paris, S. *et al.*, Fluid shear stress modulates von Willebrand factor release from human vascular endothelium. *Blood.* (1997), 90 (4), 1558-1564.

68   Garcia-Cardena, G. and Gimbrone Jr., M.A., Biomechanical modulation of endothelial phenotype: Implications for health and disease. In: The vascular endothelium II, edited by Moncada, S. and Higgs, A. Springer-Verlag Berlin, Heidelberg (2006).

69   Garcia-Touchard, A., Henry, T.D., Sangiorgi, G., Spagnoli, L.G. *et al.*, Extracellular proteases in atherosclerosis and restenosis. *Arterioscler Thromb Vasc Biol.* (2005), 25 (6), 1119-1127.

70   Geiger, B., Bershadsky, A., Pankov, R. and Yamada, K.M., Transmembrane crosstalk between the extracellular matrix--cytoskeleton crosstalk. *Nat Rev Mol Cell Biol.* (2001), 2 (11), 793-805.

71   Gerthoffer, W.T. and Gunst, S.J., Invited review: focal adhesion and small heat shock proteins in the regulation of actin remodeling and contractility in smooth muscle. *J Appl Physiol.* (2001), 91 (2), 963-972.

72   Gibbons, G.H. and Dzau, V.J., The emerging concept of vascular remodeling. *N Engl J Med.* (1994), 330 (20), 1431-1438.

73   Girard, P.R. and Nerem, R.M., Shear stress modulates endothelial cell morphology and F-actin organization through the regulation of focal adhesion-associated proteins. *J Cell Physiol.* (1995), 163 (1), 179-193.

74   Gloe, T., Riedmayr, S., Sohn, H.Y. and Pohl, U., The 67-kDa laminin-binding protein is involved in shear stress-dependent endothelial nitric-oxide synthase expression. *J Biol Chem.* (1999), 274 (23), 15996-16002.

75   Gloe, T., Sohn, H.Y., Meininger, G.A. and Pohl, U., Shear stress-induced release of basic fibroblast growth factor from endothelial cells is mediated by matrix interaction via integrin alpha(v)beta3. *J Biol Chem.* (2002), 277 (26), 23453-23458.

76   Gomez-Pinilla, F., Dao, L. and So, V., Physical exercise induces FGF-2 and its mRNA in the hippocampus. *Brain Res.* (1997), 764 (1-2), 1-8.

77   Gospodarowicz, D., Localisation of a fibroblast growth factor and its effect alone and with hydrocortisone on 3T3 cell growth. *Nature.* (1974), 249 (453), 123-127.

78   Griffioen, A.W. and Molema, G., Angiogenesis: potentials for pharmacologic intervention in the treatment of cancer, cardiovascular diseases, and chronic inflammation. *Pharmacol Rev.* (2000), 52 (2), 237-268.

79   Gu, J.W., Gadonski, G., Wang, J., Makey, I. *et al.*, Exercise increases endostatin in circulation of healthy volunteers. *BMC Physiol.* (2004), 4, 2.

80   Guay, J., Lambert, H., Gingras-Breton, G., Lavoie, J.N. *et al.*, Regulation of actin filament dynamics by p38 map kinase-mediated phosphorylation of heat shock protein 27. *J Cell Sci.* (1997), 110 (Pt 3), 357-368.

81   Guo, W. and Giancotti, F.G., Integrin signalling during tumour progression. *Nat Rev Mol Cell Biol.* (2004), 5 (10), 816-826.

82   Gupte, A. and Frangos, J.A., Effects of flow on the synthesis and release of fibronectin by endothelial cells. *In Vitro Cell Dev Biol.* (1990), 26 (1), 57-60.

83   Gustafsson, T. and Kraus, W.E., Exercise-induced angiogenesis-related growth and transcription factors in skeletal muscle, and their modification in muscle pathology. *Front Biosci.* (2001), 6, D75-89.

84   Hahn, C., Orr, A.W., Sanders, J.M., Jhaveri, K.A. *et al.*, The subendothelial extracellular matrix modulates JNK activation by flow. *Circ Res.* (2009), 104 (8), 995-1003.

85   Hall, A., Rho GTPases and the actin cytoskeleton. *Science.* (1998), 279 (5350), 509-514.

86   Heck, L.W., Blackburn, W.D., Irwin, M.H. and Abrahamson, D.R., Degradation of basement membrane laminin by human neutrophil elastase and cathepsin G. *Am J Pathol.* (1990), 136 (6), 1267-1274.

87   Hedstrom, L., Serine protease mechanism and specificity. *Chem Rev.* (2002), 102 (12), 4501-4524.

88   Helisch, A. and Schaper, W., Angiogenesis and arteriogenesis - not yet for prescription. *Z Kardiol.* (2000), 89 (3), 239-244.

89   Henriksen, P.A. and Sallenave, J.M., Human neutrophil elastase: mediator and therapeutic target in atherosclerosis. *Int J Biochem Cell Biol.* (2008), 40 (6-7), 1095-1100.

90   Honore, S., Pichard, V., Penel, C., Rigot, V. *et al.*, Outside-in regulation of integrin clustering processes by ECM components per se and their involvement in actin cytoskeleton organization in a colon adenocarcinoma cell line. *Histochem Cell Biol.* (2000), 114 (4), 323-335.

91   Hood, J.D. and Cheresh, D.A., Role of integrins in cell invasion and migration. *Nature Reviews Cancer.* (2002), 2 (2), 91-100.

92   Hornebeck, W., Derouette, J.C. and Robert, L., Isolation, purification and properties of aortic elastase. *FEBS Lett.* (1975), 58 (1), 66-70.

93   Horton, M.A., The alpha v beta 3 integrin "vitronectin receptor". *Int J Biochem Cell Biol.* (1997), 29 (5), 721-725.

94   Huang, H., Campbell, S.C., Nelius, T., Bedford, D.F. *et al.*, Alpha1-antitrypsin inhibits angiogenesis and tumor growth. *Int J Cancer.* (2004), 112 (6), 1042-1048.

95   Ichioka, S., Shibata, M., Kosaki, K., Sato, Y. *et al.*, Effects of shear stress on wound-healing angiogenesis in the rabbit ear chamber. *J Surg Res.* (1997), 72 (1), 29-35.

96   Ilic, D., Kovacic, B., McDonagh, S., Jin, F. *et al.*, Focal adhesion kinase is required for blood vessel morphogenesis. *Circ Res.* (2003), 92 (3), 300-307.

97   Ishibashi, H., Shiratuchi, T., Nakagawa, K., Onimaru, M. *et al.*, Hypoxia-induced angiogenesis of cultured human salivary gland carcinoma cells enhances vascular endothelial growth factor production and basic fibroblast growth factor release. *Oral Oncol.* (2001), 37 (1), 77-83.

98   Jalali, S., del Pozo, M.A., Chen, K., Miao, H. *et al.*, Integrin-mediated mechanotransduction requires its dynamic interaction with specific extracellular matrix (ECM) ligands. *Proc Natl Acad Sci U S A.* (2001), 98 (3), 1042-1046.

99   Jalali, S., Li, Y.S., Sotoudeh, M., Yuan, S. *et al.*, Shear stress activates p60src-Ras-MAPK signaling pathways in vascular endothelial cells. *Arterioscler Thromb Vasc Biol.* (1998), 18 (2), 227-234.

100   Jensen, L., Bangsbo, J. and Hellsten, Y., Effect of high intensity training on capillarization and presence of angiogenic factors in human skeletal muscle. *J Physiol.* (2004), 557 (Pt 2), 571-582.

101   Jin, S.W. and Patterson, C., The opening act: vasculogenesis and the origins of circulation. *Arterioscler Thromb Vasc Biol.* (2009), 29 (5), 623-629.

102   Kafienah, W., Buttle, D.J., Burnett, D. and Hollander, A.P., Cleavage of native type I collagen by human neutrophil elastase. *Biochem J.* (1998), 330 (Pt 2), 897-902.

103   Kargi, H.A., Campbell, E.J. and Kuhn, C., 3rd, Elastase and cathepsin G of human monocytes: heterogeneity and subcellular localization to peroxidase-positive granules. *J Histochem Cytochem.* (1990), 38 (8), 1179-1186.

104   Katoh, K., Kano, Y. and Ookawara, S., Role of stress fibers and focal adhesions as a mediator for mechano-signal transduction in endothelial cells in situ. *Vasc Health Risk Manag.* (2008), 4 (6), 1273-1282.

105   Katritsis, D., Kaiktsis, L., Chaniotis, A., Pantos, J. *et al.*, Wall shear stress: theoretical considerations and methods of measurement. *Prog Cardiovasc Dis.* (2007), 49 (5), 307-329.

106   Kinsella, M.G., Irvin, C., Reidy, M.A. and Wight, T.N., Removal of heparan sulfate by heparinase treatment inhibits FGF-2-dependent smooth muscle cell proliferation in injured rat carotid arteries. *Atherosclerosis.* (2004), 175 (1), 51-57.

107   Klarskov Mogensen, C., Release of bFGF from endothelial cells is mediated by protease induced HSP27 phosphorylation via p38-MAPK pathway. Dissertation, Ludwig-Maximilians-Universität, Fakultät für Chemie und Pharmazie (2006).

108   Kokubo, T., Uchida, H. and Choi, E.T., Integrin alpha(v)beta 3 as a target in the prevention of neointimal hyperplasia. *Journal of Vascular Surgery.* (2007), 45, 33a-38a.

109   Kumar, C.C., Integrin alpha v beta 3 as a therapeutic target for blocking tumor-induced angiogenesis. *Curr Drug Targets.* (2003), 4 (2), 123-131.

110   Laemmli, U.K., Cleavage of structural proteins during the assembly of the head of bacteriophage T4. *Nature.* (1970), 227 (5259), 680-685.

111   Landry, J., Lambert, H., Zhou, M., Lavoie, J.N. *et al.*, Human HSP27 is phosphorylated at serines 78 and 82 by heat shock and mitogen-activated kinases that recognize the same amino acid motif as S6 kinase II. *J Biol Chem.* (1992), 267 (2), 794-803.

112   Laurila, P. and Leivo, I., Basement membrane and interstitial matrix components form separate matrices in heterokaryons of PYS-2 cells and fibroblasts. *J Cell Sci.* (1993), 104 (Pt 1), 59-68.

113   Leake, D.S., Hornebeck, W., Brechemier, D., Robert, L. *et al.*, Properties and subcellular localization of elastase-like activities of arterial smooth muscle cells in culture. *Biochim Biophys Acta.* (1983), 761 (1), 41-47.

114   Lee, D.Y., Yeh, C.R., Chang, S.F., Lee, P.L. *et al.*, Integrin-mediated expression of bone formation-related genes in osteoblast-like cells in response to fluid shear stress: roles of extracellular matrix, Shc, and mitogen-activated protein kinase. *J Bone Miner Res.* (2008), 23 (7), 1140-1149.

115   Lepidi, S., Sterpetti, A.V., Cucina, A., Di Carlo, A. *et al.*, bFGF release is dependent on flow conditions in experimental vein grafts. *Eur J Vasc Endovasc Surg.* (1995), 10 (4), 450-458.

116   Levin, E.G. and Santell, L., Thrombin- and histamine-induced signal transduction in human endothelial cells. Stimulation and agonist-dependent desensitization of protein phosphorylation. *J Biol Chem.* (1991), 266 (1), 174-181.

117   Ley, K., Laudanna, C., Cybulsky, M.I. and Nourshargh, S., Getting to the site of inflammation: the leukocyte adhesion cascade updated. *Nature Reviews Immunology.* (2007), 7 (9), 678-689.

118   Li, S., Kim, M., Hu, Y.L., Jalali, S. *et al.*, Fluid shear stress activation of focal adhesion kinase. Linking to mitogen-activated protein kinases. *J Biol Chem.* (1997), 272 (48), 30455-30462.

119   Li, S., Piotrowicz, R.S., Levin, E.G., Shyy, Y.J. *et al.*, Fluid shear stress induces the phosphorylation of small heat shock proteins in vascular endothelial cells. *Am J Physiol.* (1996), 271 (3 Pt 1), C994-1000.

120   Li, Y.S., Haga, J.H. and Chien, S., Molecular basis of the effects of shear stress on vascular endothelial cells. *J Biomech.* (2005), 38 (10), 1949-1971.

121   Lin, C.Y., Lin, F. K., Lin, C. H., Lai, L. W., Hsu, H. J., Chen, S. H. and Hsiung, C. A., Phylogenetic web repeater (POWER), http://power.nhri.org.tw/power/home.htm, (2005).

122   Linhardt, R.J., Turnbull, J.E., Wang, H.M., Loganathan, D. *et al.*, Examination of the substrate specificity of heparin and heparan sulfate lyases. *Biochemistry.* (1990), 29 (10), 2611-2617.

123   Lodish, H., Molecular cell biology. 5. ed., 3. printing ed. Freeman, New York (2004).

124   Loeser, R.F., Forsyth, C.B., Samarel, A.M. and Im, H.J., Fibronectin fragment activation of proline-rich tyrosine kinase PYK2 mediates integrin signals regulating collagenase-3 expression by human chondrocytes through a protein kinase C-dependent pathway. *J Biol Chem.* (2003), 278 (27), 24577-24585.

125   Malek, A.M., Gibbons, G.H., Dzau, V.J. and Izumo, S., Fluid shear stress differentially modulates expression of genes encoding basic fibroblast growth factor and platelet-derived growth factor B chain in vascular endothelium. *J Clin Invest.* (1993), 92 (4), 2013-2021.

126   Malek, A.M. and Izumo, S., Mechanism of endothelial cell shape change and cytoskeletal remodeling in response to fluid shear stress. *J Cell Sci.* (1996), 109 (Pt 4), 713-726.

127   McDonald, J.A. and Kelley, D.G., Degradation of fibronectin by human leukocyte elastase. Release of biologically active fragments. *J Biol Chem.* (1980), 255 (18), 8848-8858.

128   McLean, G.W., Carragher, N.O., Avizienyte, E., Evans, J. *et al.*, The role of focal-adhesion kinase in cancer - a new therapeutic opportunity. *Nat Rev Cancer.* (2005), 5 (7), 505-515.

129   Menashi, S., Hornebeck, W., Robert, L. and Legrand, Y., Elastase-like activity in cultured aortic endothelial cells. *Thromb Res.* (1989), 53 (1), 11-18.

130   Milkiewicz, M., Brown, M.D., Egginton, S. and Hudlicka, O., Association between shear stress, angiogenesis, and VEGF in skeletal muscles in vivo. *Microcirculation.* (2001), 8 (4), 229-241.

131   Mitra, S.K., Hanson, D.A. and Schlaepfer, D.D., Focal adhesion kinase: in command and control of cell motility. *Nat Rev Mol Cell Biol.* (2005), 6 (1), 56-68.

132   Mullis, K., Faloona, F., Scharf, S., Saiki, R. *et al.*, Specific enzymatic amplification of DNA in vitro: the polymerase chain reaction. *Cold Spring Harb Symp Quant Biol.* (1986), 51 Pt 1, 263-273.

133   Mulvany, M.J., Vascular remodelling of resistance vessels: can we define this? *Cardiovasc Res.* (1999), 41 (1), 9-13.

134   Nakajima, K., Powers, J.C., Ashe, B.M. and Zimmerman, M., Mapping the extended substrate binding site of cathepsin G and human leukocyte elastase. Studies with peptide substrates related to the alpha 1-protease inhibitor reactive site. *J Biol Chem.* (1979), 254 (10), 4027-4032.

135   Nakajima, K., Shimojo, M., Hamanoue, M., Ishiura, S. *et al.*, Identification of elastase as a secretory protease from cultured rat microglia. *J Neurochem.* (1992), 58 (4), 1401-1408.

136   NCBI, National center for biotechnology information - Entrez protein database, http://www.ncbi.nlm.nih.gov/protein/.

137   Nickel, W., The mystery of nonclassical protein secretion. A current view on cargo proteins and potential export routes. *Eur J Biochem.* (2003), 270 (10), 2109-2119.

138   Noria, S., Xu, F., McCue, S., Jones, M. *et al.*, Assembly and reorientation of stress fibers drives morphological changes to endothelial cells exposed to shear stress. *Am J Pathol.* (2004), 164 (4), 1211-1223.

139   Nugent, M.A. and Iozzo, R.V., Fibroblast growth factor-2. *Int J Biochem Cell Biol.* (2000), 32 (2), 115-120.

140   Okada-Ban, M., Thiery, J.P. and Jouanneau, J., Fibroblast growth factor-2. *Int J Biochem Cell Biol.* (2000), 32 (3), 263-267.

141   Ornitz, D.M. and Itoh, N., Fibroblast growth factors. *Genome Biol.* (2001), 2 (3), REVIEWS3005.

142   Orr, A.W., Ginsberg, M.H., Shattil, S.J., Deckmyn, H. *et al.*, Matrix-specific suppression of integrin activation in shear stress signaling. *Mol Biol Cell.* (2006), 17 (11), 4686-4697.

143   Ortega, S., Ittmann, M., Tsang, S.H., Ehrlich, M. *et al.*, Neuronal defects and delayed wound healing in mice lacking fibroblast growth factor 2. *Proc Natl Acad Sci U S A.* (1998), 95 (10), 5672-5677.

144   Papaioannou, T.G. and Stefanadis, C., Vascular wall shear stress: basic principles and methods. *Hellenic J Cardiol.* (2005), 46 (1), 9-15.

145   Papetti, M. and Herman, I.M., Mechanisms of normal and tumor-derived angiogenesis. *Am J Physiol Cell Physiol.* (2002), 282 (5), C947-970.

146   Parsons, J.T., Focal adhesion kinase: the first ten years. *J Cell Sci.* (2003), 116 (Pt 8), 1409-1416.

147   Paszkowiak, J.J. and Dardik, A., Arterial wall shear stress: observations from the bench to the bedside. *Vasc Endovascular Surg.* (2003), 37 (1), 47-57.

148   Pearson, G., Robinson, F., Beers Gibson, T., Xu, B.E. *et al.*, Mitogen-activated protein (MAP) kinase pathways: regulation and physiological functions. *Endocr Rev.* (2001), 22 (2), 153-183.

149   Pichon, S., Bryckaert, M. and Berrou, E., Control of actin dynamics by p38 MAP kinase - Hsp27 distribution in the lamellipodium of smooth muscle cells. *J Cell Sci.* (2004), 117 (Pt 12), 2569-2577.

150   Piotrowicz, R.S., Martin, J.L., Dillman, W.H. and Levin, E.G., The 27-kDa heat shock protein facilitates basic fibroblast growth factor release from endothelial cells. *J Biol Chem.* (1997), 272 (11), 7042-7047.

151   Piotrowicz, R.S., Weber, L.A., Hickey, E. and Levin, E.G., Accelerated growth and senescence of arterial endothelial cells expressing the small molecular weight heat-shock protein HSP27. *FASEB J.* (1995), 9 (11), 1079-1084.

152   Platt, M.O., Ankeny, R.F. and Jo, H., Laminar shear stress inhibits cathepsin L activity in endothelial cells. *Arterioscler Thromb Vasc Biol.* (2006), 26 (8), 1784-1790.

153   Platt, M.O., Ankeny, R.F., Shi, G.P., Weiss, D. *et al.*, Expression of cathepsin K is regulated by shear stress in cultured endothelial cells and is increased in endothelium in human atherosclerosis. *Am J Physiol Heart Circ Physiol.* (2007), 292 (3), H1479-1486.

154 Platt, M.O., Xing, Y., Jo, H. and Yoganathan, A.P., Cyclic pressure and shear stress regulate matrix metalloproteinases and cathepsin activity in porcine aortic valves. *J Heart Valve Dis.* (2006), 15 (5), 622-629.

155 Pohl, U., Kreislauf. In: Anatomie, Biochemie und Physiologie der vegetativen Organsysteme, edited by Schmidt, R.F. and Unsicker, K. Deutscher Ärzte-Verlag GmbH, Köln (2003).

156 Prior, B.M., Yang, H.T. and Terjung, R.L., What makes vessels grow with exercise training? *J Appl Physiol.* (2004), 97 (3), 1119-1128.

157 Prudovsky, I., Mandinova, A., Soldi, R., Bagala, C. *et al.*, The non-classical export routes: FGF1 and IL-1alpha point the way. *J Cell Sci.* (2003), 116 (Pt 24), 4871-4881.

158 Qi, M.S. and Elion, E.A., MAP kinase pathways. *Journal of Cell Science.* (2005), 118 (16), 3569-3572.

159 Qin, J., Vinogradova, O. and Plow, E.F., Integrin bidirectional signaling: a molecular view. *PLoS Biol.* (2004), 2 (6), e169.

160 Quirt, I., Bodurth, A., Lohmann, R., Rusthoven, J. *et al.*, Phase II study of marimastat (BB-2516) in malignant melanoma: a clinical and tumor biopsy study of the National Cancer Institute of Canada Clinical Trials Group. *Invest New Drugs.* (2002), 20 (4), 431-437.

161 Ravichandran, K.S., Signaling via Shc family adapter proteins. *Oncogene.* (2001), 20 (44), 6322-6330.

162 Resnick, N., Yahav, H., Schubert, S., Wolfovitz, E. *et al.*, Signalling pathways in vascular endothelium activated by shear stress: relevance to atherosclerosis. *Curr Opin Lipidol.* (2000), 11 (2), 167-177.

163 Resnick, N., Yahav, H., Shay-Salit, A., Shushy, M. *et al.*, Fluid shear stress and the vascular endothelium: for better and for worse. *Prog Biophys Mol Biol.* (2003), 81 (3), 177-199.

164 Rhoads, D.N., Eskin, S.G. and McIntire, L.V., Fluid flow releases fibroblast growth factor-2 from human aortic smooth muscle cells. *Arterioscler Thromb Vasc Biol.* (2000), 20 (2), 416-421.

165 Rifkin, D.B. and Moscatelli, D., Recent developments in the cell biology of basic fibroblast growth factor. *J Cell Biol.* (1989), 109 (1), 1-6.

166 Rouse, J., Cohen, P., Trigon, S., Morange, M. *et al.*, A novel kinase cascade triggered by stress and heat shock that stimulates MAPKAP kinase-2 and phosphorylation of the small heat shock proteins. *Cell.* (1994), 78 (6), 1027-1037.

167 Rozen, S. and Skaletsky, H.J., Primer 3 on the WWW for general users and for biologist programmers. In: Bioinformatics methods and protocols: Methods in molecular biology, edited by Krawetz, S. and Misener, S. Humana Press, Totowa, NJ (2000), pp. 365-386.

168   Samaniego, F., Markham, P.D., Gendelman, R., Gallo, R.C. *et al.*, Inflammatory cytokines induce endothelial cells to produce and release basic fibroblast growth factor and to promote Kaposi's sarcoma-like lesions in nude mice. *J Immunol.* (1997), 158 (4), 1887-1894.

169   Schaller, M.D., Biochemical signals and biological responses elicited by the focal adhesion kinase. *Biochim Biophys Acta.* (2001), 1540 (1), 1-21.

170   Schaper, W. and Scholz, D., Factors regulating arteriogenesis. *Arterioscler Thromb Vasc Biol.* (2003), 23 (7), 1143-1151.

171   Schomburg, D., BRENDA - The Comprehensive Enzyme Information System, http://www.brenda-enzymes.info/index.php4.

172   Schretzenmayr, Über kreislaufregulatorische Vorgänge an den großen Arterien bei der Muskelarbeit. *Pflugers Arch Ges Physiol.* (1933), 232, 743-748.

173   Schwartz, M.A. and Shattil, S.J., Signaling networks linking integrins and rho family GTPases. *Trends Biochem Sci.* (2000), 25 (8), 388-391.

174   Seida, A., Wada, J., Kunitomi, M., Tsuchiyama, Y. *et al.*, Serum bFGF levels are reduced in Japanese overweight men and restored by a 6-month exercise education. *Int J Obes Relat Metab Disord.* (2003), 27 (11), 1325-1331.

175   Shattil, S.J. and Newman, P.J., Integrins: dynamic scaffolds for adhesion and signaling in platelets. *Blood.* (2004), 104 (6), 1606-1615.

176   Shikata, Y., Rios, A., Kawkitinarong, K., DePaola, N. *et al.*, Differential effects of shear stress and cyclic stretch on focal adhesion remodeling, site-specific FAK phosphorylation, and small GTPases in human lung endothelial cells. *Exp Cell Res.* (2005), 304 (1), 40-49.

177   Shyy, J.Y. and Chien, S., Role of integrins in endothelial mechanosensing of shear stress. *Circ Res.* (2002), 91 (9), 769-775.

178   Si-Tahar, M., Pidard, D., Balloy, V., Moniatte, M. *et al.*, Human neutrophil elastase proteolytically activates the platelet integrin alphaIIbbeta3 through cleavage of the carboxyl terminus of the alphaIIb subunit heavy chain. Involvement in the potentiation of platelet aggregation. *J Biol Chem.* (1997), 272 (17), 11636-11647.

179   Sinha, S., Watorek, W., Karr, S., Giles, J. *et al.*, Primary structure of human neutrophil elastase. *Proc Natl Acad Sci U S A.* (1987), 84 (8), 2228-2232.

180   Stein, R.L. and Trainor, D.A., Mechanism of inactivation of human leukocyte elastase by a chloromethyl ketone: kinetic and solvent isotope effect studies. *Biochemistry.* (1986), 25 (19), 5414-5419.

181   Steinman, L., Blocking adhesion molecules as therapy for multiple sclerosis: Natalizumab. *Nature Reviews Drug Discovery.* (2005), 4 (6), 510-U513.

182 Sterpetti, A.V., Cucina, A., Fragale, A., Lepidi, S. *et al.*, Shear-Stress Influences the Release of Platelet-Derived Growth-Factor and Basic Fibroblast Growth-Factor by Arterial Smooth-Muscle Cells. *European Journal of Vascular Surgery.* (1994), 8 (2), 138-142.

183 Sullivan, C.J., Doetschman, T. and Hoying, J.B., Targeted disruption of the Fgf2 gene does not affect vascular growth in the mouse ischemic hindlimb. *J Appl Physiol.* (2002), 93 (6), 2009-2017.

184 Sullivan, C.J. and Hoying, J.B., Flow-dependent remodeling in the carotid artery of fibroblast growth factor-2 knockout mice. *Arterioscler Thromb Vasc Biol.* (2002), 22 (7), 1100-1105.

185 Sumpio, B.E., Riley, J.T. and Dardik, A., Cells in focus: endothelial cell. *International Journal of Biochemistry & Cell Biology.* (2002), 34 (12), 1508-1512.

186 Takada, Y., Ye, X.J. and Simon, S., The integrins. *Genome Biology.* (2007), 8 (5), 215.

187 Tam, S.H., Sassoli, P.M., Jordan, R.E. and Nakada, M.T., Abciximab (ReoPro, chimeric 7E3 Fab) demonstrates equivalent affinity and functional blockade of glycoprotein IIb/IIIa and alpha(v)beta3 integrins. *Circulation.* (1998), 98 (11), 1085-1091.

188 Taverna, S., Ghersi, G., Ginestra, A., Rigogliuso, S. *et al.*, Shedding of membrane vesicles mediates fibroblast growth factor-2 release from cells. *J Biol Chem.* (2003), 278 (51), 51911-51919.

189 Teitelbaum, S.L., Osteoclasts, integrins, and osteoporosis. *Journal of Bone and Mineral Metabolism.* (2000), 18 (6), 344-349.

190 Thompson, K. and Rabinovitch, M., Exogenous leukocyte and endogenous elastases can mediate mitogenic activity in pulmonary artery smooth muscle cells by release of extracellular-matrix bound basic fibroblast growth factor. *J Cell Physiol.* (1996), 166 (3), 495-505.

191 Thoumine, O., Nerem, R.M. and Girard, P.R., Changes in organization and composition of the extracellular matrix underlying cultured endothelial cells exposed to laminar steady shear stress. *Lab Invest.* (1995), 73 (4), 565-576.

192 Traub, O. and Berk, B.C., Laminar shear stress: mechanisms by which endothelial cells transduce an atheroprotective force. *Arterioscler Thromb Vasc Biol.* (1998), 18 (5), 677-685.

193 Tremblay, G.M., Janelle, M.F. and Bourbonnais, Y., Anti-inflammatory activity of neutrophil elastase inhibitors. *Curr Opin Investig Drugs.* (2003), 4 (5), 556-565.

194 Tzima, E., del Pozo, M.A., Shattil, S.J., Chien, S. *et al.*, Activation of integrins in endothelial cells by fluid shear stress mediates Rho-dependent cytoskeletal alignment. *EMBO J.* (2001), 20 (17), 4639-4647.

195 van der Flier, A. and Sonnenberg, A., Function and interactions of integrins. *Cell and Tissue Research.* (2001), 305 (3), 285-298.

196   van Hinsbergh, V.W., Engelse, M.A. and Quax, P.H., Pericellular proteases in angiogenesis and vasculogenesis. *Arterioscler Thromb Vasc Biol.* (2006), 26 (4), 716-728.

197   van Mourik, J.A., Romani de Wit, T. and Voorberg, J., Biogenesis and exocytosis of Weibel-Palade bodies. *Histochem Cell Biol.* (2002), 117 (2), 113-122.

198   Wahlberg, E., Angiogenesis and arteriogenesis in limb ischemia. *J Vasc Surg.* (2003), 38 (1), 198-203.

199   Wang, J.H. and Thampatty, B.P., An introductory review of cell mechanobiology. *Biomech Model Mechanobiol.* (2006), 5 (1), 1-16.

200   Watanabe, H., Hattori, S., Katsuda, S., Nakanishi, I. *et al.*, Human neutrophil elastase: degradation of basement membrane components and immunolocalization in the tissue. *J Biochem.* (1990), 108 (5), 753-759.

201   Wedgwood, S., Devol, J.M., Grobe, A., Benavidez, E. *et al.*, Fibroblast growth factor-2 expression is altered in lambs with increased pulmonary blood flow and pulmonary hypertension. *Pediatr Res.* (2007), 61 (1), 32-36.

202   Wesche, J., Malecki, J., Wiedlocha, A., Skjerpen, C.S. *et al.*, FGF-1 and FGF-2 require the cytosolic chaperone Hsp90 for translocation into the cytosol and the cell nucleus. *J Biol Chem.* (2006), 281 (16), 11405-11412.

203   Widmann, C., Gibson, S., Jarpe, M.B. and Johnson, G.L., Mitogen-activated protein kinase: conservation of a three-kinase module from yeast to human. *Physiol Rev.* (1999), 79 (1), 143-180.

204   Wu, M.H., Endothelial focal adhesions and barrier function. *J Physiol.* (2005), 569 (Pt 2), 359-366.

205   Yayon, A., Klagsbrun, M., Esko, J.D., Leder, P. *et al.*, Cell surface, heparin-like molecules are required for binding of basic fibroblast growth factor to its high affinity receptor. *Cell.* (1991), 64 (4), 841-848.

206   Zakrzewicz, A., Secomb, T.W. and Pries, A.R., Angioadaptation: keeping the vascular system in shape. *News Physiol Sci.* (2002), 17, 197-201.

207   Zehe, C., Engling, A., Wegehingel, S., Schafer, T. *et al.*, Cell-surface heparan sulfate proteoglycans are essential components of the unconventional export machinery of FGF-2. *Proc Natl Acad Sci U S A.* (2006), 103 (42), 15479-15484.

208   Zhao, H., Kegg, H., Grady, S., Truong, H.T. *et al.*, Role of fibroblast growth factor receptors 1 and 2 in the ureteric bud. *Dev Biol.* (2004), 276 (2), 403-415.

209   Zhou, M., Sutliff, R.L., Paul, R.J., Lorenz, J.N. *et al.*, Fibroblast growth factor 2 control of vascular tone. *Nat Med.* (1998), 4 (2), 201-207.

APPENDIX

VII   APPENDIX

1   ABBREVIATIONS

A	Ampere
A	Area
A	Adenine
ABC	Abciximab
AG	Aktiengesellschaft
Ala	Alanine
Ang	Angiopoetin
ANOVA RM	Analysis of variance between groups for repeated measures
APS	Ammonium persulfate
AT	Annealing temperature
ATF	Activating transcription factor
ATP	Adenosine triphosphate
b	Width
BCA	Bicinchoninic acid
bFGF	Basic fibroblast growth factor
bp	Base pair
BSA	Bovine serum albumin
BSA-c	Bovine serum albumin (acetylated)
C	Celsius
c	Centi
C	Cytosine
CCD	Charge-coupled device
CD	Cluster of differentiation
cDNA	Complementary DNA
CHO	Chinese hamster ovary
CHY	Chymostatin
Co.	Company
COL	Collagen
D	Aspartic acid
Da	Dalton
DAPI	4',6-Diamidino-2-phenylindole
DMEM	Dulbecco's modified eagle's medium
DMSO	Dimethyl sulfoxide
DNA	Deoxyriblonucleic acid
dNTPs	Deoxynucleoside triphosphates
dsDNA	Double-stranded DNA

dsRNA	Double-stranded RNA
ECM	Extracellular matrix
EDHF	Endothelium-derived hyperpolarizing factor
EDTA	Ethylenediaminetetraacetic acid
EGF	Epidermal growth factor
ELA	Elastase
ELISA	Enzyme-linked immunosorbent assay
eNOS	Endothelial nitric oxide synthase
ER	Endoplasmic reticulum
ERK	Extracellular signal-regulated kinases
et al.	Et alii/et aliae
F	Force
FACS	Fluorescence-activated cell sorting
FAK	Focal adhesion kinase
FAT	Focal adhesion targeting
FCS	Fetal calf serum
FERM	Protein 4.1, ezrin, radixin, moesin homology
FGF	Fibroblast growth factor
FGFR	Fibroblast growth factor receptor
FITC	Fluorescein isothiocyanate
FL2-H	Fluorescence channel 2 height (bandpass 585/42 nm)
FN	Fibronectin
FSC-H	Forward scatter height
G	Glycine
g	Gram
G	Guanine
G	Units of gravity
GAPDH	Glyceraldehyde-3-phosphate dehydrogenase
GFP	Green fluorescent protein
GmbH	Gesellschaft mit beschränkter Haftung
GM-CSF	Granulocyte-macrophage colony-stimulating factor
Gp	Glycoprotein
Grb	Growth factor receptor-bound protein
h	Height
h	Hour
h	Planck constant
HEP	Heparinase
hMNZ	Human mononuclear cells
HRP	Horseradish peroxidase
HSA	Homo sapiens

Hsp	Heat shock protein
HSPG	Heparan sulfate proteoglycans
HTCR	Human tissue and cell research
HUVEC	Human umbilical vein endothelial cells
IB	Immunoblot
ICAM	Intercellular adhesion molecule
Ig	Immunoglobulin
IL	Interleukin
ILK	Integrin-linked kinase
Inc.	Incorporated
IP	Immunoprecipitation
JNK	C-jun N-terminal kinases
k	Kilo
KGaA	Kommanditgesellschaft auf Aktien
l	Liter
LAMP	Lysosomal-associated membrane protein
LM	Laminin
log	Logarithm
Ltd.	Limited
m	Meter
m	Milli
M	Molar
MAPK	Mitogen-activated protein kinases
MAPKAPK	Mitogen-activated protein kinase activated protein kinase
MAPKK	Mitogen-activated protein kinase kinase
MAPKKK	Mitogen-activated protein kinase kinase kinase
MCP	Monocyte chemoattractant protein
MEK	MAPK/ERK kinase
MEKK	MAPK/ERK kinase kinase
MEO	MeOSuc-Ala-Ala-Pro-Val-chloromethylketone
MeOSuc	Methoxysuccinyl
min	Minutes
MMP	Matrix metalloproteinase
mRNA	Messenger ribonucleic acid
n	Nano
N	Newton
n	Number of individual measurements
n.s.	Not significant
NA	Numerical aperture
NCBI	National center for biotechnology information

NE	Neutrophil elastase
NO	Nitric oxide
p	Phospho
p	Pico
PAEC	Porcine aortic endothelial cells
PAK	P21-activated kinase
PBS	Phosphate buffered saline
PCR	Polymerase chain reaction
PDGF	Platelet-derived growth factor
PE	Phycoerythrin
PECAM	Platelet endothelial cell adhesion molecule
PI3K	Phosphoinositide-3-kinase
pMNZ	Porcine mononuclear cells
PMSF	Phenylmethylsulfonyl fluoride
PMT	Photomultiplier tube
pNA	Para-nitroaniline
PPE	Porcine pancreatic elastase
Pro	Proline
PRR	Proline-rich region
PtdIns(3,4,5)P3	Phosphatidylinositol-3,4,5-triphosphate
Q	Flow rate
R	Arginine
r	Vessel radius
RGD	Arginine-glycine-aspartic acid
RISC	RNA-induced silencing complex
RNA	Ribonucleic acid
RNAi	RNA interference
rRNA	Ribosomal ribonucleic acid
RTK	Receptor tyrosine kinase
RT-PCR	Reverse transcription-PCR
s	Seconds
S	Svedberg
SAPK	Stress-activated protein kinase
SB	SB202190
SDS	Sodium dodecylsulfate
SDS-Page	Sodium dodecylsulfate-polyacrylamide gel electrophoresis
SEM	Standard error of the mean
Ser	Serine
SFK	Src family kinase
SH2	Src homology 2

Shc	Src homology 2 domain-containing transforming protein
siRNA	Small interfering RNA
SOS	Son of sevenless
SP	SP600125
SSC	Sus scrofa
SSC-H	Side scatter heigth
SUP	Supernatant
TBE	Tris-borate-EDTA
TBS	Tris buffered saline
TBS-T	Tris buffered saline with Tween
TEMED	N,N,N',N'-tetramethylethylenediamine
TGF	Transforming growth factor
Thr	Threonine
TIMP	Tissue inhibitor of metalloproteinase
TNF	Tumor necrosis factor
Tris	Tris(hydroxymethyl)aminomethane
Tyr	Tyrosine
U	Units
U	Uracil
U0	U0126
v	Frequency
Val	Valine
VCAM	Vascular cell adhesion molecule
VE-cadherin	Vascular endothelial cadherin
VEGF	Vascular endothelial growth factor
VN	Vitronectin
vs.	Versus
vWF	Von Willebrand Factor
w/v	Weight/volume
α	Angle
μ	Micro
μ	Viscosity
τ	Shear stress
ω	Angular velocity
Ø	Diameter

2   ALPHABETICAL LIST OF COMPANIES

Abcam	Cambridge, MA, USA
AbD Serotec	Kidlington, UK
Alexis Corporation	Laeufelfingen, Switzerland
American Diagnostica Inc.	Stamford, CT, USA
Amersham Biosciences	Freiburg, Germany
Apotheke Innenstadt	Munich, Germany
Applichem GmbH	Darmstadt, Germany
Aurion	Wageningen, The Netherlands
B. Braun Melsungen AG	Melsungen, Germany
Bachem AG	Bubendorf, Schweiz
BD Biosciences	Bedford, MA, USA
BD Pharmingen	Heidelberg, Germany
Beckman Coulter	Krefeld, Germany
Becton Dickinson	Heidelberg, Germany
Biochrom AG	Berlin, Germany
Biomers.net	Ulm, Germany
Biometra	Goettingen, Germany
Bio-Rad	Munich, Germany
Biotec-Fischer	Reiskirchen, Germany
Biozym Scientific GmbH	Hess. Oldendorf, Germany
Calbiochem	San Diego, CA, USA
Carl Zeiss MicroImaging GmbH	Goettingen, Germany
Cell Signaling	Danvers, MA, USA
Chemicon	Temecula, CA; USA
Corning Incorporated	Corning, NY, USA
Dako	Glostrup, Denmark
Eppendorf AG	Hamburg, Germany
Eurofins MWG GmbH	Ebersberg, Germany
Fermentas	St. Leon-Rot, Germany
Fluka Chemie AG	Buchs, Switzerland
GE Healthcare	Uppsala, Sweden
Genaxxon Bioscience GmbH	Biberach, Germany
Gibco Invitrogen	Karlsruhe, Germany
Greiner Bio-One	Kremsmünster, Austria
H&P Labortechnik AG	Oberschleissheim, Germany
Hamamatsu Photonics	Herrsching am Ammersee, Germany
Harbor Bio-Products	Norwood, MA, USA
Heraeus Instruments	Osterode, Germany

Hettich Zentrifugen	Tuttlingen, Germany
Hoefer	Holliston, MA, USA
Ibidi GmbH	Martinsried, Germany
Invitrogen	Eugene, OR, USA
Ismatec SA, Labortechnik	Glattbrugg, Germany
Leica Microsystems	Wetzlar, Germany
Leitz	Wetzlar, Germany
Lilly	Bad Homburg, Germany
Merck KGaA	Darmstadt, Germany
Miltenyi Biotec	Bergisch Gladbach, Germany
Molecular Probes Inc.	Eugene, OR, USA
New England Biolabs	Frankfurt, Germany
PAA Laboratories GmbH	Pasching, Austria
Peqlab Biotechnologie GmbH	Erlangen, Germany
Perbio	Bonn, Germany
Philips	Eindhoven, The Netherlands
Polysciences Inc.	Warrington, PA, USA
Promocell	Heidelberg, Germany
Qiagen	Hilden, Germany
R&D Systems	Minneapolis, MN, USA
Radiometer Copenhagen	Bronshoj, Denmark
Ratiopharm	Ulm, Germany
Reichert-Jung	Vienna, Austria
Roche	Mannheim, Germany
Rockland Immunochemicals	Gilbertsville, PA, USA
Santa Cruz	Heidelberg, Germany
Sanyo Electric Co. Ltd.	Munich, Germany
Sartorius Stedim Biotech	Goettingen, Germany
Schleicher & Schuell BioScience GmbH	Dassel, Germany
Serva Electrophoresis GmbH	Heidelberg, Germany
Sigma-Aldrich Chemie GmbH	Steinheim, Germany/ Taufkirchen, Germany
Sigma-Aldrich Inc.	St. Louis, MO, USA
SPSS Inc.	Chicago, IL, USA
Tecan	Crailsheim, Germany
Thermo Scientific	Rockford, IL, USA
Upstate	Lake Placid, NY, Germany
Vector Laboratories	Burlingame, CA, USA

3 PUBLICATIONS

3.1 ORAL COMMUNICATIONS

Elastase-dependent signaling cascades in FGF-2 release.
IV. Symposium, German Research Foundation (DFG), Research Training Group GRK 438 – Vascular Biology in Medicine, November 10–11, 2007, Herrsching am Ammersee, Germany.

Elastase treatment induces $\alpha_v\beta_3$ integrin-dependent activation of focal adhesion complexes.
88th Annual meeting, German Physiological Society, March 22–25, 2009, Giessen, Germany.

3.2 POSTER PRESENTATIONS

Elastase-dependent signaling cascades in FGF release.
Hennig, T., Pohl, U., Gloe, T.
Annual Meeting of the Society for Microcirculation and Vascular Biology 2007 and 6th International Symposium on the Biology of Endothelial Cells, October 4–6, 2007, Heidelberg, Germany.

Regulation of FGF-2 release via elastase-activated integrin $\alpha_v\beta_3$.
Hennig, T., Pohl, U., Gloe, T.
87th Annual meeting, German Physiological Society, March 2–5, 2008, Cologne, Germany.

Proteolysis of extracellular matrix proteins by elastase induces an activation of focal contacts.
Hennig, T., Pohl, U., Gloe, T.
Interact PhD Symposium 2009, April 2, 2009, Munich, Germany.

Outside-in signaling – effects of elastase on extracellular matrix, integrin $\alpha_v\beta_3$ and cytoskeleton.
Hennig, T., Pohl, U., Gloe, T.
Joint Meeting 2009 of the Society for Microcirculation and Vascular Biology and the Swiss Society for Microcirculation, October 8–10, 2009, Bern, Switzerland.

Shear stress-induced integrin $\alpha_v\beta_3$ activation is dependent on the activity of an endothelial elastase
Hennig, T., Pohl, U., Gloe, T.
Joint meeting of FEPS and the Slovenian and Austrian Physiological Societies 2009, November 12–15, 2009, Ljubljana, Slovenia.

Shear stress induces integrin activation by eliciting release of an endothelial elastase
Hennig, T., Pohl, U., Gloe, T.
Joint Meeting of the Scandinavian and German Physiological Societies, March 27–30, 2010, Copenhagen, Denmark.
accepted

3.3   ORIGINAL PUBLICATIONS

Shear stress induces the release of an endothelial elastase: role in integrin $\alpha_v\beta_3$-mediated FGF-2 release
Theres Hennig[*], Christina Mogensen[*], Ulrich Pohl and Torsten Gloe
[*] These authors contributed equally to this work.
in preparation

3.4   AWARDS

Best Poster Award
Joint meeting of FEPS and the Slovenian and Austrian Physiological Societies 2009, November 12–15, 2009, Ljubljana, Slovenia.

4 CURRICULUM VITAE

Personal data

Name	Theres Hennig
Date of birth	August 21, 1981
Place of birth	Halle/Saale, Germany
Nationality	German
Marital status	Unmarried

Academic education

Since 09/2006	Ph.D. thesis Walter-Brendel-Centre of Experimental Medicine, Prof. Dr. U. Pohl Medical Faculty, Ludwig-Maximilians-Universität, Munich, Germany
09/2006 – 06/2008	Member of the Research Training Group GRK 438 "Vascular Biology in Medicine" Scholarship German Research Foundation (DFG)
Since 01/2007	Pharmacist Apotheke am Kufsteiner Platz, Munich, Germany
05/2006	3rd State Examination, Licensure as Pharmacist
11/2005 – 04/2006	"First year resident" as Pharmacist Schlehen-Apotheke, Leipzig, Germany
05/2005 – 10/2005	"First year resident" as Pharmacist Diploma thesis Institute of Pharmaceutical Biology, Prof. Dr. J. W. Rauwald University Leipzig, Leipzig, Germany
04/2005	2nd State Examination
09/2004	Internship College of Pharmacy, Prof. Dr. H. Derendorf University of Florida, Gainesville, FL, USA
08/2002	1st State Examination
10/2000 – 05/2006	Studies of Pharmacy University Leipzig, Leipzig, Germany

School education

1992 – 2000	Grammar School: Drei-Tannen-Gymnasium, Thalheim, Germany
1988 – 1992	Primary School, Halle/Saale, Germany

5   ACKNOWLEDGEMENTS